"FEDERICO II" UNIVERSITY OF NAPLES

Dipartimento
Medicina Veterinaria
Produzioni Animali

VETERINARY SCIENCES PhD THESIS
XXX CYCLE

A functional study of the endocannabinoid system in zebrafish neurodevelopment: implications in vision and locomotion

Candidate
Rosa Maria Sepe

Tutors
Dr. Paolo Sordino
Prof. Paolo De Girolamo

Coordination - *Prof. Giuseppe Cringoli*

INDEX

LIST OF ABBREVIATIONS

2-AG, 2-Arachidonoylglycerol

ABH4/6/12, α/β-hydrolase 4/6/12

AC, amacrine cell

AC, adenylate cyclase

AEA, *N*-arachidonoylethanolamine

BC, bipolar cell

BDNF, brain-derived neurotrophic factor

BMP, bone morphogenetic protein

cAMP, Cyclic adenosine monophosphate

Cas9, CRISPR associated protein 9

cnr1/2 (gene) - CB1/2 (protein), cannabinoid receptor type 1/2

CNS, central nervous system

COX2, cyclooxygenase 2

CRISPR, Clustered Regularly Interspaced Short Palindromic Repeats

DAG, diacylglycerol

daglα/β (gene) - Daglα/β (protein), diacylglycerol lipase α/β

dpf, days post fertilization

ECS, endocannabinoid system

CB/eCB, cannabinoid/endocannabinoid

eef1a1l1, eukaryotic translation elongation factor 1 alpha 1, like 1

EMT, endocannabinoid membrane transporter

ERK, extracellular signal-regulated kinases

FAAH, fatty acid amide hydrolase

FGF, fibroblast growth factor

GCL, ganglion cell layer

GDE1, glycerophosphodiester phosphodiesterase 1

GPCR, G protein-coupled receptor

GPR18/55/119, G protein-coupled receptor 18/55/119

gRNA, guide RNA

HC, horizontal cell

hpf, hours post fertilization

INL, inner nuclear layer

IPL, inner plexiform layer

IP3, inositol 1,4,5-trisphosphate

LTD, long-term synaptic depression

LTP, long-term potentiation

MAPK, mitogen-activated protein kinase

mgll (gene) - Magl (protein), monoacylglycerol lipase

mGluR, metabotropic glutamate receptor

MO, morpholino

MSN, medium spiny neuron

NADA, *N*-Arachidonoyl dopamine

NAPE, *N*-arachidonoyl phosphatidylethanolamine

NAPE-PLD,*N*-acyl-phosphatidylethanolamine-selective phosphodiesterase

NAT, *N*-acyltransferase

OEA, Oleoylethanolamine

OKN, optokinetic nystagmus

OKR, optokinetic response

PA, phosphatidic acid

PE, pigmented epithelium

PEA, Palmitoylethanolamide

PI3K, Phosphatidylinositol-4,5-bisphosphate 3-kinase

PIP2, phosphatidylinositol-4,5-bisphosphate

PKA/C, protein kinase A/C

sPLA1/2, soluble phospholipase A1/2

PLC, phospholipase C

PLCβ, phospholipase Cβ

PLD, phospholipase D

PNS, peripheral nervous system

POA, preoptic area

PR, photoreceptor

ptgs2b, prostaglandin-endoperoxide synthase 2b

PTPN22, protein tyrosine phosphatase non-receptor type 22

RGC, retinal ganglion cell

RNE, retinal neuroepithelium

RPE, retinal pigmented epithelium

SC, superior colliculus

SNL, superficial neuropil layer

SoxB1, SRY-box containing genes B1 family

STDP, spike-timing-dependent plasticity

TALEN, Transcription activator-like effector nucleases

TNP, tectal neuropil

trpv1 (gene) - TRPV1 (protein), transient receptor potential vanilloid subtype 1 receptor

WISH, whole mount *in situ* hybridization

WNT, wingless/integrated

LIST OF FIGURES

LIST OF TABLES

1. ABSTRACT:

The endocannabinoid system (ECS) is constituted by a group of endogenous arachidonate-based lipids [endocannabinoids (eCBs)] and their receptors, capable of regulating neuronal excitability as well as a variety of physiological processes.

The 2-Arachidonoylglycerol (2-AG) is a retrograde neurotransmitter present at relatively high levels in the central nervous system, with cannabinoid neuromodulatory effects on synaptic transmission in the adult brain. Recently, several lines of evidence have demonstrated the presence of eCBs, their receptors and metabolizing enzymes, also in early stages of brain development, suggesting an important role of ECS in the regulation of neural progenitor proliferation and specification as well as migration and differentiation.

In this study we focus on the importance of 2-AG signaling in central nervous system development, with the aim to investigate the role of 2-AG in the development and differentiation of neurons, and in the formation of neuronal circuits that control spontaneous locomotion and visual system, using zebrafish as model organism.

The vertebrate *Danio rerio* (zebrafish) represents a valid animal model system to study eCB biology, since phylogenetic analyses of the zebrafish ECS have demonstrated that it is highly conserved with the mammalian counterpart.

Here we report the presence of a complete endocannabinoid system during zebrafish development and show that the genes coding for enzymes that catalyze the anabolism and catabolism (*dagla* and *mgll* respectively) of the endocannabinoid 2-AG, as well as its main receptor in the brain,

cannabinoid receptor type 1 (*cnr1*), are co-expressed in defined regions of neurogenesis and axogenesis.

Through the use of morpholino-induced transient knockdown of the zebrafish *daglα* and its pharmacological rescue, we suggest that the synthesis of 2-AG is implicated in the control of axon formation in defined areas of the developing brain, such as optic tectum, cerebellum and optic nerve. Animals lacking Daglα display defective axonal growth and fasciculation, and abnormal physiological behaviors in tests measuring stereotyped eye movement and motion perception. Moreover the use of *daglα* morpholino in the zebrafish transgenic line 'ath5:gap-gfp', in which it is possible to follow the retinal ganglion cells (RGC) pathfinding, reveals abnormalities in RGC fiber tracts and in the correct arborization in the optic tectum.

Furthermore, pharmacological treatments using antagonists of the two main zebrafish eCBs receptors (CB1 and CB2) suggest their putative role in the correct formation of the tectal neuropile in transgenic line 'ath5:gap-gfp' and in the correct lamination of neuroretina in SoFa line, in which all the major retina neuronal subtypes are labeled simultaneously.

In details, pharmacological treatments using antagonists of CB1 receptor suggest its putative role in the correct formation of the tectal neuropile in zebrafish transgenic line 'ath5:gap-gfp'. On the other hands, by using SoFa zebrafish line, in which all the major retina neuronal subtypes are simultaneously labeled, similar treatments highlight the possible role of CB2 in the correct lamination of neuroretina by regulating the number and positioning of interneurons (amacrine cells) in the inner plexiform layer of developing retina.

Animals treated with these antagonists display also defective swimming behavior, suggesting, in addition, the implication of CB1 and CB2 receptors in the correct formation of neuronal circuits that control spontaneous locomotion.

In conclusion, our results point to the important role of eCBs as mediators in axonal outgrowth with implications in the control of vision and movement, highlighting that the well-established role of 2-AG in axon guidance is required in brain areas that control locomotor and optokinetic functions. On the other hand, the eCBs receptors CB1 and CB2 can specifically regulate the formation of retinotectal system, the differentiation and lamination of zebrafish neuroretina, as well as direct the control of swimming behaviour.

2. Introduction

2.1. The Endocannabinoid System

The endocannabinoid system (ECS), known as "the body's own cannabinoid system" (*Grotenhermen*, 2012), is a complex endogenous regulation system that includes a large number of lipid and protein molecules, located throughout the central nervous system (CNS) and peripheral nervous system (PNS).

The ECS, broadly speaking, includes:

1. the endogenous arachidonate-based lipids, known as "endocannabinoids" (eCBs), that are physiological ligands for the cannabinoid receptors;
2. the enzymes that synthesize and degrade the endocannabinoids;
3. the cannabinoid receptors (*Pertwee*, 2006).

eCBs are lipid molecules principally derived from membrane phospholipids. Unlike classical neurotransmitters and neuropeptides, eCBs are not stored in vesicles in axon terminals, but rather they are synthesized on site and on demand in somata and dendrites, in response to physiological or pathological stimuli, such as neuronal depolarization or high intracellular calcium levels. They are subsequently released from cells and then exert an immediate action as signaling molecules (*Di Marzo*, 2008; *Piomelli,* 2003; *Kondo et al.*, 1998). They act as neuromodulators, not directly as neurotransmitters but rather increase or decrease the action of neurotransmitters, tuning in this way the neural circuitry of an entire brain region; not just that of an individual neuron.

Several eCBs have been identified in brain and peripheral tissues, but their function and role in ECS physiology remains to be determined. They are all eicosanoids and their structures are summarized in Fig. 1.
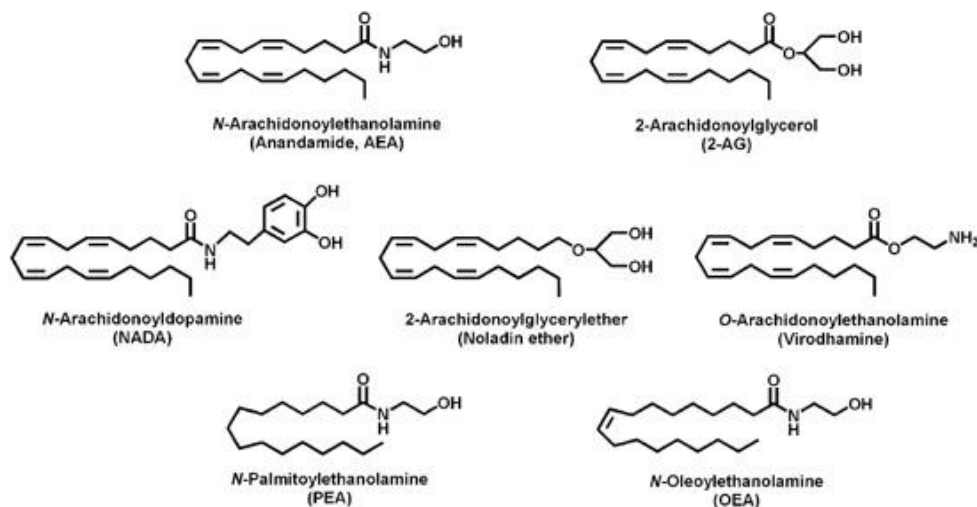
Figure 1: Molecular structure of main endocannabinoids.

The best characterized eCBs are:

- *N*-arachidonoylethanolamine (AEA), commonly known as anandamide (from Sanskrit word ananda, which means "bliss"), that was the first eCB to be identified by Lumír Ondřej Hanuš and William Anthony Devane in 1992 (*Devane et al.,* 1992),

- 2-arachidonoylglycerol (2-AG), discovered as chemical compound by Shimon Ben-Shabat at Ben-Gurion University (*Pizzorno*, 2011), and described as an endogenous agonist for the cannabinoid receptors in 1994-1995 by a research group at Teikyo University (*Sugiura et al*., 1994; *Sugiura et al.*, 1995). The 2-AG, was the second endocannabinoid to be discovered and it is the most abundant eCB present in the brain (*Reisenberg et al*., 2012).

These two eCBs are synthesized and degraded by separate pathways (Fig. 2).
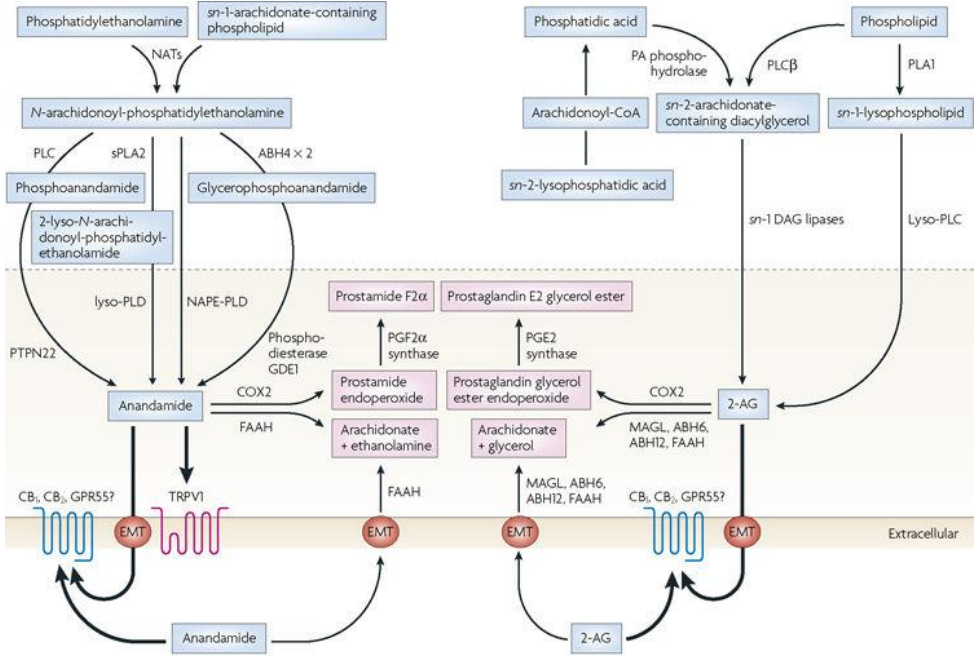
Figure 2: Biosynthesis, action and inactivation of anandamide (AEA) and 2-arachidonoylglycerol (2-AG). The biosynthetic pathways for AEA and 2-AG are shown in blue, degradative pathways are shown in pink. ABH4/6/12, α/β-hydrolase 4/6/12; CB1/2, cannabinoid receptor 1/2; COX2, cyclooxygenase 2; DAG, diacylglycerol; EMT, endocannabinoid membrane transporter; FAAH, fatty acid amide hydrolase; GDE1, glycerophosphodiester phosphodiesterase 1; GPR55, G protein-coupled receptor 55; MAGL, monoacylglycerol lipase; NAPE-PLD, N-acyl-phosphatidylethanolamine-selective phosphodiesterase; NATs, N-acyltransferases; PA, phosphatidic acid; sPLA1/2, soluble phospholipase A1/2; PLC, phospholipase C; PLCβ, phospholipase Cβ; PLD, phospholipase D; PTPN22, protein tyrosine phosphatase, non-receptor type 22; TRPV1, transient receptor potential, vanilloid subtype 1 receptor. Taken from: *Di Marzo,* 2008

The major route for the biosynthesis of anandamide is *via* the precursor *N*-arachidonoyl phosphatidylethanolamine (NAPE), which is generated by the enzyme *N*-acyltransferase (NAT) in a calcium-sensitive and -insensitive manner. AEA is then generated by hydrolysis of NAPE by four possible alternative pathways, the most direct of which (direct conversion) is catalysed by a phospholipase D (NAPE-PLD) (*Di Marzo*, 2008; *Piomelli,* 2003; *Sugiura et al*., 2002; *Wang et al*., 2009). Thus the endocannabinoid anandamide seems to be produced "on demand" and released in an activity-dependent manner by enzymatic cleavage of lipid precursors. The biological inactivation of anandamide occurs mainly through hydrolyzation mediated by fatty acid amide hydrolase (FAAH) (*McKinney et al*., 2005).

The major pathway for the biosynthesis of 2-AG comprises sequential hydrolysis of arachidonic acid-containing inositol phospholipids by phospholipase C (PLC) and diacylglycerol (DAG) lipase (DAGL) (*Di Marzo*, 2008; *Piomelli,* 2003; *Sugiura et al*., 2002). In response to many extracellular signals such as neurotransmitters, PLC catalyzes the hydrolysis of phosphatidylinositol-4,5-bisphosphate (PIP2), thereby generating two well established second messengers, inositol 1,4,5-trisphosphate (IP3) and DAG. Two different DAGL, α and β, hydrolyze DAG to yield 2-AG. Different studies strongly suggest that DAGLα, rather than DAGLβ, is the predominant 2-AG synthesizing enzyme for endocannabinoid-mediated modulation of neurotransmission (*Gao et al*., 2010; *Tanimura et al*., 2010; *Yoshino et al*., 2011), while DAGLβ is more implicated in inflammatory responses in macrophages and microglia (*Hsu et al*., 2012; *Viader et al*., 2016). 2-AG, like AEA, is transported into

neurons by endocannabinoid membrane transporters (EMT), such as heat shock proteins (Hsp70s) and fatty acid binding proteins (FABPs) (*Kaczocha et al.*, 2009), and is subsequently inactivated by the enzyme monoacylglycerol lipase (MAGL) (*Di Marzo*, 2008; *Piomelli,* 2003; *Sugiura et al.*, 2002). 2-AG is also metabolized to some extent by other recently identified lipases, the α/β-hydrolases 6 (ABH6) and 12 (ABH12), as well as FAAH, but MAGL is responsible for ~85% of this activity in the brain (*Savinainen et al.*, 2012). Both AEA and 2-AG, possibly under conditions in which the activity of MAGL or FAAH is suppressed, might become substrates for cyclooxygenase 2 (COX2) and give rise to the corresponding hydroperoxy derivatives. AEA and 2-AG hydroperoxy derivates can then be converted to prostaglandin ethanolamides (prostamides) and prostaglandin glycerol esters, respectively, by various prostaglandin synthases (*Rouzer et al.*, 2008).

2-AG synthesis and release can be driven by activation by Gq-coupled receptors, such as group I mGluRs (metabotropic glutamate receptors) and muscarinic receptors, because the signaling pathway that they activate leads to accumulation of the 2-AG precursor DAG (*Alger et al.*, 2002; *El Manira et al*, 2008; *Kano et al.*, 2009; *Kettunen et al.*, 2005). In summary, the synthesis and release of these two endogenous cannabinoids occurs on demand in an activity-dependent manner either in terms of firing of neurons or activation of Gq-coupled receptors, or a combination of the two. Separate synthesis and degradation pathways of AEA and 2-AG offer an entry point for determining their distribution and for defining their roles in controlling CNS functions.

All eCBs have in common the ability to bind to cannabinoids receptors, the same receptors that interact with phytocannabinoids.

Two cannabinoid receptors, cannabinoid receptor type 1 (CB1) and type 2 (CB2), have been identified pharmacologically, anatomically, and by molecular cloning, but other cannabinoid receptors may exist, with different tissue distribution and signaling mechanisms (*Mackie et al.*, 2006).

CB1 receptor is a G protein-coupled receptor (GPCR) from the cannabinoid receptor family that in humans is encoded by the *cnr1* gene. These receptors are expressed virtually throughout the CNS and PNS from cortical to spinal cord regions (*Katona et al.*, 2008). They are also present in minor amounts in some peripheral organs and tissues including lungs, liver, kidneys and digestive system. At the brainstem, the distribution of CB1 receptors is particularly marked in the regions responsible for motor coordination and movement, attention, and complex cognitive functions such as judgment, learning, memory and emotions (*Herkenham et al.*, 1990; *Mailleux et al.*, 1992; *Pettit et al.*, 1998). CB1 receptors may exist as homodimers or form heterodimers or other GPCR oligomers when coexpressed with one or more classes of G-protein-coupled receptors. They are predominantly localized on presynaptic terminals, at glutaminergic and GABAergic interneurons, acting as neuromodulators in a retrograde manner to inhibit release of glutamate and GABA (*Elphick et al.*, 2001), but there are also reports of a postsynaptic localization on dendrites and neuronal somata (*Marsicano et al.*, 2003). These receptors were initially thought to be coupled preferentially to a Gi/o G-protein, which decreases intracellular cAMP concentration by inhibiting its production enzyme,

adenylate cyclase (AC), and increases mitogen-activated protein kinase (MAP kinase) concentration. Alternatively, recent data show that they can be also coupled to Gq G-protein to induce release of Ca^{2+} from intracellular stores, and to Gs proteins, which stimulate adenylate cyclase (*Pertwee*, 2006). cAMP is known to serve as a second messenger coupled to a variety of ion channels, including the positively influenced inwardly rectifying potassium channels (Kir or IRK) (*Demuth et al.*, 2006) and calcium channels, which are activated by cAMP-dependent interaction with such molecules as protein kinase A (PKA), protein kinase C (PKC), Raf-1, ERK, JNK, p38, c-fos, c-jun, and others (*Pagotto et al.*, 2006).

CB2 receptor is also a G protein-coupled receptor that in humans is encoded by *cnr2* gene and it is closely related to *cnr1*, with a protein sequences identity of 44% (*Latek et al.*, 2011). CB2 receptors are expressed primarily at the peripheral level, mainly on T cells of the immune system, on macrophages and B cells, and in hematopoietic cells. Further investigation into the expression patterns of the CB2 receptors revealed that CB2 receptor gene transcripts are also expressed on peripheral nerve terminals, on some rat retinal cell types (*López et al.*, 2011), and in the brain, though not as densely as the CB1 receptor and located on different cells (*Onaivi*, 2006). Unlike the CB1 receptor, in the brain, CB2 receptors are found primarily on microglia (*Cabral*, 2008) and in some neurons within the central nervous system (*e.g.* brainstem), where their role remains not well defined (*Mackie et al.*, 2006; *Sickle et al.*, 2005). While the most likely cellular targets and executors of the CB2 receptor-mediated effects of endocannabinoids or synthetic agonists are the immune and immune-derived cells (*e.g.* leukocytes, various populations of

T and B lymphocytes, monocytes/macrophages, dendritic cells, mast cells, microglia in the brain, Kupffer cells in the liver, astrocytes, etc.), the number of other potential cellular targets is expanding, now including endothelial and smooth muscle cells, fibroblasts of various origins, cardiomyocytes, and certain neuronal elements of the peripheral or central nervous systems (*Pacher et al*., 2011).

Like CB1 receptors, CB2 receptors inhibit the activity of adenylyl cyclase through their Gi/Goα subunits. It is also known that CB2 receptors are coupled to the MAPK-ERK pathway through their Gβγ subunits (*Shoemaker et al*., 2005; *Demuth et al*., 2006; *Bouaboula et al*., 1996), regulating a number of important cellular processes in both mature and developing tissues (*Shvartsman et al*., 2009). Activation of the MAPK-ERK pathway by CB2 receptor agonists, acting through the Gβγ subunit, results also in changes in cell migration (*Klemke et al.*, 1997), as well as in an induction of the growth-related gene *Zif268* (also known as *Krox-24*, *NGFI-A*, and *egr-1*) (*Bouaboula et al.*, 1996), implicated in neuroplasticity and long-term memory formation (*Alberini*, 2009).

Different pharmacological data suggest that additional cannabinoid receptors may be present in the CNS (*Járai et al*., 1999; *McHugh et al*., 2008).

Molecular biology studies have suggested that the G protein-coupled receptor GPR55, first identified as an orphan receptor, should in fact be characterized as a cannabinoid receptor, on the basis of sequence homology at the binding site (*Baker et al*., 2006), but with a signaling profile distinct from CB1 and CB2 receptors (*Mackie et al*., 2006). Subsequent studies showed that GPR55 does indeed respond to

cannabinoid ligands (*Ryberg et al*., 2007; *Johns et al*., 2007). This profile as a distinct non-CB1/CB2 receptor which responds to a variety of both endogenous and exogenous cannabinoid ligands, has led some groups to suggest that GPR55 should be categorized as the CB3 receptor, and this re-classification may follow in time (*Overton et al*., 2006; *Ross*, 2009; *Kapur et al*., 2009; *Moriconi et al*., 2010).

Along with GPR55, GPR18 and GPR119 have been also implicated as novel cannabinoid receptors.

Recent research strongly supports the hypothesis that the N-Arachidonyl glycine receptor (NAGly receptor), also known as G protein-coupled receptor 18 (GPR18) is the molecular identity of the abnormal cannabidiol receptor and additionally suggests that NAGly, the endogenous lipid metabolite of AEA initiates directed microglial migration in the CNS through activation of GPR18 (*McHugh et al*., 2010).

G protein-coupled receptor 119, also known as GPR119, is expressed predominantly in the pancreas and gastrointestinal tract in rodents and humans, as well as in the rodent brain, with a role in reduction in food intake and body weight gain (*Overton et al*., 2006), and in incretin regulation and insulin hormone secretion (*Ning et al*., 2008; *Swaminath*, 2008; *Lan et al*., 2009).

Transient receptor potential vanilloid 1 (TRPV1), also known as the capsaicin receptor, is a nonselective cation channel expressed mainly in the nociceptive neurons of the PNS, but it is also described in many other tissues, including the CNS (*Caterina et al.*, 1997*)*. TRPV1 receptors are involved in the transmission and modulation of pain (nociception), as well as the integration of diverse painful stimuli (*Cui et al*., 2006; *Huang et al*.,

2002). These receptors are activated by a wide variety of exogenous and endogenous physical and chemical stimuli, sending a pain signal to the brain. The best-known activators of TRPV1 are: capsaicin, the irritating compound in hot chili peppers, heat, proinflammatory substances and acidic conditions. Interestingly, anandamide and other endocannabinoids, like N-oleyl-dopamine, and N-arachidonoyl-dopamine, are activators of the TRPV1 channel. Since sensory neurons often co-express both CB1 and TRPV1, they could regulate pain sensation in the brain, with potential implications in the treatment of inflammatory disorders (*Ross*, 2003).

Thus, it is thought that cannabinoid signaling in the brain is mediated primarily by CB1 receptors, but that additional receptors may also be present. In addition, the anatomical localization of the receptors in relation to the site of synthesis and release of endocannabinoids will determine the direction of their signaling and physiological function, like motor control, memory and learning, pain perception, energy balance regulation, food intake, endocrine function, vascular response, immune system modulation, and neuroprotection.

2.2 The Retrograde Signalling of Endocannabinoids

In the study of synaptic transmission, the field of endocannabinoid research is flowering. A wealth of recent findings has revealed critical molecular underpinnings of endocannabinoid generation and signal transduction, and the subcellular localization of these processes within neurons has been mapped with increasing detail. Sophisticated techniques of neuronal imaging and electrophysiological recording are combined to yield new insights into the timing and regulation of endocannabinoid signaling at synapses throughout the brain, and these discoveries are beginning to influence models of synaptic computation and plasticity at a profound level (*Gerdeman*, 2008).

Endocannabinoids are now known to act as a widespread system of retrograde signaling at central synapses, whereby the stimulus-dependent synthesis of endocannabinoids in postsynaptic neurons leads to the activation of presynaptic CB1 receptors, and a subsequent inhibition of neurotransmitter release via multiple presynaptic mechanisms.

In fact, multiple lines of evidence have led to general consensus that in many brain areas, the molecular synthetic pathways for AEA and 2-AG exert their function postsynaptically to both excitatory and inhibitory synapses (*Matyas et al.*, 2006; *Katona et al.*, 2006; *Yoshida et al.*, 2006) (Fig. 3).

Postsynaptically released endocannabinoids that are triggered by membrane depolarization, intracellular Ca^{2+} elevation, and/or activation of $G_{q/11}$-coupled metabotropic receptors, act at presynaptic CB1 receptors to mediate retrograde synaptic inhibition at both excitatory and inhibitory

synapses, and on timescales that are either transient (on a scale of seconds) or long lasting.

Accordingly, endocannabinoids in the CNS intervene in both short-term and long-term forms of synaptic plasticity, including depolarization-induced suppression of both excitatory and inhibitory neurotransmission, long-term potentiation and depression, and long-term depression of inhibition (*Wilson et al.*, 2002; *Freund et al.*, 2003).

Multiple lines of evidence including localization of CB1 receptors on presynaptic terminals (*Herkenham et al.*, 1991; *Egertova et al.*, 1998; *Katona et al.*, 1999), preferential coupling to $G_{i/o}$ proteins (*Howlett et al.*, 2002), and inhibition of voltage-gated Ca^{2+} channels (VCCs) (*Twitchell et al.*, 1997; *Shen and Thayer*, 1998), indicate that endocannabinoids would cause suppression of vesicular neurotransmitter release.

By dynamically modulating synapse reliability, synaptic suppression mediated by endocannabinoids provides a means for postsynaptic neurons to "tune" the sensitivity of their synaptic inputs to afferent patterns of stimulation. This mechanism may in turn help to regulate burst firing, or to generate or maintain synchronous membrane oscillations in interconnected neuronal populations. Endocannabinoid-dependent long-term synaptic depression (LTD) has also been recently demonstrated to underlie multiple forms of spike-timing-dependent plasticity (STDP) in the cerebral cortex, long thought to regulate the neuronal representation of sensory maps.

In many ways, the activity and functional potential of a neural circuit is defined by the moment-to-moment state of its many synapses (*Hebb*, 1949; *Bear*, 1996; *Abbott and Regehr*, 2004). In recent years, the endocannabinoids have emerged as a system for modulating synaptic

efficacy within many brain areas, by acting as postsynaptically released retrograde messengers to presynaptic CB1 receptors. Short- and long-term synaptic suppression by CB1 receptors is a widespread mechanism to fine-tune synaptic filtering properties, and to facilitate associative modes of plasticity as a coincidence detector. In addition, endocannabinoid-mediated LTD has now redefined many known forms of synaptic plasticity, clarifying these processes on a new level of mechanistic detail.

The endocannabinoid system is thus central to many cellular mechanisms of stable neuronal plasticity, information that has wide-ranging implications for understanding brain function and the etiology and treatment of neurological diseases.
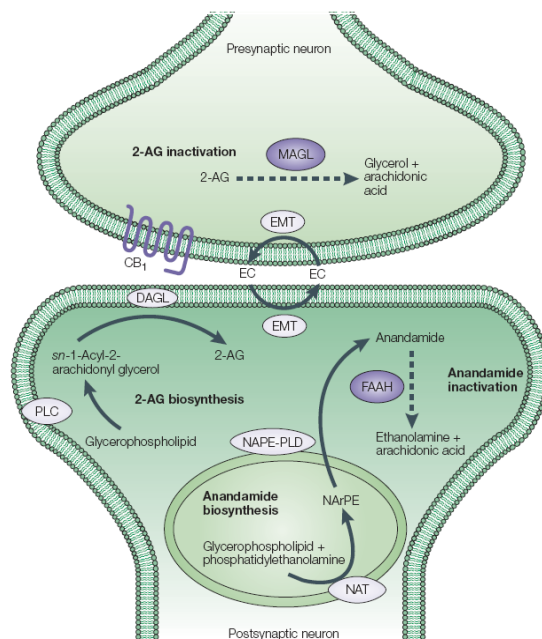
Figure 3: Subcellular localization of endocannabinoid metabolic pathways. This overview highlights potential factors controlling the physiology of 2-AG or AEA at postsynaptic sites of generation and release, as well as presynaptic signaling by CB1 receptors (CB1). Taken from: *Di Marzo et al.*, 2004.

2.3 ECS and Neurodevelopment

Endocannabinoids act as retrograde messengers that control synaptic plasticity, that is the ability of the nervous system to alter the functional efficiency of neuronal connections (synapses), to establish new ones and to eliminate some others. This mechanism occurs in many areas of the postnatal brain, including neocortex, hippocampus, cerebellum, and basal ganglia.

But, besides this well-established neuromodulatory role in adults, it has just begun to emerge that the endocannabinoid signaling also subserves fundamental mechanisms of CNS development: this family of lipid mediators is pivotal in controlling neurogenesis, neuronal progenitor proliferation and fate specification, lineage segregation, neuronal migration, differentiation and survival, influencing the formation of complex neuronal circuits in the embryonic brain that directly translate into retrograde synaptic signaling once synapse establishment concludes (*Fernandez-Ruiz et al*., 2000; *Fride*, 2004; *Harkany et al*., 2008).

Neuroanatomical findings furnish the concept that the endocannabinoid system is expressed and positioned during CNS development such that its activity can ideally tune a broad array of developmental processes in both neural progenitors and in lineage-committed neuronal precursors.

During brain development, the expression of CB1, CB2, GPR55 and TRPV1 receptors, and enzymes associated with endocannabinoid synthesis and degradation coincides with the expansion of neural progenies and their engagement in establishing neuronal diversity (*Galve-Roperh et al*., 2006; *Harkany et al*., 2007). The presence of functional endocannabinoid signaling networks in neurogenic proliferative zones of the developing

brain, and also in neurogenic niches of the adult, suggests that endocannabinoid signals could provide extracellular cues instructing the cellular program of neural progenitors such that they generate appropriate contingents of cell lineages required to build the developing brain (*Aguado et al*., 2005). The endocannabinoids and related lipid mediators regulate neural progenitor commitment and survival, guaranteeing a fine-tuned balance between progenitor cell proliferation and programmed cell death thus leading to the generation of adequate quantities of neural cells during brain development (*Guzman et al*., 2002; *Guzman*, 2003; *Aguado et al*., 2006).

The concept that on-demand endocannabinoid signaling links axonal specification in the early embryonic brain to synaptogenesis and synaptic plasticity during the neonatal period is supported by recent evidence identifying endocannabinoids as a novel class of axon guidance cues (*Berghuis et al*., 2007). An attractive hypothesis is that autocrine endocannabinoid signaling regulates growth cone differentiation and axon guidance (*Bisogno et al*., 2003). This concept stems from the finding that 2-AG stimulates neurite outgrowth of cerebellar neurons *via* a mechanism dependent on intrinsic DAGLα/β activity within axonal growth cones (*Williams et al*., 2003). Also the activation of CB1 receptor controls neurite outgrowth and synaptogenesis, processes that are required to generate functionally mature neurons. In fact, the CB1 localization in developing brain has recently been identified as a prerequisite for guiding the elongating axons to their targets, and to achieving proper synapse positioning of postsynaptic target cells (*Berghuis et al*., 2007).

Furthermore the endocannabinoid effects also extend to the regulation of neuronal migration, and the attainment of particular morphological, physiological, and molecular phenotypes occurring during terminal neuronal differentiation. Notably, endocannabinoid-induced neuronal migration (*Song and Zhong*, 2000) acts in cooperativity with brain-derived neurotrophic factor (BDNF), a prime migration (*Fukumitsu et al.*, 2006) and prodifferentiation factor (*Ventimiglia et al.*, 1995; *Horch and Katz*, 2002; *Dijkhuizen and Ghosh*, 2005), for a variety of CB1 receptor-expressing neurons, including GABAergic, serotonergic, and dopaminergic cells.

Finally, on-demand recruitment of second messengers to the CB1 receptor, e.g., the Src/Stat3 (*Jordan et al.*, 2005; *He et al.*, 2005), extracellular signal-regulate kinase (ERK1/2) (*Galve-Roperh et al.*, 2000; *Rueda et al.*, 2002; *Berghuis et al.*, 2007), and PI3K/Akt pathways (*Molina-Holgado et al.*, 2002), and the modulation of sphingolipid-derived signaling mediators and cell death pathways (*Guzman*, 2003), enhances the ECS potential to dynamically regulate fundamental developmental processes, including neural progenitor proliferation and migration, fate decision, survival, and lineage specification, in a spatially and temporally coordinated manner (*Harkany et al.*, 2007; *Galve-Roperh et al.*, 2007).

2.4 ECS and Locomotion

Motor behavior represents the overt expression of integrated CNS processing. The final motor output is the result of a sophisticated integration of the activity of different CNS networks, that display a continuous plasticity to allow their activity to adapt to changes in the internal and external environments (*Destexhe and Marder*, 2004). The plasticity of neural circuits can be changed by modulatory systems that have been classically considered to depend on release of modulatory transmitters from pre-synaptic terminals that can act post-synaptically on axon terminals or dendrites to change synaptic strength (*Katz and Frost,* 1996; *Nusbaum et al*., 2001). This view has been revised following the discovery of retrograde signaling (*Ohno-Shosaku et al*., 2001), and the eCBs represent a prominent example of retrograde signaling in synaptic plasticity in many regions of the CNS. Most studies of eCB-mediated plasticity in the brain have concentrated on mechanisms related to learning and memory (*Chevaleyre et al*., 2006; *Heifets and Castillo*, 2009; *Kano et al*., 2009), but they have been confronted with the difficulty of quantifying cognitive changes in the aim to link synaptic plasticity with behavior. A major advantage of motor circuits is that their outputs can be readily measured and correlated to the motor behavior. Activity-dependent changes in synaptic efficacy play a critical role in shaping the functional architecture of neural circuits and determining their operational range. In this regard, eCBs have attracted much attention in recent years because of their unconventional way of regulating synaptic transmission.

One region of the CNS where the link between eCB-mediated synaptic plasticity can be directly related to circuit function and motor behavior is

the spinal cord. Locomotor movements are generated by spinal networks comprised primarily of interconnected populations of excitatory glutamatergic and inhibitory glycinergic interneurons that lead to the temporally sequenced muscle contractions underlying locomotion.

Because eCBs can in principle be released from all neurons in the spinal locomotor networks, they provide an important modulatory mechanism that is not only involved in fine-tuning of the ongoing activity but that may be also necessary for the generation of the locomotor activity (Fig.4).

In vitro studies have demonstrated that eCBs play an important role in setting the baseline locomotor frequency. The blockade of CB1 receptors, in the isolated spinal cord, using a specific antagonist, reduced the baseline frequency of the locomotor rhythm, showing that eCBs are released within the locomotor circuitry and that they contribute to the expression of the motor pattern (*Kettunen et al*., 2005; *Kyriakatos and El Manira*, 2007; *Thorn Perez et al*., 2009). This indicates that activation of CB1 receptors by eCBs released during locomotion, regulates inhibitory and excitatory synaptic transmission in such a manner as to increase the excitability in the spinal circuitry and thus to accelerate the locomotor behavior (*El Manira et al*., 2008; *Kettunen et al*., 2002; *Kyriakatos and El Manira*, 2007).

Also the basal ganglia are thought to be responsible for the selection of appropriate motor behavior. They consist of a set of interconnected nuclei with the striatum as the primary input nucleus receiving excitatory inputs from cortex and thalamus and a dense dopaminergic innervation from midbrain nuclei.
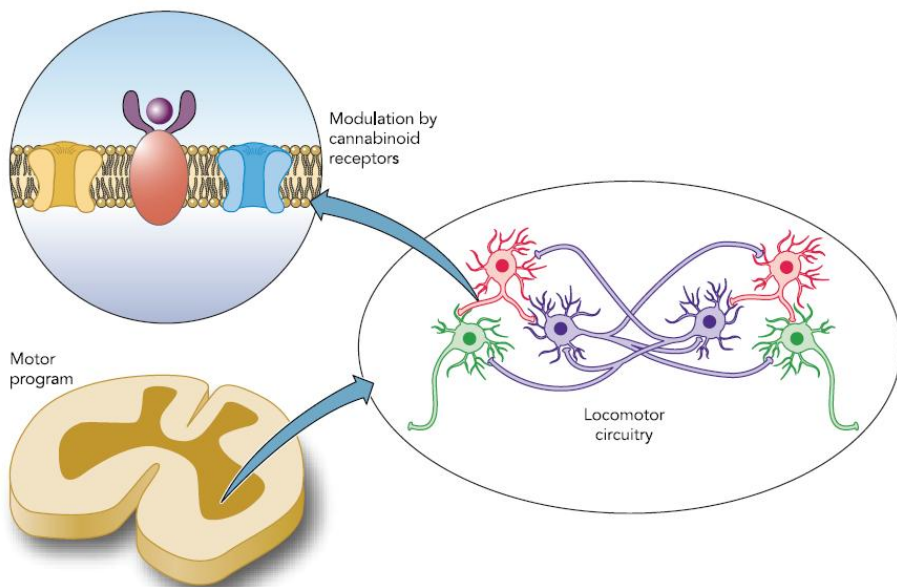
Figure 4: Levels of analysis of neural circuits controlling motor behavior. A defined motor behavior is generated by networks of excitatory and inhibitory neurons. The activity of the neurons and their synaptic interactions is modulated by G-protein-coupled receptors that can be activated by endocannabinoids. Taken from: *El Manira and Kyriakatos*, 2010.

The vast majority of neurons in the striatum are GABAergic medium spiny neurons (MSNs), with a few cholinergic and other GABAergic interneurons. The excitatory input to MSNs displays a strong activity-dependent plasticity in the form of LTD and long-term potentiation (LTP). The striatal LTD requires the elevation of Ca^{2+} levels in postsynaptic neurons and a convergence of modulatory inputs activating group I mGluRs and dopamine receptors D2 (*Kreitzer and Malenka*, 2008; *Surmeier et al.,* 2009). This combination of several signals leads to release of eCBs from MSNs that act retrogradely to depress synaptic transmission from excitatory terminals. The treatment with eCB degradation inhibitors in animals with depleted dopaminergic innervation significantly enhanced

locomotor activity. These results provide evidence that eCB-mediated synaptic plasticity in the striatum can be important in controlling motor function. However, it should be noted that eCB signaling cannot alone be responsible for balancing the activity of the direct and indirect pathways because other mechanisms are also necessary for the normal function of the basal ganglia circuitry and selection of motor behavior (*Surmeier et al.,* 2009).

Finally, the cerebellum plays an important role in fine-tuning of motor behavior and in learning of new motor tasks, contributes to the precision and smooth execution of motor tasks, and furthermore mediates motor learning in the vestibulo-ocular reflex pathway (*Ito*, 1972). Purkinje cells are the only output from the cerebellar cortex and project to the deep cerebellar nuclei. Each Purkinje cell receives excitatory inputs from many parallel fibers arising from granule cells and from a single climbing fiber originating in the inferior olive. Excitatory synaptic transmission to Purkinje cells displays both short and long-term changes that depend on release of eCBs and activation of CB1 receptors. eCBs have been shown to mediate depolarization-mediated suppression of both inhibitory and excitatory synaptic transmission to Purkinje cells (*Diana et al*., 2002; *Kreitzer and Regehr*, 2001; *Yoshida et al*., 2002).

Although endocannabinoid-mediated plasticity has been studied extensively in the cerebellum, very little is known about its significance for cerebellar function and motor behavior. To understand the function of endocannabinoid-mediated plasticity in terms of motor function, the analysis needs to be broadened from single synapses to circuit operation and ultimately to behaviorally relevant tasks.

2.5 ECS and Vision

In the last decade, there has been a growing interest for eCBs in the retina and their role in visual processing and perception, and recent reports suggest that the ECS could play an instrumental role at all levels of the visual system. But the vast majority of these studies focused on the expression and functions of the ECS in the adult retina and visual system, and only a few investigated the expression and functions during embryonic development.

Physiological and biochemical studies demonstrated the presence of the ECS in various ocular tissues. The presence of different eCBs and the expression profiles of CB1 and CB2 receptors in the adult retina of various species are summarized in Tables 1, 2 and 3.

Most of the studies comparing AEA to 2-AG expression in the adult retina concluded that 2-AG levels are significantly higher than AEA (*Chen et al*., 2005; *Bisogno et al*., 1999), and found that the content of eCBs varies in certain disease states, suggesting the importance of eCBs in maintaining ocular homeostasis (*Chen et al*., 2005; *Matias et al*., 2006).

In the retina and in the primary visual cortex, cannabinoids act inhibiting the release of various neurotransmitters. Indeed, it has been found that CB1 receptor agonists decrease the release of noradrenaline and dopamine *via* a Gi/o-dependent mechanism (*Schlicker et al*., 1996; *Weber and Schlicker*, 2001; *Savinainen and Laitinen*, 2004), and can regulate the glutamate release in photoreceptors and bipolar and ganglion cells (*Yazulla*, 2008). Some evidence also suggests a regulatory effect on GABA$_A$ receptor-mediated inward currents by CB1/CB2 receptor agonists in amacrine cells (*Warrier and Wilson*, 2007). Moreover, *in vivo* electrophysiological studies

indicate that CB2 receptor appears to cause changes light responses in the mouse retina (*Cécyre et al*., 2013).

Taken together, these various effects may suggest a possible cannabinoid-mediated tone in transmitter release.

So far, few studies have looked at the effects of eCBs on retina development. Most works are based on the study of the expression profile of different eCBs receptors and metabolic enzymes in different animal species, and few others showed the functional impact of cannabinoids on retinal development.

It has been reported that CB1 and CB2 receptor specific agonists induce a collapse of the growth cone of retinal ganglion cells and decrease axon growth (*Argaw et al*., 2011; *Duff et al*., 2013). Conversely, the application of CB1 and CB2 receptor specific inverse agonists increases the growth cone surface area and the number of filopodia present on the growth cone and increases axon growth.

GPR55 also modulates growth rate and target innervation of retinal projections during development. For instance, the application of GPR55 agonists increases the growth cone surface area and the number of filopodia and also triggers axon growth (*Cherif et al.*, 2013).

Furthermore, $gpr55^{-/-}$ mice revealed a decreased branching in the dorsal terminal nucleus and a lower level of eye-specific segregation of retinal projections. Altogether, these studies identify a mechanism by which the ECS modulates retino-thalamic development and offer a potential model to explain why cannabinoid agonists affect CNS development.

In summary, CB1 and CB2 receptors are both present in various retinal tissues where they modulate neurotransmitter release in the most part *via*

retrograde signaling, and where they inhibit potassium and calcium currents. These effects can thus modulate visual activity as early as at the retina level. More studies are obviously needed to assess to what extent a cannabinoid-mediated modulation in the retina could impact visual perception. This is especially true given that cannabinoid receptors are present in most retinal cell types. As cannabinoids are also present in the visual cortex, it may well be that cannabinoids modulate visual perception at each level of visual system hierarchy.

Furthermore, as it has been previously demonstrated in the CNS, cannabinoids play an important role in neuronal development and axon guidance. It would now be of interest to see if a similar variation in the concentration of receptors, enzymatic machinery, and endogenous ligands occur also during retinal development.

Table 1: Endocannabinoid levels in the adult retina of various species.

Endocannabinoids	Concentration (pmol/g)	Species
2-arachidonoyl glycerol (2-AG)	2,970 1,393 1,600	Rat Human Bovine
Anandamide (AEA)	Under detection level 36 64	Rat Human Bovine
Palmitoylethanolamide (PEA)	130 200	Rat Human
Oleoylethanolamide (OEA)	55	Rat

Table 2: Cannabinoid receptor type 1 protein distribution in the adult retina of various species.

Retinal cell types	Sub-cellular localization
Photoreceptors	Expression in the inner and outer segments Strong labeling in the cone pedicles
Horizontal cells	Expression in the membrane but not in dendrites
Bipolar cells	Expression in the dendrites, cell body, and axons of rod bipolar cells
Amacrine cells	Expression in amacrine cells, including GABAergic amacrine cells
Inner plexiform layer	Unspecified expression in the IPL Expression in the synapses of rod bipolar cells Higher expression in the synapses of ON cone bipolar cells compared to OFF cone bipolar cells
Ganglion cells	Expression in the cell body and fibers
Müller cells	Absence of expression Expression in the goldfish retina only

Table 3: Cannabinoid receptor type 2 protein distribution in the adult retina.

Retinal cell types	Sub-cellular localization
Photoreceptors	Expression in the outer and inner segments of cones Absence of expression in cone pedicles Expression in the inner and outer segments and cell body of rods
Horizontal cells	Expression at the membrane of the soma and in horizontal cells, dendrites
Bipolar cells	Expression in the membrane of the soma and axons of rod bipolar cells Expression in the membrane of the soma of cone bipolar cells
Amacrine cells	Expression in some subtypes
Ganglion cells	Expression in the soma
Müller cells	Absence of expression at the membrane of the soma, in Müller cells, inner and outer processes Expression in Müller cells' processes in the vervet monkey only

Tables 1-2-3: Adapted from: *Bouchard et al.*, 2015.

3. Zebrafish as Experimental Model

Danio rerio, better known as zebrafish, is a small tropical fresh water fish, belonging to the Cyprinidae family and native to the Gange region in eastern India. It commonly inhabits streams, canals and other slow moving or stagnant water bodies but it is also widely sold as an aquarium fish (*Mayden et al.* 2007). It is so called because of a characteristic pattern of blue-black horizontal stripes that run along the body and in the anal and tail fins.

Zebrafish reach sexual maturity at around three months of age and exhibit sexual dimorphism, with the female characterized by a larger belly and the male by its comparative slimness and a more yellowish hue (Fig. 5).

Ever since George Streisinger pioneered his research using zebrafish in Eugene, at the University of Oregon in 1972, this fish species has become a great animal model both in basic and biomedical research.

Figure 5: Adult male (left) and female (right) zebrafish.

Being a vertebrate, zebrafish share a high degree of genomic sequence and functional homology with mammals, including humans. Due to the conservation of cell biological and developmental processes across all vertebrates, studies in fish can help understanding protein functions and human disease processes. However, the genetic similarity to mammalians is not the only relevant reason to choose zebrafish as research model. A leading motive is for sure the optical transparency of zebrafish embryos, making them ideally suited for microscopic imaging of live processes. The fertilization of eggs is external, avoiding animal sacrifice as in case of murine models, and, in each spawn, zebrafish give a large number of offspring (200 embryos per mating) that develop relatively fast, ensuring a big and ready supply of animals for research purposes.

Fluorescent markers can be also used to 'light up' different cells and organs in the embryo giving the possibility to follow the impact of a genetic manipulation or pharmacological treatment using non invasive imaging techniques. Importantly, many simple and highly efficient genetic manipulation techniques have been developed (like zinc-finger, TALEN, CRISPR/Cas9, TOL-2), that allow targeted mutagenesis or generation of transgenic lines.

Moreover, zebrafish embryos are able to absorb many chemicals by simple dissolution of them in the embryo medium, thus representing a useful tool for drug screenings.

Zebrafish can thus contribute significantly to meeting the challenge of the post-genome sequencing era to understand gene function on a global scale. Its value as model has been further increased significantly by parallel

developments in microscopy technologies, which now allows us imaging intact live embryos at subcellular resolution.

Another reason for the popularity of the zebrafish among the developmental biologists is the rapid development of its transparent embryos (Fig. 6).

Cell divisions begin soon after the fertilization process and, during the blastula period, epiboly takes place, when cells proliferate, thinning and starting to coat the yolk. This stage ends at 30% epiboly. Epiboly goes on with the following period of gastrula stage, ranging from 5 to 10 hours post fertilization (hpf). During this developmental stage, cell induction movements of convergence and extension take place, leading to the formation of mesoderm, ectoderm and endoderm. It is also possible to recognize the anterior (that will generate the head) from the posterior (that will generate the tail) part of the main body axis, the ventral from the dorsal and medial tissue from the lateral ones. This stage is followed by the segmentation period, so called because of segmentation of the nervous system. Furthermore, the formation of somites, which are the structures giving rise to the trunk muscles, and sketches of the different organs are also evident. Embryo is fully transparent up to 22 hpf, by which stage, the melanocytes start to differentiate and the embryo begins to be pigmented. Movements are irregular and non-controlled. Major organ systems are formed over the next 24 to 36 hours. In the pharyngula period (24-48 hpf), the formation of the pharynx occurs, the head is extended and the pectoral fins are formed. The hatching period is the last embryonic phase, when the embryo exits the chorion (membrane surrounding the zygote) and the embryonic development is completed. After hatching, the embryo becomes

a free-swimming larva wherein all anatomical structures are fully established (*Kimmel et al*., 1995).
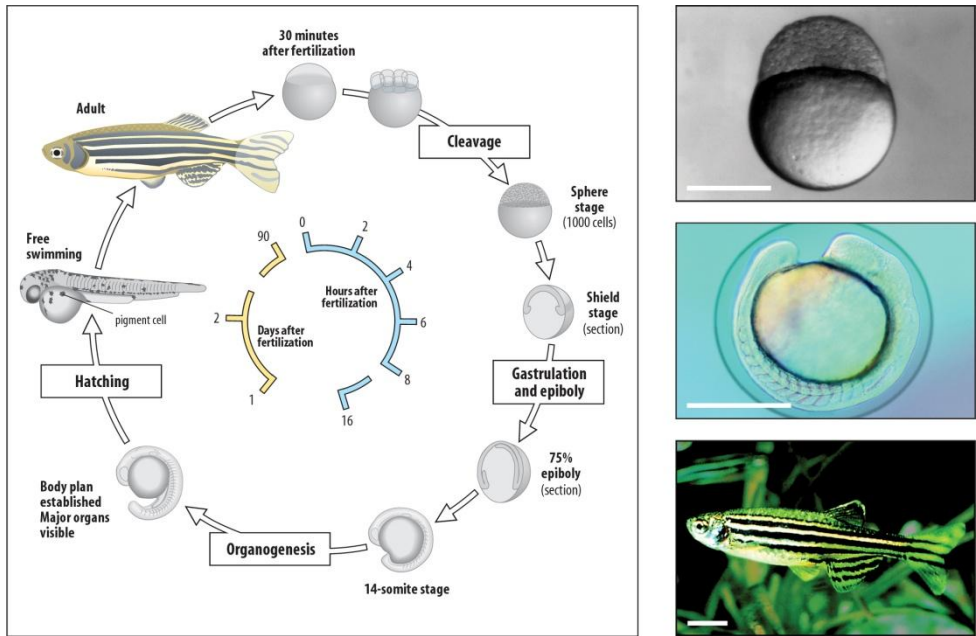
Figure 6: Stages of zebrafish development.

3.1 Neurogenesis in Zebrafish Embryos

Neurogenesis describes the process by which undifferentiated neural progenitor cells generate mature and functional neurons. The first steps in neurogenesis are the induction of neural progenitors and a phase of cell division that enlarges the pool of progenitors. This is followed by a sequence of events leading to specification of committed progenitors, and differentiation of post-mitotic neurons. Each of these steps is spatially and temporally orchestrated to generate the multiple neuronal and glial cell types that will eventually populate the mature CNS. The zebrafish has proven to be an excellent model organism to study neurogenesis, providing many contributions in neural development.

The first phase in the development of the vertebrate nervous system is called "neural induction" and is initiated during early embryonic development. At the onset of gastrulation, the forming mesodermal layer involutes and comes into contact with the overlying ectoderm, inducing or inhibiting neural induction in the ectodermal layer (*Doniach and Mushi*, 1995; *Lumsden and Krumlauf*, 1996; *Spemann and Mangold*, 2001; *Streit et al.*, 2000), due to complex interactions between extrinsic (*e.g.* bone morphogenetic protein, BMP; wingless/integrated, Wnt; fibroblast growth factor, Fgf) and intrinsic factors (*e.g.* SRY-box containing genes B1 family, SoxB1) (*Streit et al.*, 1997; *Avilion et al.*, 2003). Once specified, the neural ectoderm forms the neural plate, a pseudostratified epithelial structure in zebrafish. During the process of neurulation in zebrafish, unlike other vertebrates, the neural plate forms a solid neural keel instead of folding up immediately into a tube with a lumen. However, the topological arrangement of cells in zebrafish during formation of the neural

keel from the neural plate is similar to that of other vertebrates. In the so-called "secondary neurulation", the fish neural rod inflates and forms a typical vertebrate tube. Thus, although there are differences between mammals and fishes, neurulation leads to the formation of a highly similar structure: the neural tube (*Papan et al.*, 1999). Three primary vesicles develop in the rostral portion of the neural tube: the prosencephalon (forebrain), mesencephalon (midbrain) and rhombencephalon (hindbrain). The caudal neural tube remains undifferentiated and will form the mature spinal cord. Secondary vesicles emerging from the prosencephalon give rise to the telencephalon (cerebral hemispheres) and diencephalon (thalamus and hypothalamus) (Fig. 7). The fish brain represents the anterior portion of the CNS: (antero-posteriorly) from a forebrain region (telencephalon and diencephalon), through the midbrain with its swellings (optic lobes), to the hindbrain (cerebellum and medulla). Subsequently, the CNS continues toward the caudal fin with the spinal cord. The mesencephalon or midbrain of fishes is relatively large; it consists of the optic tectum dorsally, appearing in dorsal view as two optic lobes, and the tegmentum ventrally (*Lagler et al.*, 1967).
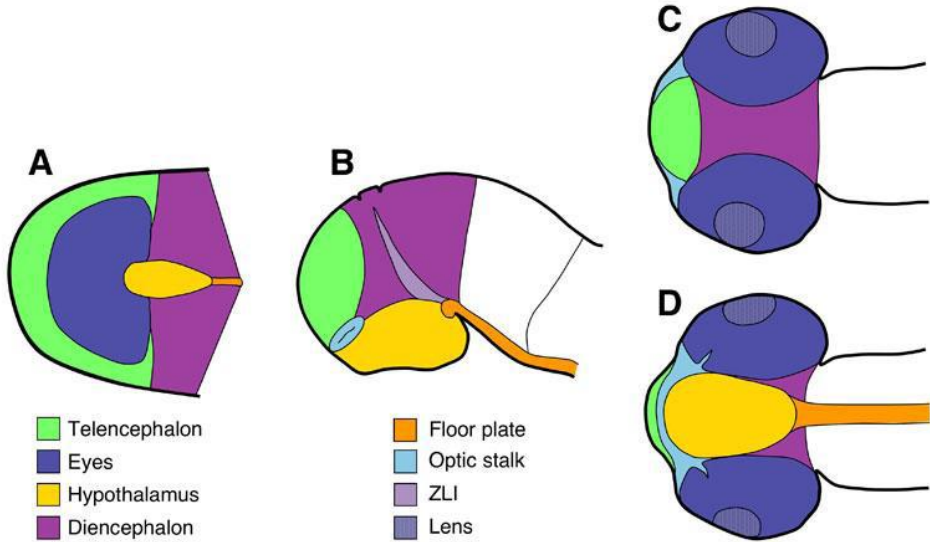
Figure 7: Zebrafish central nervous system. (A) Organization of the brain territories at neural plate stage. The groups of cells giving rise to each territory are shown in different colors. (B-D) The same color code is used to show the relative positions of the different territories in embryonic brains at a later stage of development, from lateral (B), dorsal (C) and ventral (D) views. Taken from *Cavodeassi et al.*, 2009.

3.2 Development of the Zebrafish Motor Behavior

Developmental patterns of network organization, including that of the locomotor network, are common among all vertebrates (*Butler and Hodos, 1996; Stein et al.,* 1997). Cellular and molecular principles and mechanisms underlying neuronal specification by transcription factors (*Jessel,* 2000) and axon guidance (*Tessier-Lavigne,* 1996) during early development have also been revealed.

The zebrafish is a useful model for developmental studies and, especially, offers the possibility of studying the developmental genetics of the locomotor network in the living embryos (*Brustein et al.,* 2003). The motor activity of the developing zebrafish changes and newly appearing behavioral traits are specific to different developmental stages. The stereotypic movements of developing zebrafish include three subsequent phases (Fig. 8):

- a transient period of alternating coilings (~17 hpf), which exhibits two types of network-driven episodic activity. The first one represents a periodic depolarization that trigger action potentials and generate coils, while the second one originates bursts of glynergic inputs (synaptic events). However, the role of these bursts at this stage has not yet been clarified (*Saint-Amant and Drapeau,* 2000*; Brustein et al.,* 2003).

- a touch response (~21 hpf), characterized by an over-the-head and fast coiling of the trunk. This was suggested as the embryonic manifestation of the mature escape response (*Saint-Amant and Drapeau*, 1998; *Eaton et al.*, 2001; *Brustein et al.*, 2003).

- finally, the appearance of organized swimming, in which the swimming rate increases gradually. Newly hatched larvae (two-three days post

fertilization, dpf) are generally inactive, with only occasional episodes of spontaneous "burst" swimming, and by three-four dpf the larvae switch to a "beat-and-glide" mode of swimming (*Saint-Amant and Drapeau*, 1998; *Buss and Drapeau*, 2001; *Brustein et al.*, 2003).
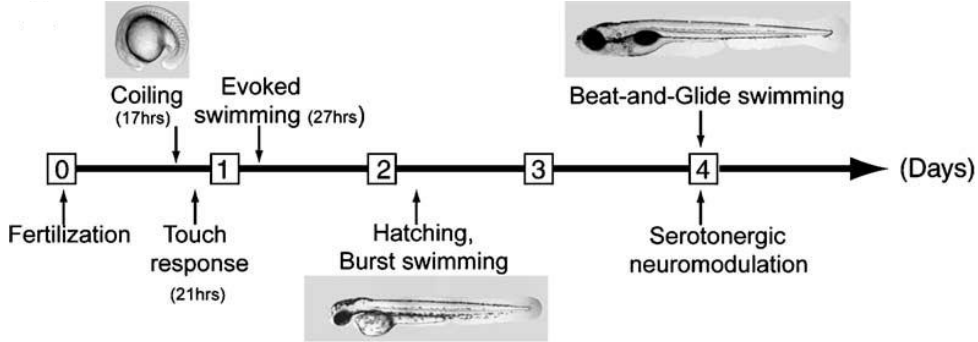
Figure 8: The chronological sequence of the appearance of motility patterns during development of the zebrafish. Taken from *Brustein et al.*, 2003.

3.3 Neurogenesis in the Zebrafish Retina

As in other vertebrate species, the zebrafish retina is simpler than other regions of the central nervous system. This relative simplicity along with rapid development, and accessibility to genetic analysis make the zebrafish retina an excellent model system for studies of neurogenesis in the vertebrate CNS.

The remarkable evolutionary conservation of the vertebrate eye provides the basis for using the zebrafish as a model system for the detection and analysis of genetic defects potentially related to human eye disorders. In fact, the zebrafish possesses a canonical vertebrate retina (Fig. 9) composed of one glial cell type (Müller glia) and six neuronal cell types distributed in three nuclear layers separated by two synaptic (plexiform) layers already apparent at 3 dpf.
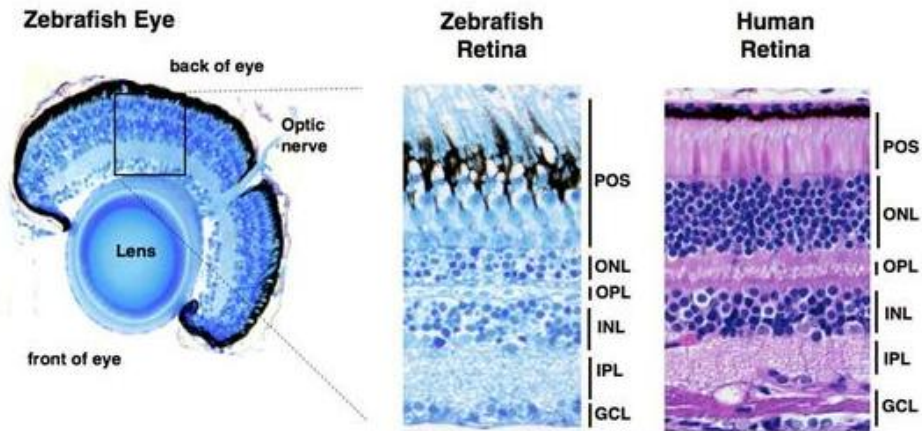
Figure 9: Similarity between the zebrafish and the human retina layers.

An important advantage of the zebrafish retina for genetic and developmental research is that it forms and becomes functional very early in development, indeed it is essentially complete by 60 hpf (*Nawrocki*, 1985) and, as judged by the startle and optokinetic responses, the zebrafish eye detects light stimuli surprisingly early, starting between 2.5 and 3.5 dpf (*Clark*, 1981; *Easter and Nicola*, 1996).

The optic lobes become evident during neurulation (12.5 hpf) as bilateral thickenings of the anterior neural keel, that gradually become more and more prominent and protrude laterally on both sides of the brain (*Schmitt and Dowling*, 1994) (Fig. 10 A-C).

At approximately 13 hpf, the posterior portion of the optic lobe starts to separate from the brain, while its anterior part remains attached, forming later the optic stalk (Fig. 10 D). As its morphogenesis advances, the optic lobe turns around its antero-posterior axis so that its ventral surface becomes directed toward the brain while the dorsal surface starts to face the outside environment (Fig. 10 G).

At ca. 15 hpf, cells migrate from the medial to lateral epithelial layer of the optic lobe (Fig. 10 G) (*Li et al*., 2000). The medial layer becomes thinner and subsequently differentiates as the retinal pigmented epithelium (RPE) (Fig. 10 H-K). At about the same time, an invagination forms on the lateral surface of the optic lobe (*Schmitt and Dowling*, 1994), accompanied by the appearance of the lens rudiment.

Subsequently, over a period of several hours, both the invagination and the lens placode become increasingly more prominent, transforming the optic lobe into the optic cup (Fig. 10 J-L).
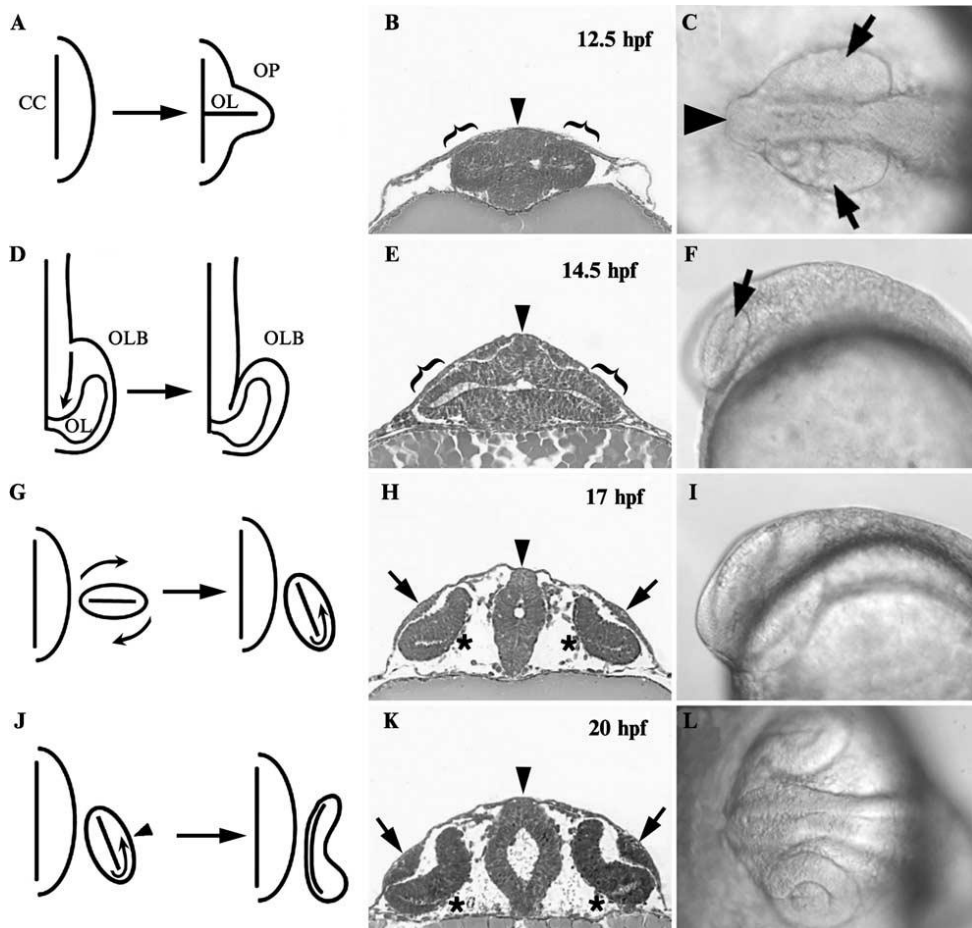
Figure 10: Early morphogenetic events leading to the formation of the optic cup. Taken from: *Avanesov and Malicki*, 2004.

Starting at about 24 hpf, melanin granules appear in the cells of the pigmented epithelium, and at the beginning of day 2, the optic cup consists of two closely connected sheets of cells: the pseudostratified columnar neuroepithelium (RNE) and the cuboidal pigmented epithelium (PE) (Fig.11 A) (*Kimmel et al.*, 1995; *Schmitt and Dowling*, 1994). The optic stalk gradually becomes less prominent and provides support for the axons of ganglion cells that begin to differentiate.

Lastly, the optic cup rotates around its mediolateral axis, and this rotation is the final major morphological transformation in zebrafish eye development (72 hpf), with the complete differentiation of the optic nerve (*Macdonald et al*., 1997).
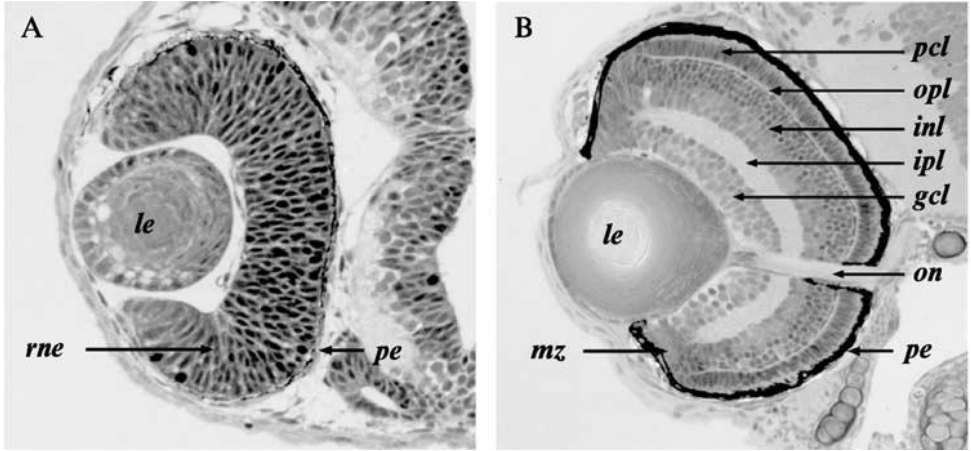
Figure 11: Neurogenesis in the zebrafish retina. (A) A section through the zebrafish eye at approximately 36 hpf, when the retina mostly consists of two epithelial layers: the pigmented epithelium and the retinal neuroepithelium. (B) A section through the zebrafish eye at 72 hpf, when neurogenesis is mostly completed. The major nuclear and plexiform layers, as well as the optic nerve and the pigmented epithelium, are well differentiated. gcl: ganglion cell layer; inl: inner nuclear layer; ipl: inner plexiform layer; le: lens; mz: marginal zone; on: optic nerve; opl: outer plexiform layer; pcl: photoreceptor cell layer; pe: pigmented epithelium; rne: retinal neuroepithelium. Taken from: *Avanesov and Malicki*, 2004.

As the morphogenetic movements that shape and orient the optic cup come to completion, the first retinal cells become postmitotic and begin to differentiate. Gross morphological characteristics of the major retinal cell classes are very well conserved in all vertebrates. Six major classes of neurons arise during neurogenesis together with the Müller glia: ganglion,

amacrine, bipolar, horizontal, interplexiform, and photoreceptor cells, taking place in different layers of the retina (Fig. 12).
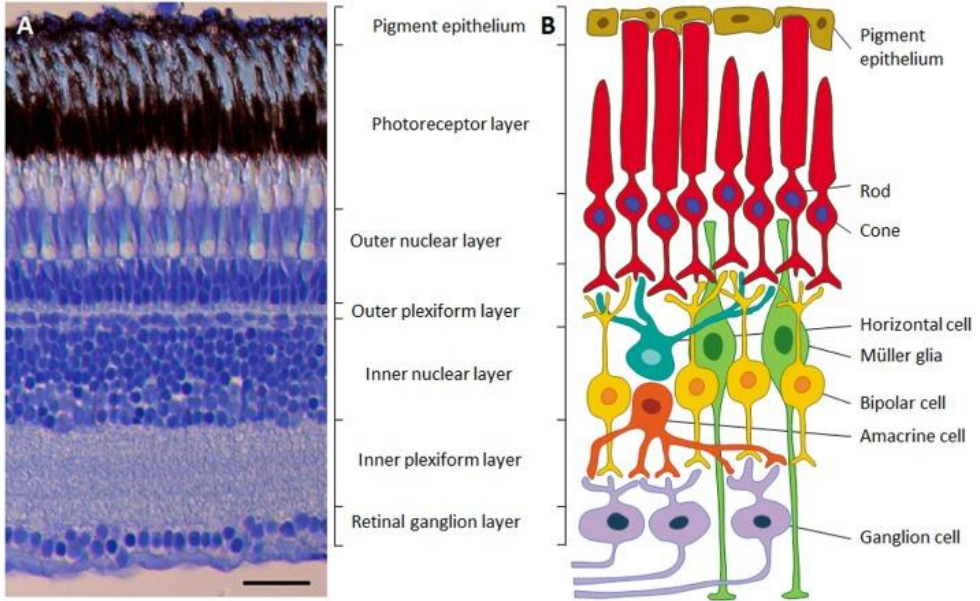
Figure 12: Structure of the retina. A: Microphotograph of a cross-section through the retina of an adult zebrafish, showing the different cellular and synaptic retinal layers. B: Diagram of the neural circuit of the retina, showing the six neuronal cell-types and the two supporting cell types (Müller glia and retinal pigmented epithelium). Taken from: *Gramage et al*., 2014.

The neuronal network of the retina is largely self-contained. The only retinal neurons that send their projections outside are ganglion cells. At ca. 36 hpf, their axons start to exit the eye and navigate through the midline of the ventral diencephalon into the dorsal part of the midbrain, the optic tectum (*Burrill and Easter*, 1995; *Macdonald and Wilson*, 1997).

After crossing the midline, the axonal projections of ganglion cells split into the dorsal and ventral branches of the optic tract. The ventral branch contains mostly of axons of the dorsal retinal ganglion cells, the dorsal

branch being mostly composed of axons of the ventral retinal ganglion cells (*Baier et al.*, 1996). The growth cones of retinal ganglion cells first enter the optic tectum between 46 and 48 hpf, when the spatial coordinates of retina and tectum are reversed. The ventral-nasal ganglion cells of the zebrafish retina project to the dorsal-posterior optic tectum; whereas the dorsal-temporal cells innervate the ventral-anterior tectum (Fig. 13) (*Stuermer*, 1988; *Karlstrom et al.*, 1996; *Trowe et al.*, 1996). By 72 hpf, axons from all quadrants of the retina are in contact with their target territories in the optic tectum. Moreover, zebrafish have topographic tectal afferents connecting directly from the zebrafish cerebellum. The deep layers of the tectum have topographic outputs to the hindbrain and can send output commands to motor centers, initiating swimming, hunting, and escape behaviors with respect to the location of the stimuli. In this manner, the tectum combines sensory inputs and rapidly generates survival behaviors in response to visual stimuli.
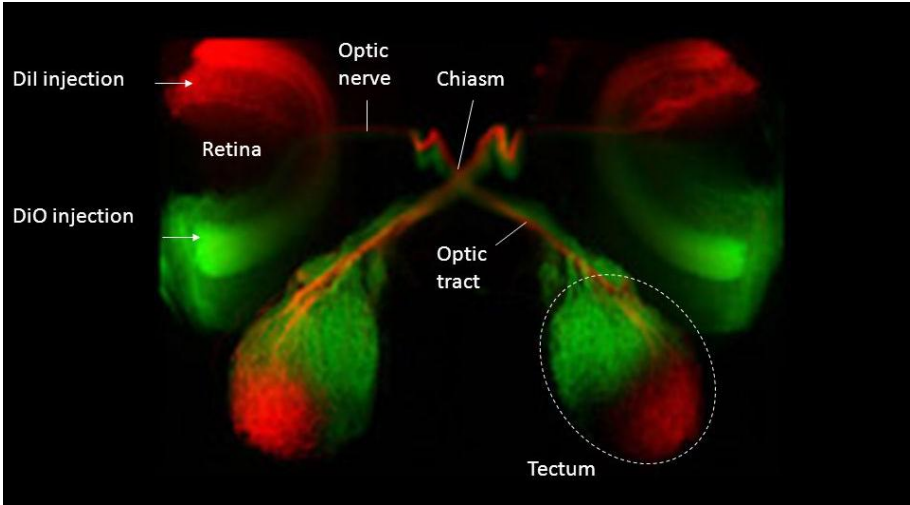
Figure 13: Representation of zebrafish retinotectal projections.

3.4 Zebrafish to Study the ECS

The complexity of how eCB signaling regulates the activity of circuits within the CNS is further obscured by the promiscuous signaling dynamics that are characteristic of this system. Numerous genes have been identified that provide alternate routes of eCBs degradation or synthesis, thereby resulting in region-specific ligand signaling profiles (*Ahn et al*., 2008; *Di Marzo*, 2011). Moreover, in addition to cannabinoid receptor 1 and cannabinoid receptor 2, eCBs bind to many non-CB receptors, that comprise a complex multipartite signaling system where a host of ligands bind to multiple receptors with differential affinities (*Alexander and Kendall*, 2007). Finally, the effects of eCBs receptors signaling depend on the specific cell type involved, which may be associated with opposing outcomes such as the inhibition or excitation of a neural circuit.

These complicated dynamics that define eCBs signaling, coupled with the increasing use and development of exogenous CBs that differentially target this system, mandates scientific investigation of the toxicological and therapeutic potential of altered CB signaling. To this end, many research groups have sought to use the unique advantages of different model organisms to further explore eCB biology. Although the bulk of eCB literature published to date consists of experiments using *in vitro* approaches or rodent models, zebrafish have recently gained traction as a powerful *in vivo* model for complementing and expanding upon the findings of these existing studies. One useful application of zebrafish is pharmacological screening in a whole vertebrate system, well suited for rapidly assessing the effects of exogenous CB exposure.

Zebrafish are able to absorb small molecules across the skin from the surrounding water at all stages of development and even in adulthood. In addition, the fecundity of adult mating pairs, which can produce clutches of several hundred offspring per week, readily enables high-throughput screening.

Due to the diverse scope of physiological processes that involve eCB signaling, zebrafish could be also used to identify novel therapeutic strategies. Exogenous CBs could be screened using disease models to identify compounds that corrected the pathological phenotypes of interest.

Moreover, zebrafish are highly amenable to genetic manipulation, and are well suited for both reverse and forward genetic screening applications, representing an additional tool for the investigation of individual ECS gene functions.

In recent years, developments in genome editing techniques have enabled precise and highly efficient modification of the zebrafish genome (*Blackburn et al*., 2013). Custom nuclease technology such as transcription activator-like effector nucleases (TALENs) and clustered regularly interspersed short palindromic repeat/Cas9 (CRISPR/Cas9) may be used for targeted mutagenesis of loci *via* non-homologous end joining, or the incorporation of new sequences using small single stranded oligonucleotide donors for homology directed repair (*Blackburn et al*., 2013; *Campbell et al*., 2013). This technology has provided an accessible methodology for studying the roles of individual genes in the zebrafish model. With regard to eCB biology, establishing zebrafish lines with mutations in individual genes will be indispensable for studying their

function in this organism, which could be obscured by the potential off-target effects associated with pharmacological investigations.

Although zebrafish can significantly advance the understanding of eCBs biology with the use of pharmacological or genome editing approaches, the greatest contribution of this small model verterbate to the field will likely result from studies enabled through combined approaches (Fig.14).

Any observed alterations in physiology or behavior could then be linked to specific molecular signaling cascades, which could be ideally analyzed with the use of comprehensive methodologies such as RNA sequencing and behavioral assays.

Phylogenetic analyses of the zebrafish ECS have demonstrated that it is highly conserved with the mammalian counterpart, and ontogenetic analyses have revealed that ECS gene expression begins early in zebrafish development. In addition to the conservation of ECS genes themselves, many of the zebrafish ECS gene expression patterns also appear to be homologous. For instance, *cnr1* and *dagla* are co-expressed in the zebrafish brain (*Watson et al*., 2008) and exhibit homologies with rodent distribution patterns as early as 2 dpf, which are maintained into adulthood (*Lam et al*., 2006; *Ahn et al*., 2008).

For these reasons, zebrafish have already been used to study eCBs biology in diverse contexts including addiction, anxiety, development, energy homeostasis and food intake, immune system function, and learning and memory (summarized in Table 4). Nevertheless, the only study on zebrafish neural development was performed by Watson *et al.* (2008), showing that knockdown of *cnr1* gene activity by morpholino antisense oligonucleotides resulted in defects of axonal growth and fasciculation.
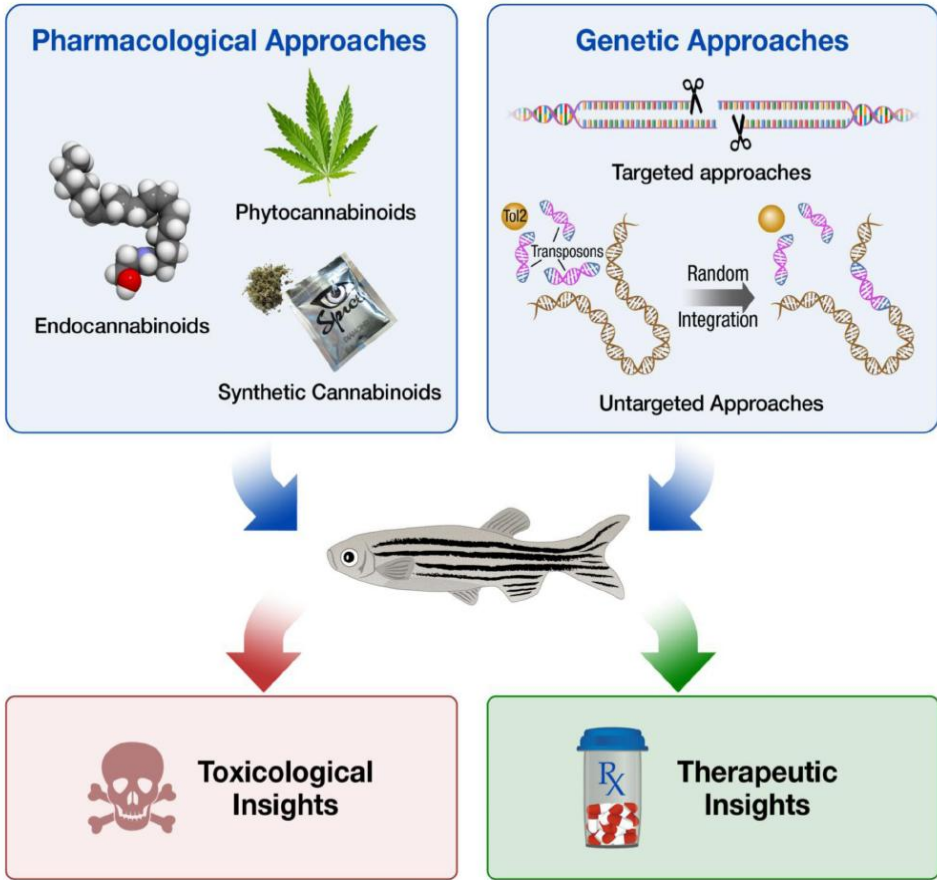
Figure 14: Strategies for providing toxicological and therapeutic insights about cannabinoid biology using zebrafish. Taken from: *Krug II et al.*, 2015.

Table 4: Summary of Zebrafish Endocannabinoid Gene Function Studies

eCB Gene Function Studies	Zebra fish Ages	Pharmacological Approaches	Genetic Approaches	Key Experimental Endpoints
Addiction				
Braida et al., 2007	Adult	SR141716A (sCB)	NA	Locomotor Activity, & Conditioned Place Preferences
Anxiety				
Barba-Escobedo & Gould, 2012	Adult	WIN55212-2 (sCB)	NA	Visual Social Choices
Connors et al., 2014	Adult	WIN55212-2 (sCB)	NA	Light-Dark Plus Maze Behaviors
Ruhl et al., 2014	Adult	Δ9-THC (pCB)	NA	Locomotor Activity, & Escape Responses
Stewart & Kalueff, 2014	Adult	Δ9-THC (pCB)	NA	Assorted Spatiotemporal Behavioral Parameters
Development				
Akhtar et al., 2013	Juvenile	Δ9-THC (pCB), AM251 (sCB), CP55940 (sCB), & WIN55212-2 (sCB)	NA	Morphology, & Mortality Locomotor Activity, & Visual Motor Responses
Migliarini & Carnevali, 2009	Juvenile	AM251 (sCB)	NA	Morphology, & Hatching Rates Locomotor Activity
Thomas, 1975	Juvenile	Δ9-THC (pCB)	NA	Morphology, & Mortality Spontaneous Tail Muscle Twitches
Watson et al., 2008	Juvenile	NA	*cnr1* Knockdown (Whole Organism)	Axonal Outgrowth, & Fasciculation
Energy Homeostasis & Food intake				
Migliarini & Carnevali, 2008	Juvenile, & Adult	AEA (eCB), & AM251 (sCB)	NA	CB1, IGF1, IGF2, & SREBP mRNA Expression
Nishio et al., 2012	Juvenile,	SR141716A (sCB,) & WIN55212-2 (sCB)	*cnr1 & cnr2* Knockdown (Whole Organism)	CB1, & CART1–3 mRNA Expression Yolk Sac Size, & Lipid Metabolism

eCB Gene Function Studies	Zebra fish Ages	Pharmacological Approaches	Genetic Approaches	Key Experimental Endpoints
Pai et al., 2013	Juvenile, & Adult	AEA (eCB), & AM251 (sCB)	cnr1 Overexpression (Hepatic)	Lipotoxic, & Lipogenic Markers Lipid Metabolism, & Liver Morphology
Piccinetti et al., 2010	Adult	NA	NA	CB1 mRNA, & Protein Expression Food Intake
Shimada et al., 2012	Juvenile	SR141716A (sCB,)	cnr1 Knockdown (Whole Organism)	Locomotor Activity, & Food Intake
Silvestri et al., 2015	Juvenile	Δ9-THCV (pCB), & CBD (pCB)	NA	Lipid Metabolism
Immune System Function				
Liu et al., 2013	Juvenile	JWH-015 (sCB), & WIN55212-2 (sCB)	cnr2 Knockout (Whole Organism)	Alox5, & JNK Signaling Leukocyte Inflammatory Migration
Learning & Memory				
Ruhl et al., 2014	Adult	Δ9-THC (pCB)	NA	Telencephalic Akt, & Erk Phosphorylation Associative, & Spatial Memory

Taken from: *Krug II et al*., 2015.

4. THESIS AIMS

The endocannabinoid system (ECS) comprises neuromodulatory lipids and their receptors, capable of regulating neuronal excitability. It is involved in a variety of physiological processes and in specific brain functions, such as nociception, control of movement, memory and neuroendocrine regulation. Recently, it has also been suggested that the ECS may play an important role in early neuronal development, regulating neural progenitor proliferation, differentiation and specification. Because of redundancy and promiscuity that characterize this system, it becomes indispensable to establish roles, functions, and contributions of single genes involved in ECS. The vertebrate *Danio rerio* represents a valid model system to study eCB biology, since phylogenetic analyses of the zebrafish ECS have demonstrated that it is highly conserved with the mammalian counterpart. For this reason the first goal of my PhD thesis was to evaluate the spatial-temporal expression profiles of different ECS genes during zebrafish development. Moreover, since the 2-arachidonoylglycerol (2-AG) is synthesized at high levels in CNS by diacylglycerol lipase α (Daglα), the second objective was to investigate the role of 2-AG in the development and differentiation of neurons, and in the formation of neuronal circuits that control spontaneous locomotion and visual system in zebrafish embryos.

Particularly, considering the key role of eCB signalling during neurogenesis, we hypothesized that *daglα* downregulation could affect axonal pathfinding during zebrafish embryogenesis, as it has been demonstrated in previous studies on *cnr1*, the CB1 coding gene (*Watson et al.*, 2008). In this thesis work, our hypothesis is that the alteration of the

function of the 2-AG synthesis enzyme can produce similar effects in terms of alterations of the axonal phenotype, revealing as well unexplored aspects of the 2-AG during vertebrate neurogenesis.

Finally, the third purpose of this work was to highlight the role of 2-Ag and its main receptors (CB1 and CB2) in the correct differentiation and lamination of zebrafish neuroretina, and in the correct formation of retinotectal system. Moreover we intended to understand if CB1 and CB2 receptors could also direct the correct formation of neuronal circuits that control spontaneous locomotion during zebrafish embryogenesis.

In summary, in the present work we aimed to:

- characterize the spatial-temporal expression profiles of ECS genes during zebrafish development by qPCR and *in situ* hybridization;
- inhibit the 2-AG synthesis in zebrafish embryos by morpholino-induced knockdown for Daglα;
- reveal disorganization of neurons in defined area of the brain by acetylated tubulin immunostaining;
- test the role of 2-AG in swimming behaviour by locomotor assays and in visual sensitivity by oculomotor analysis;
- rescue of the morphant phenotype by administration of a 2-AG analog;
- analyze the role of Daglα, CB1 and CB2 in correct formation of neuroretina and retinotectal system by using morpholino and pharmacological treatments in zebrafish transgenic lines;
- test the role of these two receptors also in swimming behaviour by locomotor assays.

5. RESULTS

The complexity of how eCB signaling regulates the activity of nerve circuits within the central nervous system is further obscured by the fact that numerous genes have been identified that provide alternate routes of eCBs degradation or synthesis, thereby resulting in region-specific ligand signaling profiles (*Ahn et al*., 2008; *Di Marzo*, 2011). Moreover, the effects of CB receptor signaling depend on specific cell types involved, which may be associated with opposing outcomes such as inhibition or excitation of a neural circuit. For this reason, it becomes indispensable to establish when and where eCB genes are expressed, in order to permit later studies of the CB signalling system at any given time in the zebrafish lifespan. Therefore, we described the spatial and temporal expression profile of different ECS genes during zebrafish development.

5.1 Temporal expression profile of ECS genes during zebrafish development

Using 17 human endocannabinoid genes as reference, a recent bioinformatics analysis identified a well-conserved repertoire of ECS genes in the zebrafish genome (*McPartland et al.,* 2007). This finding prompted us to profile the expression of different ECS genes at different stages of zebrafish embryonic development, in collaboration with the Endocannabinoid Research Group, Institute of Biomolecular Chemistry (ERG-ICB) in Pozzuoli, Naples, coordinated by Dr Vincenzo Di Marzo.

We designed a set of primers that target the orthologous genes involved in AEA and 2-AG metabolism and in the synthesis of ECS receptors (Table 5), and we chose 12, 24, 48 (before and after hatching), 72 hpf and 4 dpf as

developmental time points. By using quantitative PCR and *eef1a1l* (eukaryotic translation elongation factor 1 alpha 1, like 1) as reference gene, we found detectable mRNA expression starting from 12 hpf for all analyzed genes, except for *cnr1*, which was first detectable at 24 hpf (Fig. 15).

More interestingly, the temporal dynamics of AEA biosynthetic (*nape-pld*, *abhd4*) and catabolic (*faah*) enzyme expression significantly increased during the developmental period under investigation (Fig. 15A).

The 2-AG biosynthetic enzyme (*daglα*) also increased its expression during the same time, while, conversely, 2-AG catabolic enzyme genes *mgll* and *ptgs2b* were down-regulated during the pre-hatching period (24-48 hpf; Fig. 15B).

While ECS receptors (*cnr1*, *trpv1*, and *gpr55*) increased their expression in a time dependent manner, of note, only marginal *cnr2* mRNA expression was observed during zebrafish development, with no increase even in later larval stages (Fig. 15C).

	Primer 5'-3'	

TABLE 5. *Quantitative PCR primer pairs used for ECS temporal dynamics during zebrafish development*

Gene	Forward	Reverse
daglα	GAGGGTTTCCGTCGTCAC	TGTTCCTCCAGCAATGATCC
mgll	AAGTGAAGGTGAGAGGAT	AATGTCCAACGATGAAGA
nape-pld	CTCAAGGACATGCACTCA	GAGCACAATCTTCAAGACAAT
abhd4	GCGTCACTCTTATTGAAG	TTAGTCCACCGTATTACA
faah	TTTGGATATAAGGGTCATG	CTTCTTCAGCACTGTAAC
ptgs2b	ATCCAGGATGAAGTCTACAAT	GCTGTTGACGCCATAATC
cnr1	TACTGGAAGAGGTCAATC	AGAGTCAATAGTGAGCAA
gpr55	AACTGAAGGTGTGGATAC	ACGCCATAATGTTTAACG
trpv1	TTGGATTGACTACAGATAAC	AATGGTGAACTTGAACAG
cnr2	TGGAGAACAAACTGGAACAA	GGTCAGCAGGACCAAAATGT
eef1a1l1	CTTCTCAGGCTGACTGTGC	CCGCTAGCATTACCCTCC

55
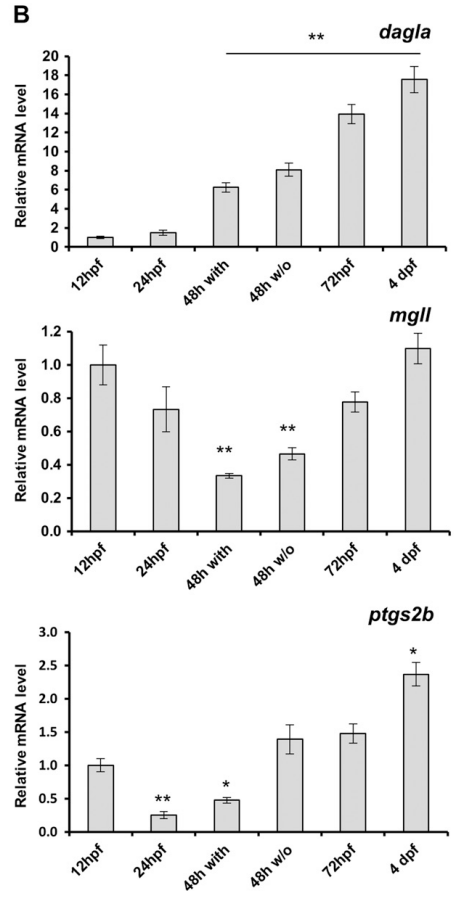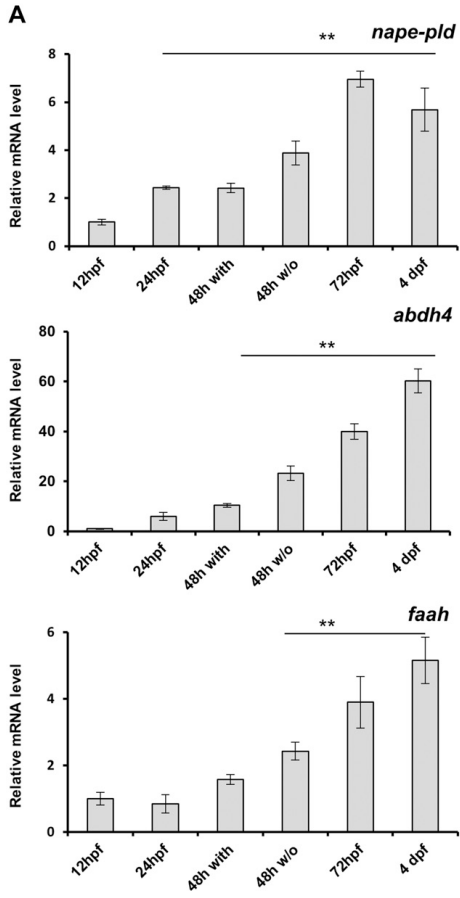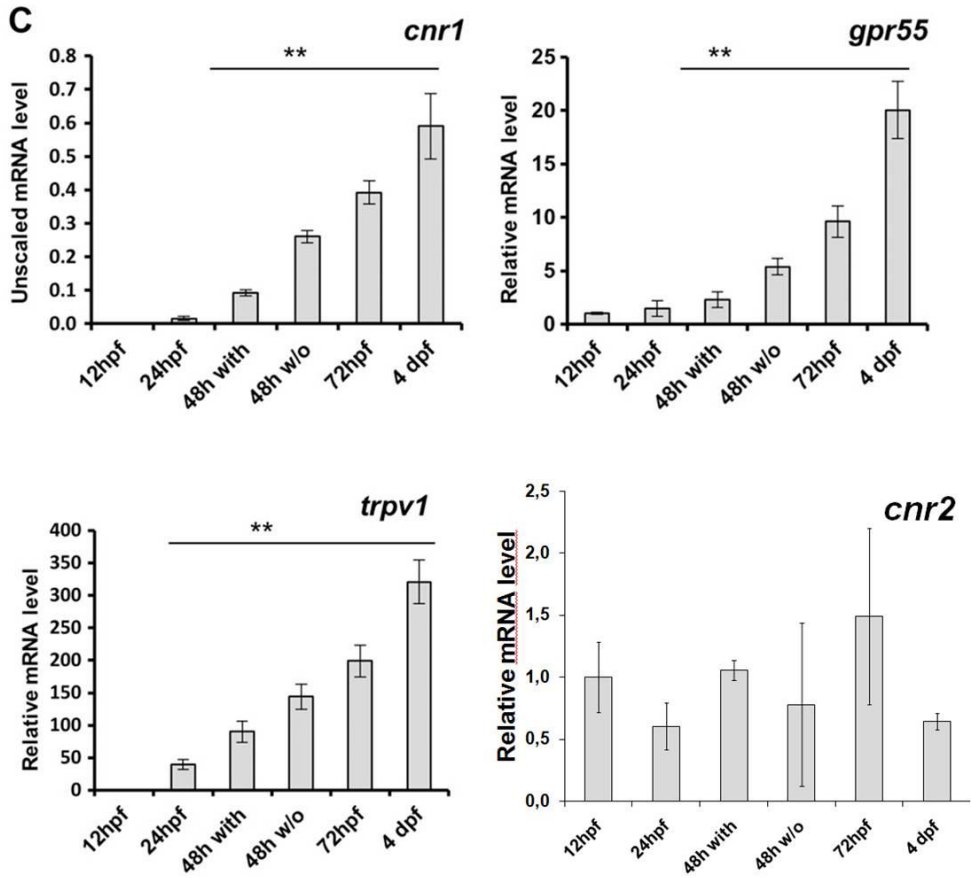
Figure 15. ECS genes are expressed in zebrafish embryos and larvae at levels that increase during development. Quantitative PCR values of each sample group were obtained from a pool of 20 whole embryos at different embryonic and larval stages. (A-C) ECS genes are arranged in AEA metabolic enzymes (A), 2-AG metabolic enzymes (although *ptgs2b* is also involved in AEA catabolism) (B), and eCBs receptors (C). Stages 48 hpf with andwithout refer to the chorion presence/absence in synchronous embryos. Results are the mean of 3 separate experiments. Data and statistical significance are expressed relative to the 12 hpf group. Relative expression ± SEM as determined by Bio-Rad CFX Manager software. *P , 0.05; **P , 0.01.

5.2 Analysis of endocannabinoid levels during zebrafish embryonic and larval developmental stages

Having found expression of a complete ECS genetic system during the different developmental stages analyzed in collaboration with ERG, we next investigated the presence of eCBs and their congeners at different time points by means of liquid chromatography-mass spectrometry analyses on pre-purified lipid extracts. Of interest, 2-AG was found to be the most abundant eCB in the zebrafish developing embryos, and its levels followed a profile that closely resembled that of *dagl*α mRNA transcript levels (Figs. 15B and 16A). Of importance, unfertilized eggs instead displayed higher contents of eCBs, such as 2-AG, palmitoylethanolamide (PEA) and oleoylethanolamide (OEA) compared with embryos at 12 hpf, which suggested a possible maternal source required for egg fertilization (Fig. 16 A, C). Temporal dynamics during embryonic development toward hatching showed increasing levels of 2-AG, whereas AEA, PEA, and OEA levels did not change appreciably (Fig. 16). With the exception of PEA, levels of all compounds tended to decrease in hatched embryos (comparing 48 hpf embryos with and without chorion), although this effect was statistically significant only for 2-AG, which indicated that a significant amount of this eCB was retained in the chorion. An increase, which was statistically significant only for PEA and 2-AG, was again noted at early larval stage (72 hpf; Fig. 16 A, C).
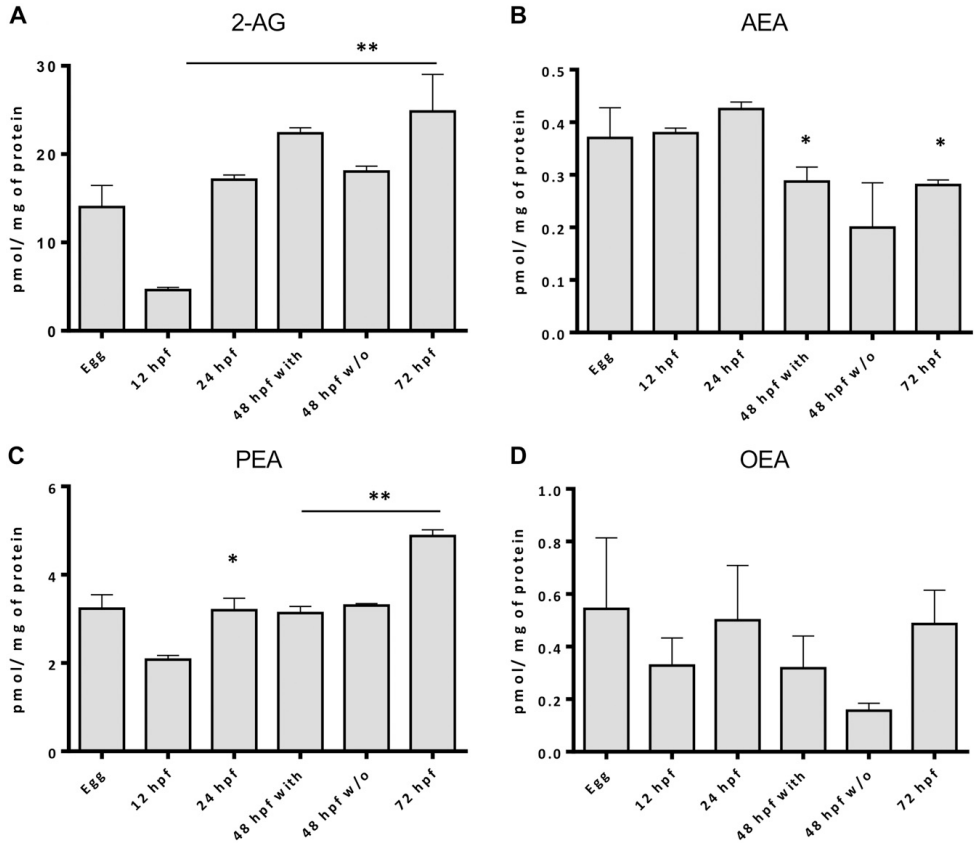
Figure 16: eCB levels during zebrafish development. 2-AG levels are higher in unfertilized zebrafish eggs, embryos, and larvae compared with AEA and related mediators during development (A-D). Liquid chromatography-mass spectrometry quantification of the main eCBs and N-acylethanolamines: 2-AG (A), AEA (B), PEA (C), and OEA (D). Each sample was obtained from a pool of 50 unfertilized eggs, embryos (12, 24, and 48 hpf), or larvae (72 hpf). Stages 48 hpf with and 48 hpf w/o refer to the chorion presence/absence in synchronous embryos. Data are expressed as means ± SD of 3 independent experiments. *P , 0.05; **P , 0.01.

5.3 Dagls and Magl enzymatic activities reflect increased 2-AG turnover during embryonic development

Since 2-AG appears to be the most abundant eCB during zebrafish development, we proceeded, in collaboration with Di Marzo's group, to evaluate the endogenous enzymatic activities involved in its metabolism. By using radiolabeled substrates we were able to extrapolate the enzymatic rate for different developmental time points. Both Dagls and Magl activities showed an increased trend with time (Fig. 17), although Dagls increase starts to be significant from 48 hpf. The absolute activity of these anabolic enzymes was consistently higher than Magl for all developmental time points and corresponds with the *daglα* expression pattern (Fig. 15).
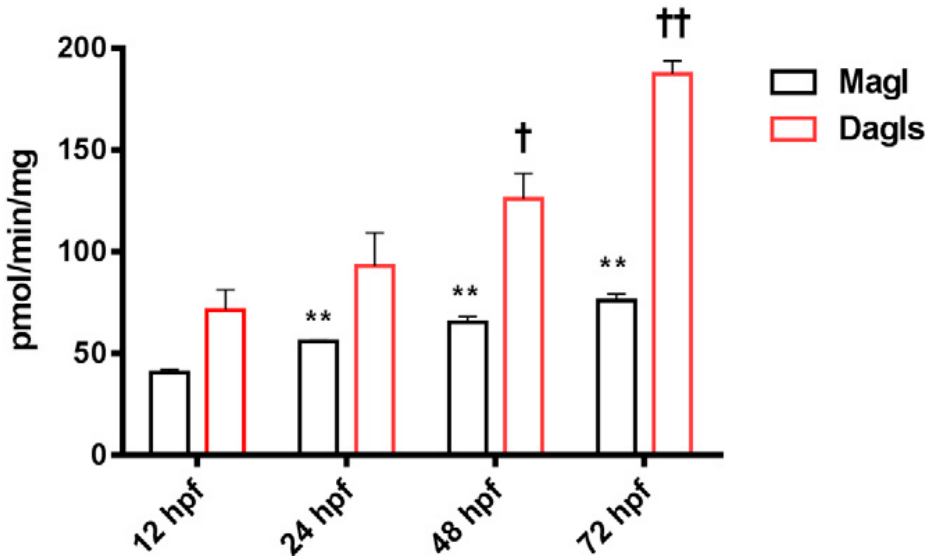
Figure 17: Enzymatic activities of biosynthetic (DAGLs) and catabolic (MAGL) 2-AG enzymes. Each sample was obtained from a pool of 50 embryos or larvae. Data are expressed in pmol/min/mg of protein and as means ± SD of 3 independent experiments. Statistical significance is given with respect to the 12 hpf group. P , 0.05; **P , 0.01.

5.4 Spatial-temporal characterization of ECS gene expression profiles

The establishment of endocannabinoid signalling requires the temporal and spatial coincidence of metabolic enzyme and receptor expression during brain development.

Despite efforts directed toward understanding endocannabinoid signaling in the postnatal brain, a surprising lack of data exists with regard to detailed developmental studies on the distribution of sn-1 diacylglycerol lipases (Dagls), the prime 2-arachydonoylglycerol (2-AG) synthetic enzymes, monoacylglycerol lipases (Magl), the 2-AG hydrolyzing enzyme, and the by far well known cannabinoid receptors during brain development.

Therefore, in order to better understand and define the basic developmental and signaling principles controlled by eCBs, we identified possible sites of action for eCB signaling in zebrafish neurogenesis, analyzing the expression patterns of several ECS genes at different developmental stages: 24, 48 and 72 hpf *via* whole mount *in situ* hybridization (WISH).

In this way, we confirmed data already available in the literature, such as those for *daglα* and *cnr1* (*Lam et al.*, 2006; *Watson et al.*, 2008), and identified new ones, not yet present in literature, as in the case of transcriptional profiles of *daglβ*, *mgll*, and *trpv1*, as well as of *daglα* at 24 and 72 hpf. As for expression profiles of *cnr2* and *gpr55* receptors, we were not able to detect specific staining patterns at any of the zebrafish developmental stages analyzed.

5.5 Spatial-temporal characterization of 2-AG metabolic enzymes expression profiles

Since 2-AG seems to be the most abundant eCB during zebrafish development, we proceeded, to evaluate the expression profiles of its metabolic enzymes during different zebrafish developmental stages.

First, we analyzed the expression patterns of *daglα* and, for the first time, *daglβ*, the paralogous genes that encode for the major synthesizing enzymes for 2-AG.

At prim5 stage (24 hpf) it is possible to observe that the expression profile of *daglα* is localized in the dorsal telencephalon (olfactory placode), ventral hypothalamus, tegmentum, hindbrain and spinal cord. By the long pec stage (48 hpf), as reported by Watson and collaborators (*Watson et al.*, 2008), the transcript was still expressed in the telencephalon, hypothalamus, tegmentum, and hindbrain, and it appeared in midbrain and cranial ganglia, thus showing widespread distribution in all major compartments of the brain and in the ganglion layer of the retina (Fig. 18 A-C, G). This expression profile remained unchanged at 72 hpf.

daglβ exhibited an expression profile spatially and temporally similar to that of its paralogue *daglα* in telencephalon, hypothalamus, midbrain, hindbrain, spinal cord, and retinal ganglion layer, but with slightly broader expression levels (Fig. 18 D, E, F, H) from 24 to 72 hpf.
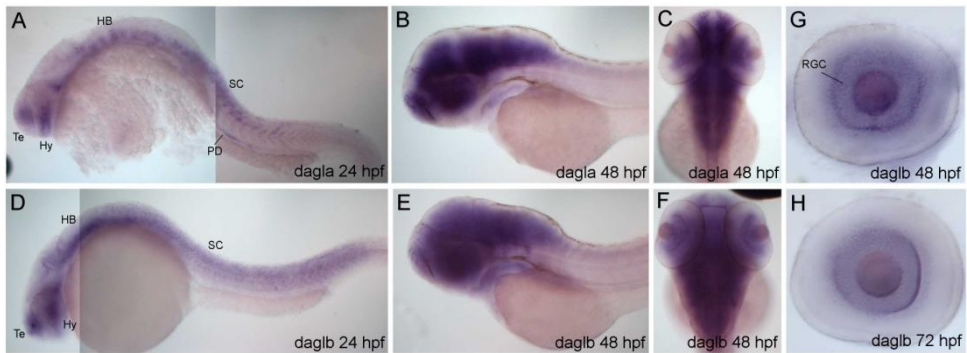
Figure 18: *daglα and daglβ* **gene expression profiles during zebrafish neurogenesis.** Whole-mount *in situ* hybridization analysis shows the expression of *daglα* in telencephalon, hypothalamus, hindbrain, and spinal cord at the stage of 24 hpf (A). At 48 hpf, mRNA labeling is restricted to the central nervous system with a widespread distribution in all major brain compartments (B, C) and in the ganglion cell layer of the retina (G). *daglβ* shows a very similar expression profile, including telencephalon, hypothalamus, hindbrain, and spinal cord from 24 to 72 hpf but slightly more diffuse (D, E, F, H). (A, B, D, E) Anterior to left and (C, F) to top. (A, B, D, E) Lateral and (C, F) dorsal views. (G, H) Several focal plans were combined lateral views of explanted eyes. Abbreviations: Te, telencephalon, HB, hindbrain; Hy, hypothalamus; PD, pronephric duct; RGC, retinal ganglion cells.

Next, we analyzed for the first time, by WISH, the expression pattern of *mgll*, the gene that encodes for the major catabolic enzyme for 2-AG. At the blastula stage and throughout epiboly, maternal, and zygotic stages, *mgll* transcripts were ubiquitously distributed (Fig. 19 A-C). During early somitogenesis, *mgll* expression became restricted to a single domain in the rostral brain that encompasses telencephalon, diencephalon, and tegmentum (Fig. 19 D, E), and to a region of the pronephric ducts encompassing the proximal straight and distal early segments (Fig. 19 F).

By late somitogenesis (22 hpf) and early post-somitogenesis (25 hpf), *mgll* mRNA was clearly visible in neuronal clusters associated with the dorsal

pallium, preoptic area, and epiphysis, and more weakly in tegmentum (Fig. 19 G-J).

The signal in the pronephric ducts was restricted to one somite length of tubule epithelium in the distal early segment (25 hpf; Fig. 19 L). As development proceeds, *mgll* expression remained in the telencephalon, anterior hypothalamus, and epiphysis (Fig. 19 M, N), whereas additional *mgll* mRNA signals became progressively discernable. At 28 hpf, transcript expression was extended to distinct neuronal clusters that stretched dorsally in the molecular layer of the cerebellar primordium or that were located latero-ventrally in each rhombomere (Fig. 19 M, O). At 48 hpf, instead, expression was detected also in the optic tectum, pectoral fin mesenchyme, and in a region of the eye that seems to include the retinal ganglion cell layer as suggested by co-localization of *mgll* and *fgf8a* transcripts – the latter being a marker of retinal ganglion cells (Fig. 19 P, Q) – and later at 72 hpf *mgll* the signal was restricted to the ventricular zone.

A germ ring
B germ ring
C 70% epiboly
D Te Tg Hy 14 hpf
E Tg Te Hy 14 hpf
F PD 14 hpf
G Te * Tg Hy 22 hpf
H * Te Hy 22 hpf
I PD 25 hpf
J Te * PO 25 hpf
K * Te PO 25 hpf
L 25 hpf
M Te * Tg Ce HB PO 28 hpf
N * Te 28 hpf
O HB Ce 28 hpf
P TO Ce Rh PF * Te 48 hpf
Q RGC *mgll* *fgf8a* 48 hpf
R vz 72 hpf

64
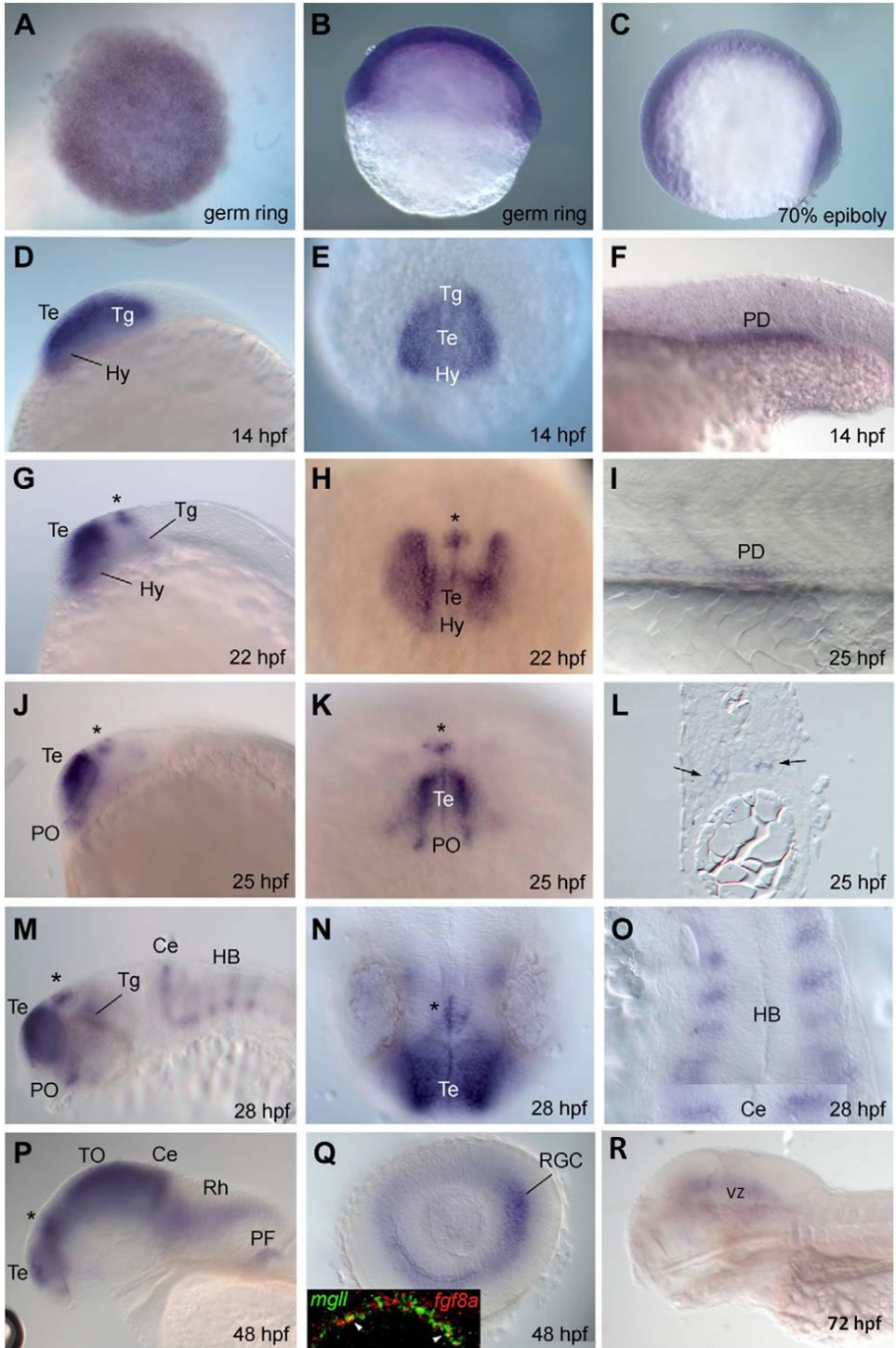
Figure 19: Dynamic expression of *mgll* during zebrafish neurogenesis. WISH shows maternal contribution (A) and ubiquitous expression during gastrulation (B, C). During somitogenesis (14 hpf), *mgll* mRNA is seen in a rostral domain, including telencephalon, diencephalon, and tegmentum (D, E), and in a large segment of the pronephric ducts (F). During late somitogenesis (22 and 25 hpf), mgll expression is found in neuronal clusters located in dorsal pallium, preoptic area, epiphysis (*), and tegmentum (G-J). Expression in the tubular epithelium of the pronephros is seen in lateral view (K) and in section through the trunk (L). Additional expression becomes progressively discernable in the cerebellum, hindbrain (M, N), optic tectum (P), pectoral fins (P), and eye (Q). Inset in panel Q highlights co-expression of *fgf8a*, a marker of retinal ganglion cells, and *mgll* as shown by signal merging (arrowheads). At 72 hpf *mgll* is expressed in the ventricular zone (R). Different focal planes were combined in O. Animal pole and dorsal view in A and O, respectively; lateral view in B and C; anterior to the left and lateral view in D, F, G, I, J, M, P and R; anterior view in E, H, K, and N. Ce, cerebellum; HB, hindbrain; Hy, hypothalamus; OT, optic tectum; PD, pronephric duct; PF, pectoral fin; PO, preoptic area; RGC, retinal ganglion cell layer; Rh, rhomboencephalon; Te, telencephalon; Tg, tegmentum, vz, ventricular zone.

5.6 Spatial-temporal characterization of 2-AG main receptor expression profiles

After analyzing the expression profiles of the principal genes involved in synthesis and degradation of 2-AG, we investigated the expression territories of its major receptors. Even if we were able to isolate and clone various transcripts coding for the main 2-AG receptors, only WISH experiments for *cnr1* and *trpv1* mRNAs generated a good signal, while no or very weak signal was detected for *cnr2* and *gpr55* transcripts, maybe due to low RNA abundance.

Largely in agreement with previous studies (*Lam et al*., 2006; *Watson et al*., 2008), we found that *cnr1* gene was expressed by the prim 5 stage, 24 hpf, in the preoptic area, hypothalamus, dorsal telencephalon, ventral thalamus, ventral tegmentum, and posterior hindbrain (Fig. 20 A, B). As development proceeds, its expression extended also to other neuronal populations. Thus, by the long pec stage, 48 hpf, *cnr1* was expressed in the telencephalon, preoptic area, hypothalamus, ventral thalamus, and ventral tegmentum. mRNA was also distributed in midbrain and hindbrain though more weakly (Fig. 20 C, D). At 72 hpf, the signal persisted in the above regions, and appeared also in the dorsal thalamus, optic tectum, and cerebellum.

Comparing the expression patterns of *cnr1*, *daglα*, *daglβ* and *mgll*, it seems that these genes are tightly co-regulated in specific areas of the telencephalon, hypothalamus, midbrain, and hindbrain (Fig. 20 F).
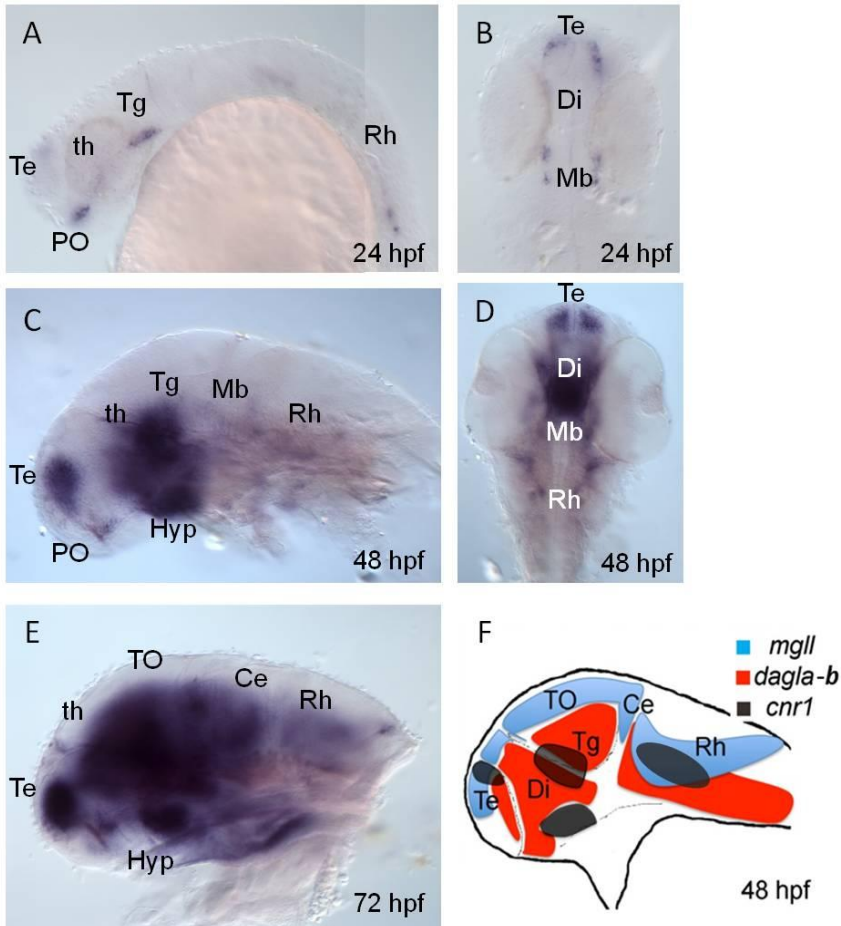
Figure 20: *cnr1* gene expression profile during zebrafish neurogenesis. Whole-mount *in situ* hybridization analysis shows the expression of *cnr1* in telencephalon, preoptic area, ventral thalamus, ventral tegmentum and caudal hindbrain at 24 hpf (A–B). At 48 hpf, expression was seen in telencephalon, preoptic area, hypothalamus, thalamus, and tegmentum (C–D). At 72 hpf, the transcript is widely distributed in all major compartments of the brain (E). The images were acquired in lateral (A, C, E) and dorsal (B, D) view. Abbreviations: Te, telencephalon; PO, preoptic area; th, thalamus; Tg, tegmentum; Rh, rhombencephalon; Hyp, hypothalamus; Di, diencephalon; Mb, midbrain; TO, optic tectum.

Since recent studies have demonstrated that intact 2-arachidonoylglycerol is an endogenous Trpv1 activator that contributes to phospholipase C-dependent Trpv1 channel activation and Trpv1-mediated anti-nociceptive signalling in the brain (*Zygmunt et al*., 2013; *Petrosino et al*., 2016), we lastly analyzed for the first time *trpv1* gene expression.

At prim5 stage (24 hpf) it was possible to observe that the expression profile of zebrafish *trpv1* was localized in few neural and sensory cell types within sensory cranial ganglia flanking the hindbrain, and in the Rohon–Beard cells localized in the dorsal aspect of spinal cord (Fig. 21 A). At long pec stage (48 hpf), and protruding mouth stage (72 hpf), *trpv1*-positive cells were similarly distributed as they were seen in two columns projecting toward the eye in the ventral head mesenchyme, and in trigeminal sensory neuron subtypes (Fig. 21 B-E). Cells expressing *trpv1* also were found at the base of the pectoral fins, suggesting a correspondence to pectoral motor nerve ganglia (Fig. 21 B-E). No spinal cord labelling was detected at this stage.
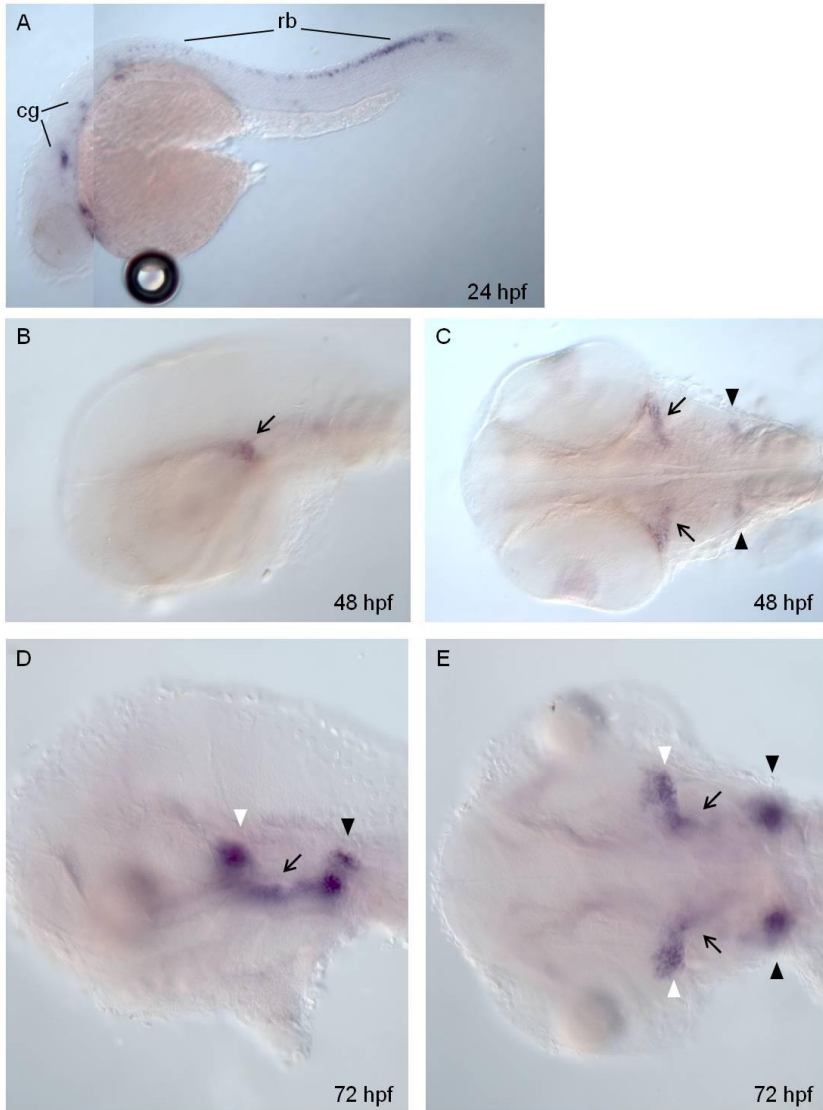
Figure 21: Few neural and sensory cell types expressing *trpv1*: Whole-mount RNA *in situ* hybridization of *trpv1* from 24 to 72 hpf. Embryos are oriented with head toward the left in lateral views (A, B, D) and head toward the left in dorsal views (C, E). (A) *trpv1* mRNA in cranial ganglia (cg) and Rohon-Beard (rb) neurons at 24 hpf. (B-E) Expression in trigeminal (white arrowhead), cranial (arrow) and pectoral (black arrowhead) neurons at 48 and 72 hpf.

5.7 *daglα* down-regulation to decrease 2-AG levels

From mass spectrometry analysis that was performed in collaboration with Dr. Di Marzo (ERG, ICB-CNR, Pozzuoli, Naples), we found that 2-AG levels were elevated and actively produced during zebrafish embryogenesis (Fig. 16).

To ascertain its function during development, we knocked down the 2-AG biosynthetic enzyme *daglα* in order to decrease 2-AG levels in embryos and larvae by using morpholino (MO), an antisense oligonucleotide that inhibits translation by "steric blocking", binding to a specific target sequence within an RNA. Considering the key role of EC signalling during neurogenesis, we hypothesized that MO-induced down-regulation of *dagla* would impair axonal pathfinding during zebrafish embryogenesis as it has been shown in *cnr1* knockdown experiments (*Watson et al.*, 2008).

We used two different antisense MOs for this gene, one directed against the translational start site of the coding sequence (daglα-Tb1) and the other targeting the exon 3 – intron 3 splice site boundary (daglα-Sb1).

As control, in order to increase the 2-AG levels, we knocked down the 2-AG catabolic enzyme *mgll*, using also in this case two different antisense MOs: one directed against the translational start site of the coding sequence (mgll-Tb1) and the other targeting the exon 2 – intron 2 splice site boundary (mgll-Sb1). The binding sites of the different MOs are schematized in Fig. 22.

Dose-response relationships were investigated to assess toxicity and determine the working concentration of MOs (Fig. 23).

Figure 22: Representation of oligo-Morpholino binding sites. A) At the top, the physical map of the *daglα* gene is illustrated with the corresponding domains represented in different colors. It is highlighted the region comprising the binding sites of morpholino daglα-Tb1 (green line), ATG translation site starting site; daglα-Sb1 (blue line), between the exon3-introne3 (ATACGCCTAG-gtaagacgta) junction. This last is also represented in red in the corresponding amino acid sequence of the gene (A'). B) Below it is represented the physical map of the *mgll* gene. Morpholino mgll-Tb1 (green line) binds to the ATG translation start site; morpholine mgll-Sb1 (blue line) between the exon 2-intron 2 (GTCCTCCGAA-gtaagtgtga).
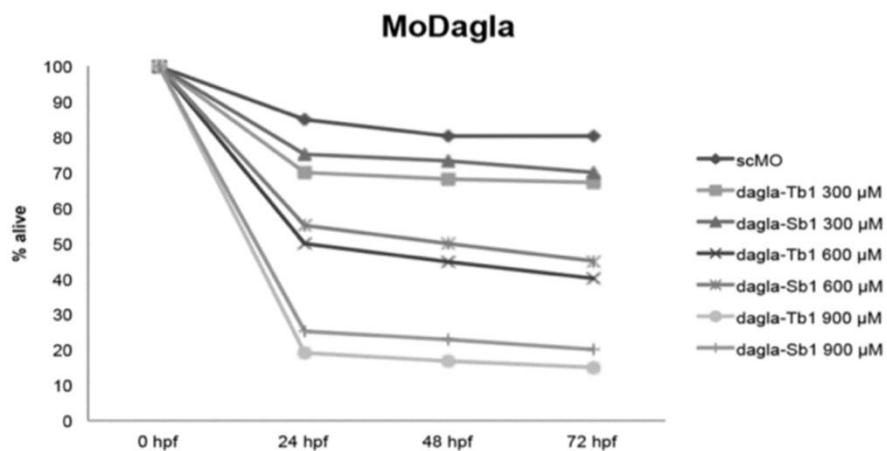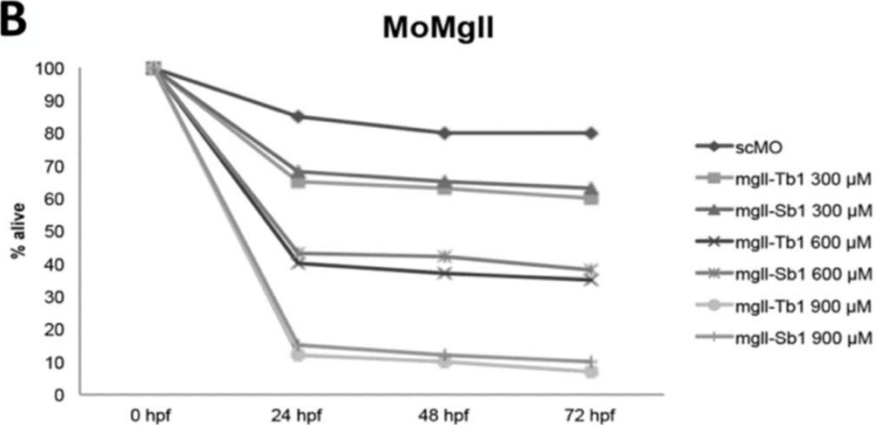
Figure 23: Dose-response relationship of oligo-morpholino. Statistical analysis of mortality induced by control, daglα (A) and mgll (B) morpholinos at different concentrations (300, 600 and 900 μM) and at different stages of zebrafish development (24, 48 and 72 hpf) to define the optimal working concentration (300 μM) with the highest survival rate (alive).

Zebrafish 1-cell stage embryos were injected with either MO, then sampled at different developmental stages for 2-AG level measurement. In line with the biochemical function of Daglα, MO-based knockdown produced a significant reduction in endogenous 2-AG after microinjection of either daglα-Tb1 or daglα-Sb1 MOs compared with uninjected embryos or *vs*. those injected with control MO (Fig. 24 A).

These data are in agreement with the notion that Daglα is the major 2-AG biosynthetic enzyme. Of interest, on the other hand, we found a significant increase of 2-AG levels in mgll-Tb1 and mgll-Sb1 MO-injected embryos, also here in line with the catabolic function of this enzyme (Fig. 24 B).
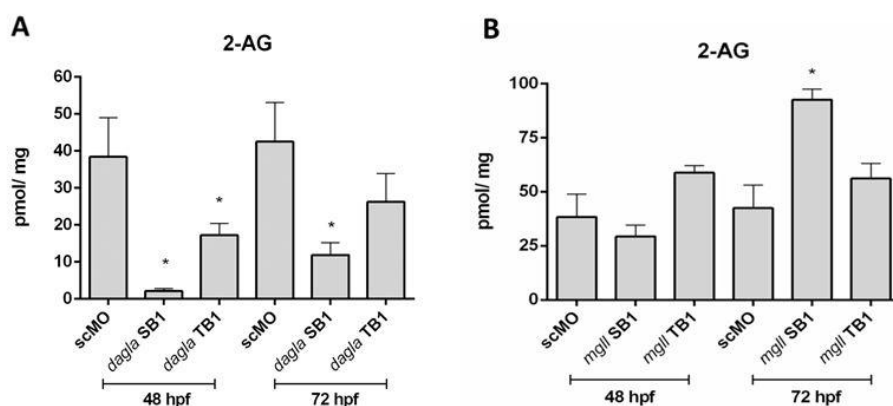
Figure 24: Analysis of 2-AG levels in *daglα* and *mgll* morphants. Quantification of 2-AG by liquid chromatography-mass spectrometry in fish at 48 and 72 hpf shows a significant reduction in daglα-Tb1 and daglα-Sb1-MO injected embryos (A) and a significant increase in mgll-Tb1 mgll-Sb1 MO-injected embryos (B). Standard control MO (scMO) indicates the values in corresponding synchronous stages, which did not differ significantly from each other. Data obtained in collaboration with Dr. Di Marzo's research group (ERG, ICB-CNR, Pozzuoli, Naples).

Finally, to confirm that the morphologic abnormalities as well as the changes in 2-AG levels were specific effects of MO injections, we decided to analyze *daglα* and *mgll* transcripts by RT-PCR. These analyses clearly showed that both MOs for the splicing site induced a premature stop codon in *daglα* and *mgll* mRNA. Specifically, cDNA sequencing revealed a partial exon 3 skipping and partial intron 2 retention generating premature stop codons in *daglα* and *mgll* mRNAs, respectively (Fig. 25).
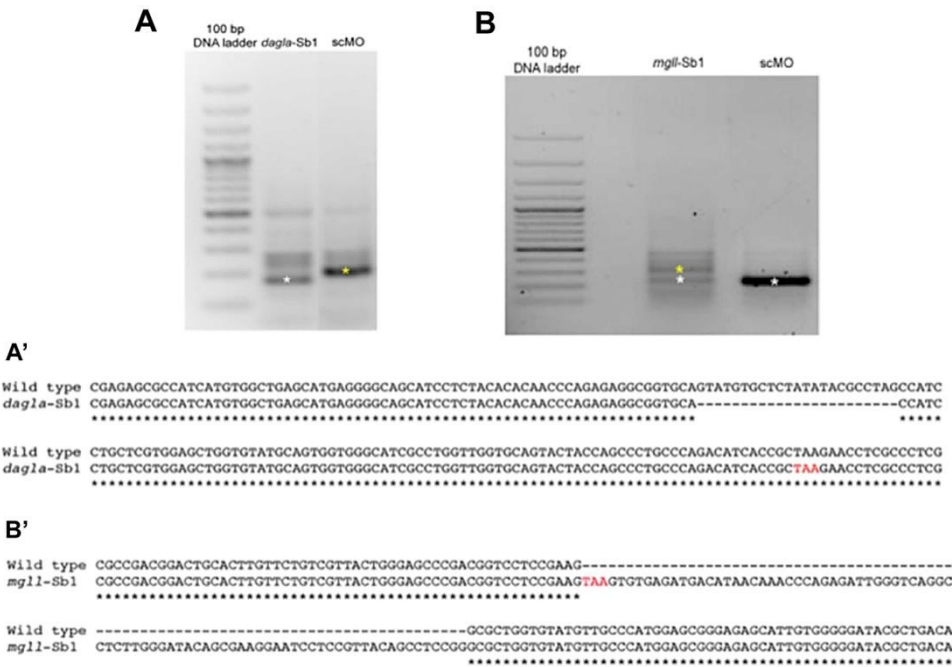
Figure 25: RT-PCR analysis of embryos injected with daglα-Sb1 and mgll-Sb1 morpholinos. From the agarose gel electrophoretic analysis, compared to the control (scMO), it is possible to see a lower band due to the 23 bp deletion in exon 3 of the *daglα* transcript (A), resulting in alteration of the reading frame and formation of a premature stop codon (highlighted in red), confirmed by sequencing analysis (A'). On the contrary, there is a higher band due to the 84 bp insertion in the intron 2 of *mgll* transcript (B), leading also in this case an alteration of the reading frame and formation of a premature stop codon (highlighted in red), also confirmed by sequencing analysis (B').

5.8 Role of Daglα in axon growth

Whereas both ATG and splice site targeted MOs seemed to perturb 2-AG levels and axon formation in a similar manner (60–80% of larvae analyzed showed defects in axon growth), thereby implying a link between *daglα* down-regulation and neuronal phenotype, only results obtained with daglα-Tb1 MO are presented here. To minimize the potential for confounding results from morphological abnormalities (*daglα* morphant larvae that showed severe defects in body morphology had defective axon growth), we analyzed only those MO-microinjected larvae at 3 dpf that were not disturbed in their overall morphology (70%), but, however, appeared darker in pigmentation pattern (Fig. 26).
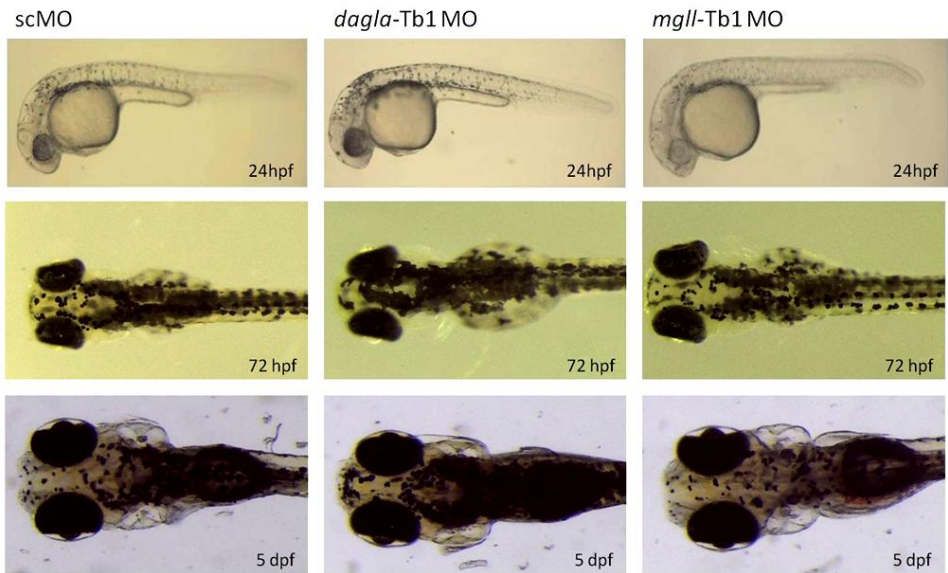
Figure 26: Body morphology of daglα-Tb1 injected fish. Compared to the control, in 70% of cases, daglα-Tb1 MO or mgll-Tb1 MO-injected fish did not show significant abnormalities in the structure of the body, neither the curvature of the tail, nor even cardiac edema.

Analysis of daglα-Tb1 MO-microinjected larvae stained with an antibody against acetylated α-tubulin (component of the neuronal microtubules, marker of the structural function of the axon) revealed abnormalities in disparate fiber tracts in specific brain regions.

Previous studies reported that the majority of neuron cell bodies of the optic tectum are located in the superficial periventricular layer, which contains the main tectal neuropil (TNP) and axons of the superficial neuropil layer (SNL) just under the epidermis (*Robles et al.*, 2011). A comparison with controls illustrated that:

- the number of SNL axons was significantly reduced in 71% of *dagla* morphant larvae, with fewer or no axons reaching the dorsal midline from the TNP (Fig. 27 A, B, M);

- in support of the correlation between ECS and axon growth, analysis of the cerebellum underscored the abnormal axonal patterning of knockdown larvae. The projection pattern of nerve fibers in the rhombic lip of the cerebellum revealed a statistically significant difference between groups. Indeed, cerebellar fibers from both halves stopped their elongation prematurely and were not properly extended toward the dorsal midline in 80% of *daglα* knockdown larvae (Fig. 27 D, E, N);

- investigating also the retinal ganglion cell axons in the optic nerves and tracts, 61% of dagla morphants displayed hypoplastic optic nerves, which appeared restricted rostrocaudally relative to the control region (Fig. 27 G, H);

- furthermore, anterior vagal nerves were disorganized, with misrouted or extra axons in 60% morphant larvae (Fig. 27 J, K).

To gain further evidence that impaired axonal outgrowth is really the consequence of *daglα* knockdown and subsequent reduction of 2-AG levels – Daglα enzyme also produces other 2-acylglycerols with little or no action at CB1 receptors – we treated Daglα-deficient embryos from 70% epiboly until 72 hpf with the CB1 cannabinoid receptor agonist and non-hydrolysable 2-AG analog, noladin ether (2-Arachidonylglycerylether) (*Hanuš et al*., 2001). Of interest, we found that the axonal phenotype of noladin ether administered *daglα* morphants did show a partial rescue of SNL axon loss, and nerve elongation defects in the molecular layer of the cerebellum (Fig. 27 C, F, I, L, M, N). These results suggest that primary axon tract formation in Daglα-depleted zebrafish is impaired as a result of decreased 2-AG levels. We subsequently decided to investigate functional traits of *daglα* morphant larvae in terms of vision and locomotion.
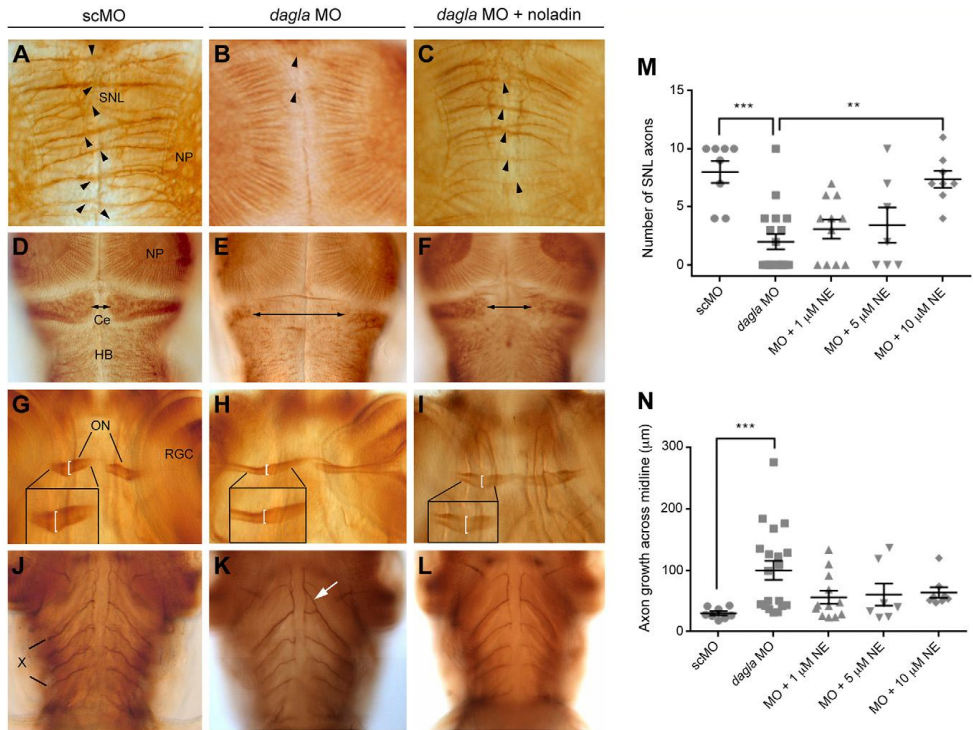
Figure 27: Loss of Daglα causes specific defects in axonal outgrowth. A–L) daglα-Tb1 MO-injected larvae (72 hpf) are characterized by substantial reduction of SNL axons (black arrowheads) (A–C), limited extension of cerebellar nerves (double arrows) (D–F), reduced thickness of the optic nerves (square brackets) (G–I), and abnormal branches in the anterior facial motor neurons (white arrow) (J–L). Axonal defects are less severe in daglα-Tb1 MO-injected larvae that were treated with noladin ether, a stable 2-AG analog. M, N) Statistical analysis showing a substantial reduction in the number of SNL axons (M) and the distance between cerebellar axons across the midline in *daglα* morphant larvae (N). M) Treatment of knockdown larvae with noladin ether causes significant rescue of SNL axons in a dose-dependent manner. Scattered dots at the same level are individual larvae with the same number of axons. Molar concentration refers to the concentration of noladin ether. Statistical analysis was performed by using Kruskal-Wallis test followed by Dunn's multiple comparison test. Scatter plots represent means ± SEM of 3 independent experiments (n = 180). Anterior to the top. Dorsal views in A–F; ventral views in G–L. Ce, cerebellum; L, lens; ON, optic nerve; RGC, retinal ganglion cell axon; scMO, standard control MO; x, vagal sensory nerve. **P , 0.01; ***P , 0.001.

5.9 Vision acuity and sensitivity in Daglα-deprived larvae

A functional ECS is thought to be required in the developing visual system to shape retinal responses to light and in visual processing (*Ryskamp et al.*, 2014; *Keimpema et al.*, 2010; *Cécyre et al.*, 2013).

Investigations into the visual system development and functions necessitate quantifiable behavioral models of visual performance that are easy to elicit, and that are robust and simple to manipulate. A suitable model has been found in the optokinetic response (OKR), a reflexive behavior present in all vertebrates due to its high selection value. The OKR is a stereotyped eye movement in response to movement in the surround and involves slow stimulus-following movements of eyes alternated with rapid resetting saccades. This serves to stabilize the visual image on the retina, and allows for high-resolution vision. In the laboratory, OKR is usually elicited using a black-and-white striped drum that ideally revolves around the subject. The resulting slow eye movements following the drum rotation (slow phase) are interrupted by fast resets in opposite direction (fast phase), referred to as optokinetic nystagmus (OKN). Eye movements are recorded and automatically analyzed in real time. Data analysis enables immediate recognition of parameters such as slow and fast phase duration, movement cycle frequency, slow-phase gain, visual acuity, and contrast sensitivity (Fig. 28). The measurement of this behavior is easily carried out in zebrafish larvae, due to its early and stable onset (fully developed after 96 hpf). OKR can be used as a screening assay, enabling the analysis of sensory-motor control and visual system performance in great detail (*Huang and Neuhauss*, 2008; *Mueller et al.*, 2011).

The hypothesized role of ECS in vision, together with the axonal growth deficits that we detected here in zebrafish *daglα* morphants, prompted us to test whether optokinetic performance was altered in Daglα-deficient larvae. In collaboration with Prof. Stephan Neuhauss at the Institute of Molecular Life Sciences, University of Zurich, Switzerland, we determined visual acuity and contrast sensitivity in daglα-Tb1 MO injected embryos, by measuring larval OKR, which is the stereotyped eye movement in response to movements in the field of vision (*Haug et al.*, 2010). Perturbation of optokinetic behavior, which is regulated by the optical and neuronal properties of the visual system, could be a result of defects in sensory inputs or motor outputs. In OKR experiments, we examined contrast sensitivity (Fig. 29 A), spatial sensitivity (Fig. 29 B), and temporal sensitivity (Fig. 29 C), and in all cases we observed significantly reduced eye velocity (repeated measurement ANOVA P, 0.005), which suggested that the visual system is not intact in *daglα* morphants and that 2-AG production is required for proper detection of motion stimuli.

On the other hand, we did not find any significant alteration of eye velocity in mgll-Tb1 MO injected embryos in terms of contrast (Fig. 30 A), spatial (Fig. 30 B), and temporal sensitivity (Fig. 30 C), indicating that an increase in 2-AG amount could not compromise visual acuity and optokinetic behavior.
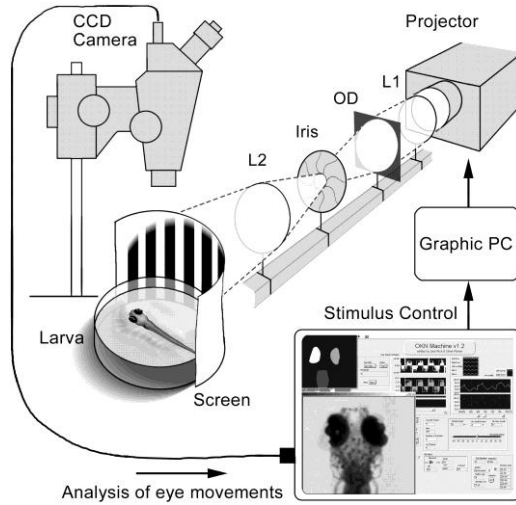
Figure 28: Schematic drawing of the setup used to stimulate and record optokinetic responses. Immobilized zebrafish larvae are stimulated with gratings projected onto a cylindrical screen. Projection is focused through two convex lenses (L1, L2). Intensity is adjusted by optical density filters (OD). Eye movements are recorded with a CCD camera and evaluated in real-time in terms of eye angle and velocity. Taken from *Rinner et al.*, 2005.
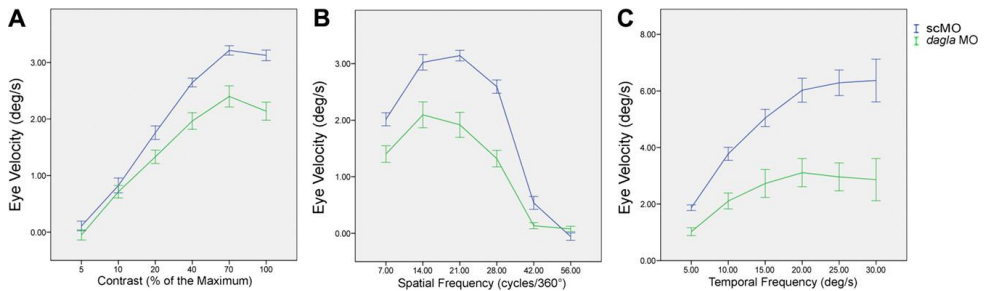
Figure 29: OKR is reduced in Daglα-deficient larvae. OKR was recorded in 5 dpf larvae injected with standard control MO (scMO) (blue) and daglα-Tb1 MO (green) in response to different contrast (A control n = 17; daglα MO, n = 15); spatial frequency (B control, n = 17; daglα MO, n = 17) and angular velocity (C control, n = 18; daglα MO, n = 18). In all cases, we observed significantly reduced eye velocity. scMO, standard control MO; Data are shown as means ± SD of 3 independent experiments (repeated measures ANOVA P , 0.005).
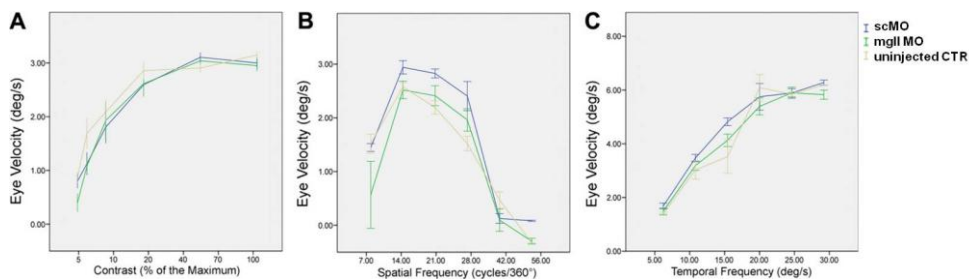
Figure 30: OKR is not compromised in Mgll-deficient larvae. OKR was recorded in 5 dpf larvae injected with standard control MO (scMO) (blue), mgll-Tb1 MO (green) and uninjected larvae (beige) in response to different contrast (A control n = 17; mgll MO, n = 15); spatial frequency (B control, n = 17; mgll MO, n = 17) and angular velocity (C control, n = 18; mgll MO, n = 18). In all cases, we did not observe any significant alteration of eye velocity. scMO, standard control MO.

5.10 Locomotor phenotype caused by Daglα depletion

It is well-known that eCBs play an important role in the activation and modulation of the motor system (*El Manira and Kyriakatos*, 2010). Zebrafish larvae are highly motile and display a variety of stereotypical movement behaviors, including cyclic swimming and fast-startle responses (*Brustein et al.*, 2003).

To characterize the role of 2-AG with respect to the spontaneous motor activity of zebrafish larvae, we examined the swimming behavior in Mgll and Daglα-deficient embryos at 72 hpf by using DanioVision (Noldus) technology. Mgll-depleted embryos featured mild locomotor hyperactivity, showing an increase of distance moved and speed (Fig. 31). Differently from mgll-MO, we found that Daglα-depleted embryos had a lower mean velocity and moved less compared with control embryos during the observation period, both in terms of distance moved and velocity (Fig. 31). Therefore, these data lend support to the hypothesis that 2-AG is needed for the proper function of the locomotor system. We concomitantly treated Daglα-deficient embryos with different concentrations of noladin ether from 70% epiboly stage until 72 hpf. Of interest, although the rescue effect was statistically significant for the distance moved, mean velocity reduction was only partially mitigated in treated *daglα* morphant embryos (Fig. 32).
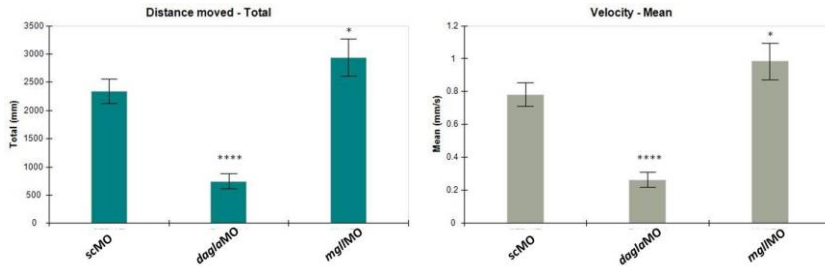
Figure 31: Locomotor phenotype in Daglα and Mgll-deficient larvae. *daglα* morphants have impaired spontaneous movement compared with standard control MO (scMO) – injected larvae, instead Mgll-depleted embryos featured mild locomotor hyperactivity. This was quantitatively assessed by using Ethovision XT software analysis. Distance moved and mean velocity graphs obtained from 3 independent experiments. Statistical analysis was performed by using Kruskal-Wallis test followed by Dunn's multiple comparison test. Bars represent mean ± SEM. *P , 0.05; ****P , 0.0001.
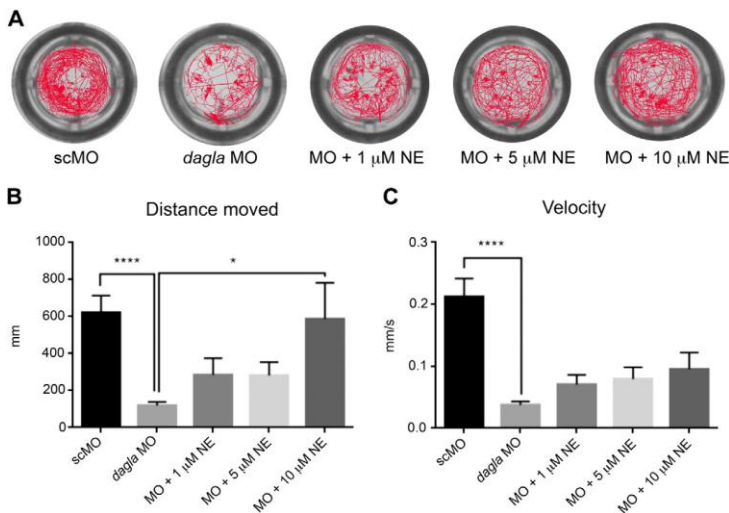
Figure 32: Locomotion is impaired in Daglα-deficient larvae. Motion-tracking plots suggest that *daglα* morphants have impaired spontaneous movement compared with standard control MO (scMO)–injected larvae, and that this locomotor phenotype was, at least in part, ameliorated by treatment with CB1-specific agonist noladin (A). This was quantitatively assessed by using Ethovision XT software analysis. Mean distance moved (B) and mean velocity (C) graphs obtained from 4 independent experiments. Statistical analysis was performed by using Kruskal-Wallis test followed by Dunn's multiple comparison test. Bars represent mean ± SEM. *P , 0.05; ****P , 0.0001.

5.11 Locomotor phenotype caused by cannabinoid receptors antagonists

To address the question if the reduction of 2-AG levels could induce locomotor alterations *via* CB1 and/or CB2, spontaneous locomotion analysis was conducted on larvae treated with cannabinoid receptors antagonists. These are a type of cannabinoidergic drugs that bind to cannabinoid receptors and prevent their activation by endocannabinoids. They include antagonists, inverse agonists, and antibodies of CBRs.

In this study, we used two different inverse agonists for CB1, AM251 and SR141716 (also known as Rimonabant), which are structurally very similar, and one inverse agonist for CB2, AM630. Their structures are illustrated in Fig. 33.
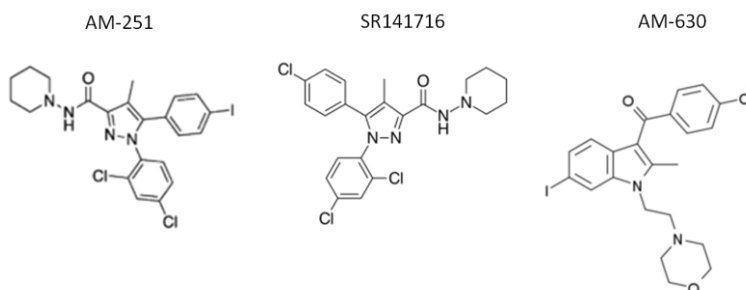
Figure 33: Molecular structure of cannabinoid receptors antagonists. AM-251 and SR141716 are inverse agonists for CB1 receptor, while AM-630 is an inverse agonist for CB2 receptor.

Zebrafish embryos were exposed to CB1/CB2 antagonists at different concentrations (0,5-1-2,5-5 μM) from 70% epiboly (~7 hpf), corresponding to the end of gastrulation, when the neural plate border gene markers are already expressed but neurulation has not yet begun, until 5 dpf.

Treatments were daily renewed with fresh solution, and embryos were evaluated on the basis of standard parameters. Embryos exposed to highest drug concentrations (2,5 and 5 μM) did not show any sign of toxicity until 72 hpf. Moreover, at 5 dpf, the highest doses of AM-251 and SR141716 induced a slight pericardic edema and alteration of branchial arches, but not brain necrosis, hemorrhages and bent spine (Fig. 34). Mortality reached the value of 100% at 5 dpf with highest drug concentrations (10 μM for AM-251 and AM-630, and 5μM for SR141716).
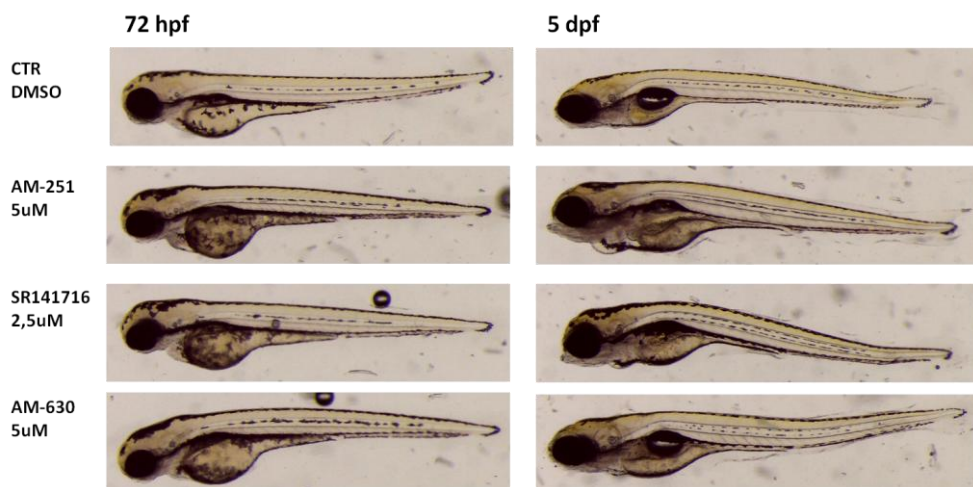
Figure 34: Phenotypic characterization of treated animals. Pharmacological treatment with cannabinoid receptors antagonists did not manifest developmental abnormalities at 72 hpf, while treatments with maximum concentration of CB1 antagonists caused pericardic edema and branchial arches alteration in 5 dpf larvae.

Free-swimming ability of treated animals was compared to vehicle controls at 72 hpf and 5 dpf by using DanioVision (Fig. 35-36). Row data were analyzed by EthoVision XT software, showing that animals treated with CB1 antagonists had a significant reduction in motility, even at lower concentrations, both in terms of distance and velocity. At higher concentrations, this behavioral phenotype was drastically more severe (Fig. 35 and 36).

On the other hand, 5 dpf larvae treated with CB2 antagonist showed a lower mean velocity and moved less compared to the control larvae during the observation period only when exposed to higher concentrations (2,5 and 5 μM) (Fig. 36).

Collectively, these data suggest that CB1 and CB2 receptors are needed for the proper function of the locomotor system. Of interest, since we found that 2-AG reduction is responsible for motility alterations, we hypothesize that this neuromodulator plays an important role in motor control *via* CB1 and CB2 activation.
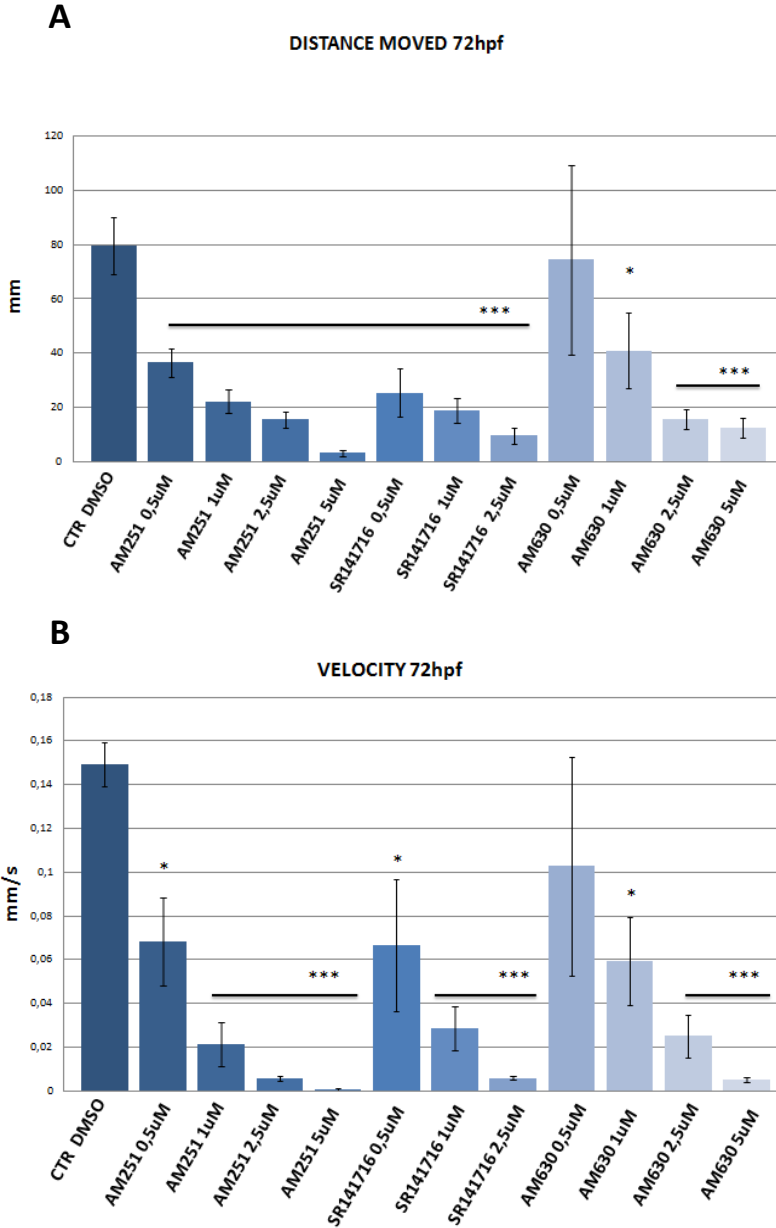
Figure 35: Locomotion is impaired in pharmacological treated larvae at 72 hpf. Treated larvae had impaired spontaneous movements compared with control in term of distance (A) and velocity (B). This phenotype was quantitatively assessed by using Ethovision XT software analysis. Data are shown as means ± SEM of 3 independent experiments; *P < 0.05; ***P < 0.0001.
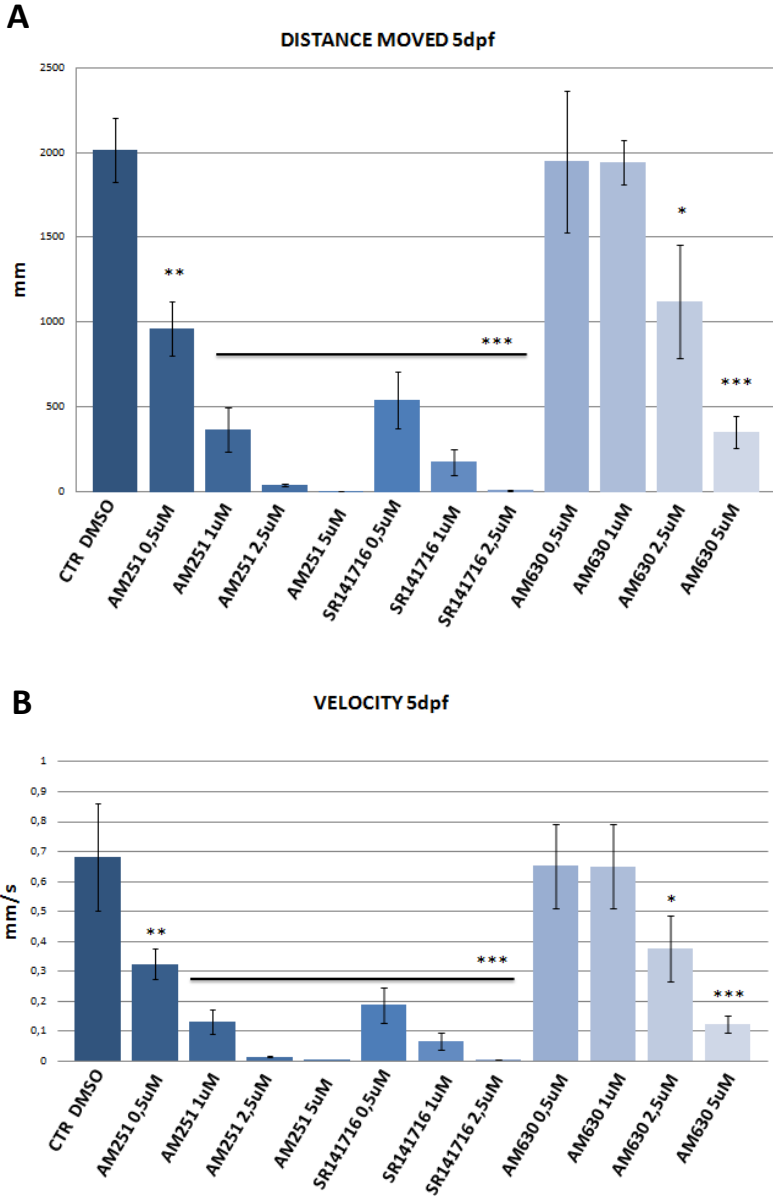
Figure 36: Locomotion is impaired in pharmacological treated larvae at 5 dpf. Treated larvae had impaired spontaneous movements compared with control in term of distance moved (A) and velocity (B). This phenotype was quantitatively assessed by using Ethovision XT software analysis. Data are shown as means ± SEM of 3 independent experiments; *P < 0.05; **P < 0.01; ***P < 0.0001.

5.12 The role of ECS in retinotectal axon guidance

Since malformations of the optic nerve lead to reduced vision or even blindness, the axonal outgrowth deficits that we detected in zebrafish *daglα* morphants, together with the alterations in optokinetic performance, prompted us to test whether the ECS could have a role in the correct orientation of axons in the developing retino-tectal system. This system consists of a variety of cell types, and retinal ganglion cells (RGCs) are an excellent model system to tackle the above question. Restricted to a layer adjacent to the inner basement membrane, RGCs show typical neuronal polarity, with basally oriented axons and apically oriented dendritic trees. RGCs, whose cell bodies are located in the ganglion cell layer (GCL), send axons *via* the optic nerve that relay information outside of the retina, to the optic tectum in non-mammalian vertebrates and to the superior colliculus (SC) in mammals. The journey of elongating RGC axons is complex. As RGCs differentiate, their axons navigate to the optic disc (optic nerve head), fasciculate and exit the eye as the optic nerve (*Oster et al.*, 2004; *Bao et al.*, 2008). After leaving the eye, axons navigate to the ventral diencephalon midline where they form the optic chiasm in the preoptic area (POA) with axons from the contralateral eye by crossing to the contralateral optic tract on their way to the tectum/SC. In animals with monocular vision such as zebrafish, all RGC axons cross the midline (*Petros et al.*, 2008). Innervation of the tectum/SC forms a retinotopic map, such that axons from cells located adjacently in the GCL project to adjacent locations in the tectum/SC (*Oster et al.*, 2004; *Reese*, 2011). Transgenic animals expressing reporter genes in specific classes of neuronal cells are powerful tools for the study of gene expression dynamics

and neuronal network formation. In zebrafish, through the use of a transgene that drive fluorescent proteins under the control of an enhancer-promoter from the *ath5* gene (*atoh7*), it is possible to analyze the differentiation of RGCs from their final mitosis at the apical surface, through the initiation of their axonal and dendritic processes (*Poggi et al.*, 2005). Thus, for this study, we used the zebrafish transgenic line Tg(*pBatoh7:gap43-gfp*)[cb1] ('ath5:gap-gfp') generated in the laboratory of Prof. William A. Harris at the Department of Physiology, Development and Neuroscience, University of Cambridge (UK). This transgenic line, that express a fluorescent protein [enhanced green fluorescent protein (EGFP)] fused to the GAP43 N-terminal palmitoylation signal under the control of the zebrafish *ath5* promoter (*Zolessi et al.*, 2006), allowed us to examine the consequences of genetic and pharmacological manipulations, thus providing an immediate read-out of RGC-specific behaviours. In zebrafish, RGCs begin to differentiate around 28 hpf, then axons exit the eye around 32 hpf, cross the chiasm at 34-36 hpf and fully innervate the tectum at 72 hpf.

We analyzed the zebrafish 'ath5:gap-gfp' larvae at 5 dpf when the RGC are completely formed, finding that dagla-Tb1 MO-microinjected larvae, in 65% of cases, showed an abnormal optic nerve development, whose axons appeared to project abnormally and to stray from the optic nerve before reaching the optic tectum (Fig. 37). Moreover, we compared the size of the tectal neuropil observing that, in 65% of cases, it was ~50% smaller on average in morphants than in their control counterparts (Fig. 38). Also, axonal projections abnormally projecting outside the optic tectum area were observed in 35% of cases.
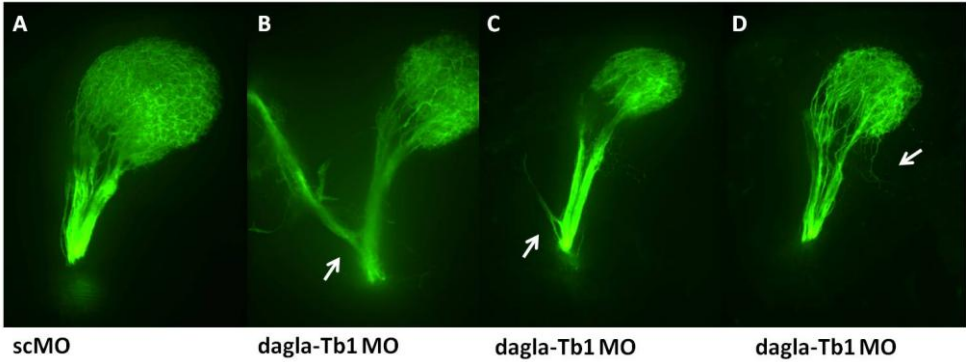
Figure 37: Daglα-depleted embryos show aberrant RGC projections at 5 dpf.
Compared to controls injected with standard control MO (scMO) (A), knock-down of *dagla* causes guidance defects of RGC axons (white arrows), that stray from the optic nerve in 65% of cases (B-C) and project far from the optic tecum area in 35% of cases (D).
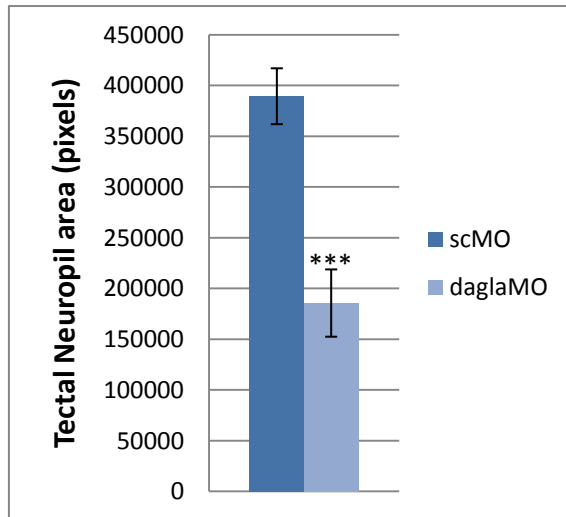
Figure 38: Daglα-depleted embryos have smaller tectal neuropil at 5 dpf. Size comparison of the tectal neuropils in 5 dpf scMO injected larvae and daglα morphant embryos. The area (in pixels) of the tectal neuropils was measured using ImageJ. Data are shown as means ± SEM of 5 independent experiments (repeated measures ANOVA ***P < 0.0001).

In parallel, we performed pharmacological treatments with CB1 and CB2 antagonists on 'ath5:gap-gfp' embryos from the stage of 70% epiboly to 5 dpf. We used two different drug concentrations for CB1 antagonists (2,5 and 5 μM for AM251; 1 and 2,5 μM for SR141716) and two different drug concentrations for CB2 antagonist (AM630: 2,5 and 5 μM). Analyzing CB1 antagonists-treated larvae at 5 dpf, we did not reveal any considerable abnormalities in the development of the optic nerve. Only in few cases (25%) we found some few axons projecting outwardly from the optic tectum in larvae treated with the highest concentration of SR141716. No external projections in the optic nerve fiber tracts were observed in larvae treated with AM251 and AM630 at both concentrations (Fig. 39).

Nevertheless, comparing tectal neuropil in treated larvae with CB1 antagonists with control counterparts, we observed that its size was significantly smaller on average (Fig. 40).

These results suggest that 2-AG synthesized by Daglα could have an important role in proper retinotectal axon guidance and in correct arborization of tectal neuropil, which also requires the activation of the CB1 receptor for its complete formation.
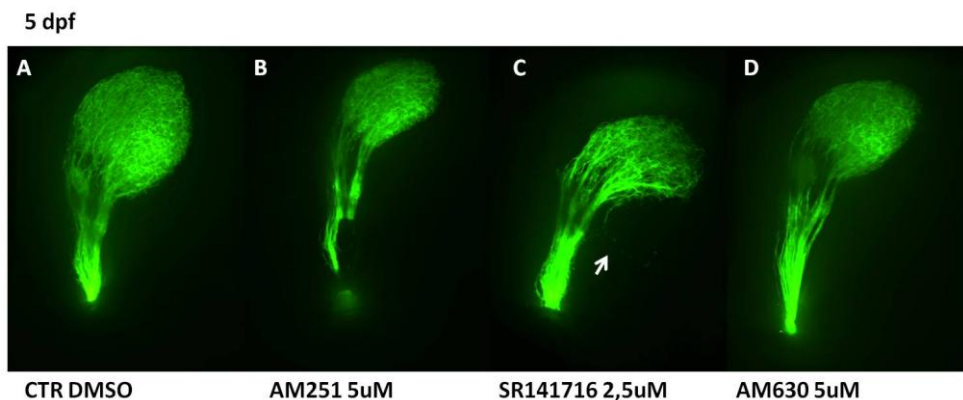
Figure 39: RGC projections in treated larvae at 5 dpf. Compared to control (A), treated larvae did not show any significant defects of RGC axons. (B and D) RGCs of animals treated with the highest concentration of AM251 and AM630. Only in few cases (25%), we found few axons projecting outside the optic tectum (white arrow) in larvae treated with the highest concentration of SR141716 (C).
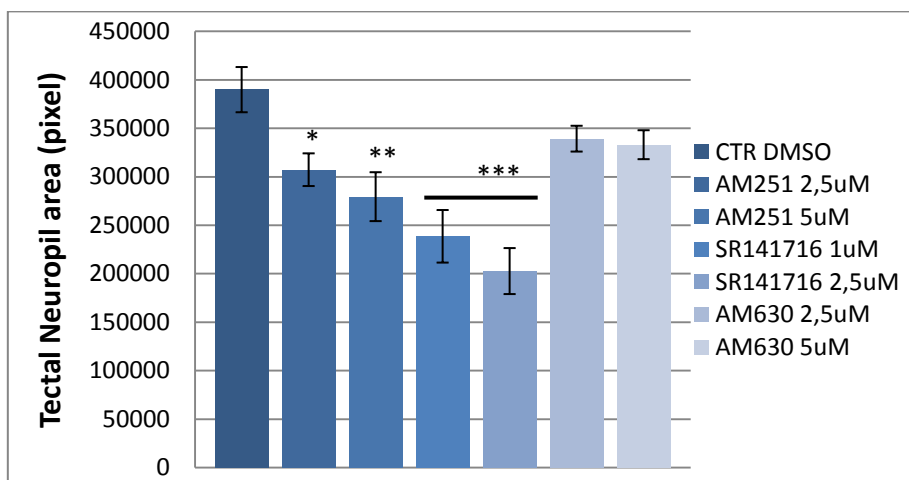
Figure 40: Tectal neuropil area in treated larvae at 5 dpf. Comparison of tectal neuropil size in 5 dpf control and treated larvae. The area (in pixels) of the tectal neuropils was measured using ImageJ. Data are shown as means ± SEM of 3 independent experiments (repeated measures ANOVA *P < 0,05, **P < 0,01, ***P < 0.0001).

5.13 The role of CB2 in retinal lamination

To address the question if the ECS could have a role also in retinal neurogenesis and eye circuit formation, we took advantage of the zebrafish SoFa transgenic line, engineered by the research group led by Prof. W. A. Harris, at the University of Cambridge (UK).

By using SoFa transgenic line it is possible to simultaneously follow the differentiation of major neuronal subtypes in zebrafish retina.

As explained in the Introduction chapter, the zebrafish retina comprises five major neuronal types: photoreceptors (PRs), horizontal cells (HCs), bipolar cells (BCs), amacrine cells (ACs), and retinal ganglion cells (RGCs), and a single type of glial cell, Müller glia.

To generate a SoFa retina, a combination of three different promoter sequences, each driving a different fluorescent protein, was used, so that all main subsets of retinal neurons were labelled in distinct spectral combinations (Fig. 41):

1. Atoh7, a bHLH transcription factor, to mark RGCs and labelled with gapRFP,

2. Ptf1a, a bHLH transcription factor, to label retinal inhibitory neurons, the ACs and HCs, with cytGFP,

3. Crx, a homeodomain transcription factor, expressed in BCs and PRs and labelled with gapCFP.

In SoFa retina, gapRFP expression is first detected in the ventronasal retina adjacent to the choroid fissure at ~28-30 hpf. While gapRFP expression begins to spread through the retina over the next few hours, expression of gapCFP, followed shortly after by the expression of cytGFP, also starts

ventronasally and then follows the gapRFP expression around the retina until ~72 hpf (*Almeida et al*., 2014).
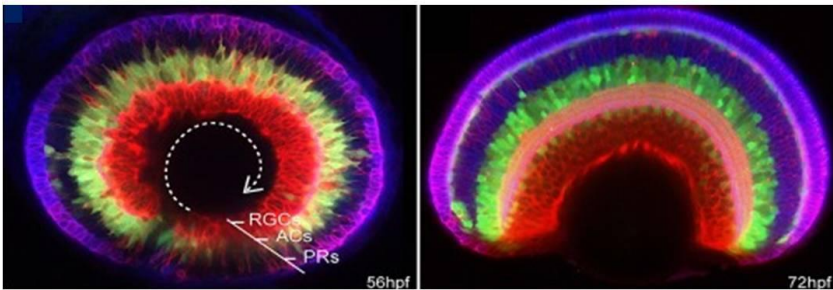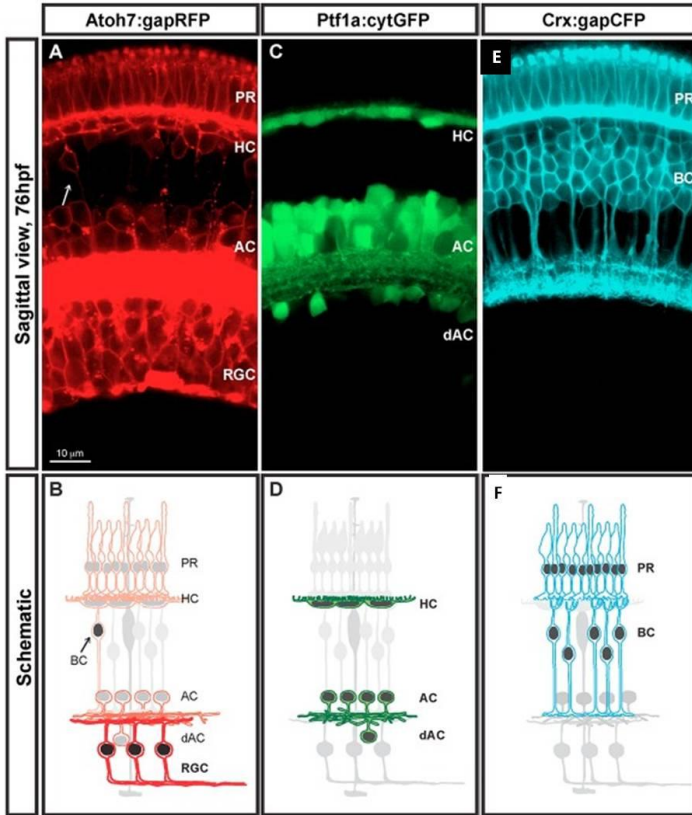
Figure 41: SoFa transgenic line. Reporter protein expression profile and corresponding diagram of each of the three transgenes used to generate the SoFa line (A-F). Adapted from: *Almeida et al*., 2014.

Thanks to the use of zebrafish SoFa line we examined the consequences of genetic and pharmacological manipulations, discovering that treatment with 5 μM CB2 antagonist (AM630) from 70% epiboly to 5 dpf led to the alteration of retina lamination. In particular, we observed a large number of retinal inhibitory neurons retained in the basal RGC layer at 72 hpf and 5 dpf, instead of a correct positioning in the inner nuclear layer (INL) (Fig. 42-43).

The zebrafish retina also contains displaced amacrine cells with their somas in the ganglion cell layer immediately adjacent to the inner plexiform layer (IPL), towards which they project their dendritic arbors (*Jusuf and Harris*, 2009), but in our experimental treatments the soma of Ptf1a-positive cells completely penetrated in the ganglion cell layer.

Of interest, we didn't reveal any significant changes in daglα-MO injected, as well as in CB1 antagonist treated SoFa embryos. This may suggest that the role of CB2 receptor in the zebrafish retina could be mediated by other kind of endocannabinoids different from 2-AG. It remains to be understood whether this could be due to a defect of differentiation, proliferation, or migration.
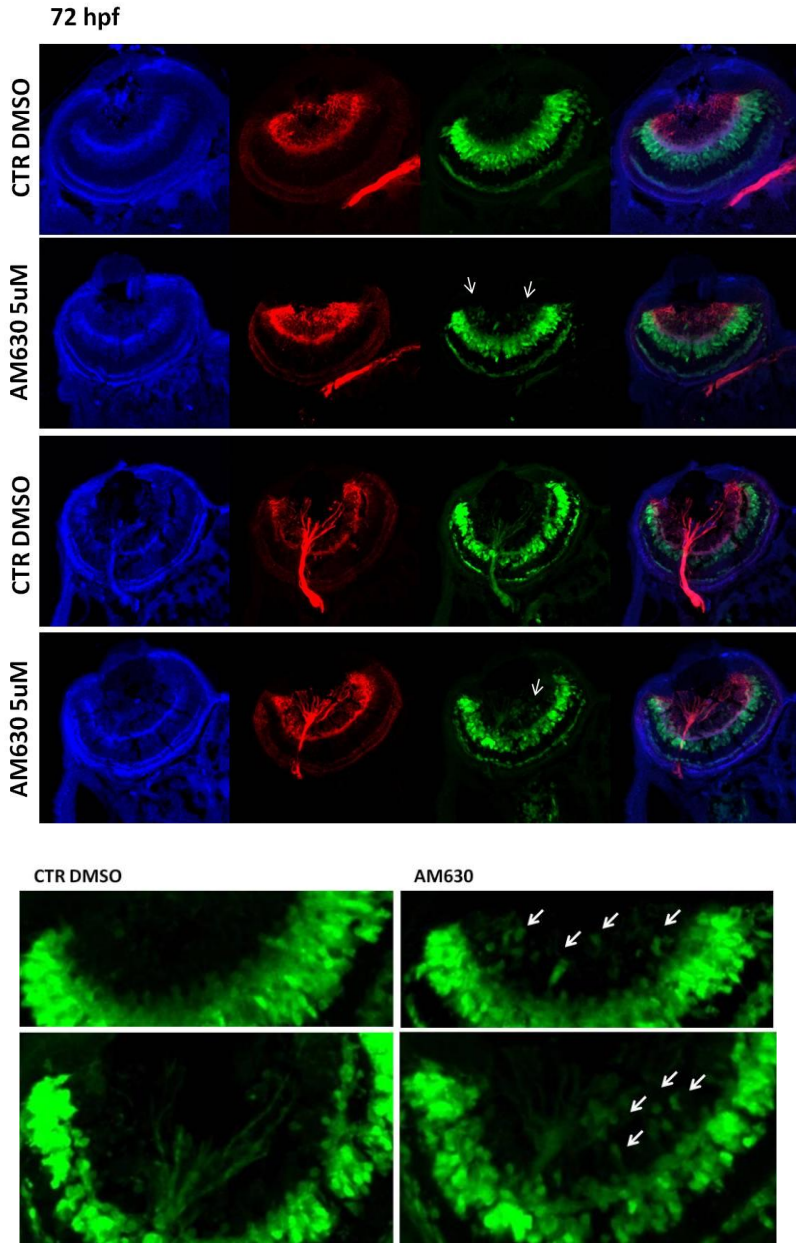
Figure 42: Trasversal sections of SoFa retina treated with CB2 antagonist at 72 hpf. A large number of retinal inhibitory neurons are retained in the basal RGC layer at 72 hpf (white arrows).
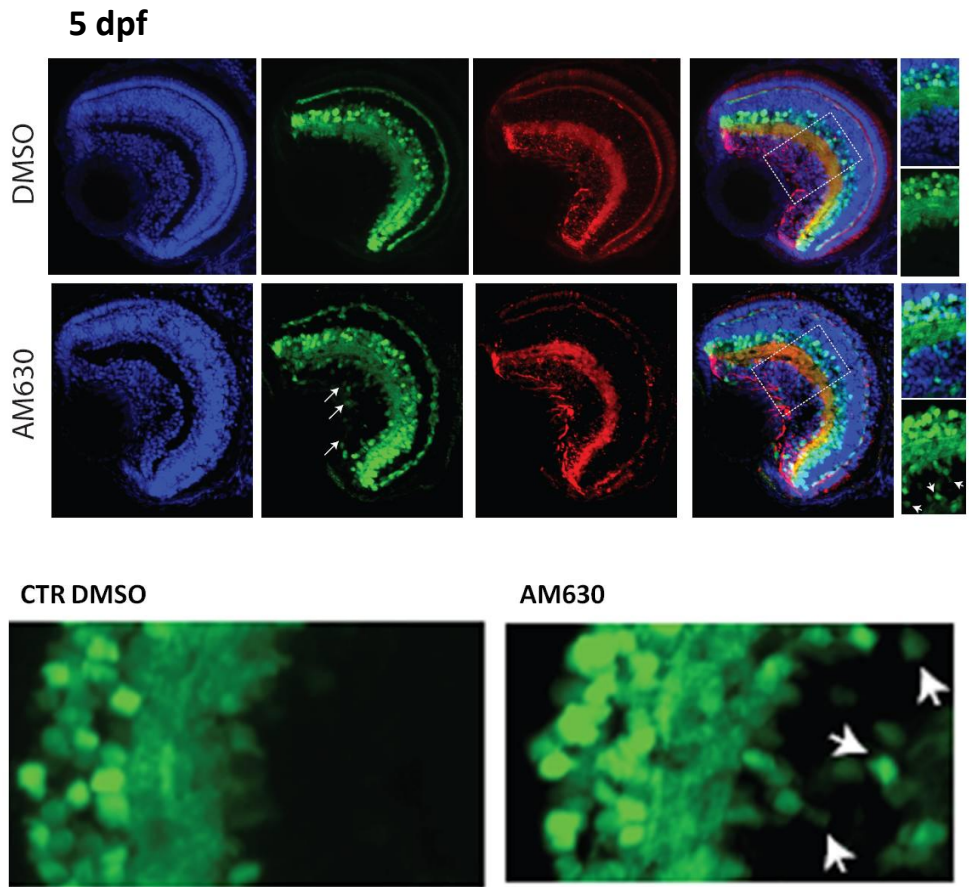
Figure 43: Trasversal sections of SoFa retina treated with CB2 antagonist at 5 dpf. A large number of retinal inhibitory neurons are retained in the basal RGC layer at 5 dpf (white arrows).

5.14 Generation of zebrafish mutants for *dagla* and *cnr1* by CRISPR/Cas9 Technology

Recently, a new tool based on a bacterial CRISPR-associated protein-9 nuclease (Cas9) from *Streptococcus pyogenes* has been generated to make precise, efficient and reliable targeted changes to the genome of living cells.

CRISPR-Cas9 technology was adapted from a naturally occurring genome editing system in bacteria and archaea as a defense mechanism to silence foreign nucleic acids of viruses and plasmids.

By using this system it is possible to direct site-specific genome editing with a small piece of RNA containing a short "guide" sequence (gRNAs) that binds to a specific DNA target sequence in a genome. gRNA also binds to Cas9 nuclease directing a site-specific DNA cleavage.

This mechanism generates DNA double-strand breaks (DSBs) in the target site, that are then repaired via non-homologous end-joining (NHEJ) recombination, resulting in repair errors that generate small insertions and deletions (indels) that disrupt the functions of the targeted gene.

This genome editing technology has provided an accessible tool for studying the role of individual genes in the zebrafish model. With regard to eCB biology, establishing zebrafish lines with mutations in individual genes is indispensable for more precisely studying their function, which could be obscured by potential off-target effects associated with morpholino and pharmacological investigations.

Any observed alterations in physiology or behavior could then be linked to specific molecular signaling cascades, which could be ideally analyzed

with the use of comprehensive methodologies such as RNA sequencing and behavioral assays.

In our study we decided to produce different zebrafish knock-out lines for different genes involved in ECS, starting with *daglα* and *cnr1* in three different genetic background (wilde type AB/TL; ath5:gap-gfp transgenic line and SoFa transgenic line).

Gene-specific gRNAs were prepared using the design tool at https://chopchop.rc.fas.harvard.edu, which finds and ranks all 23-bp gRNA sequences ending in the NGG motif and outputs predictable off-target sites on the basis of sequence relatedness.

We chose two different gRNA for *daglα* (one targeting a region of coding exon 2, one a region of exon 6) and *cnr1* genes (both targeting a different region of coding exon 1) with no predictable off-target sites. Their sequences are presented in Table 6 and their targeting regions illustrated in Fig. 44 and 45.

TABLE 6. gRNA sequence 5'-3'	
daglα coding exon 2	GACAACTGACCAAGATGCCG
daglα coding exon 6	GCTGCTCCGACAGAGACAAC
cnr1 coding exon 1_a	GCTGCGAACGGCTTGGGCAG
cnr1 coding exon 1_b	GCCGATGTACTGCAGGCCGG
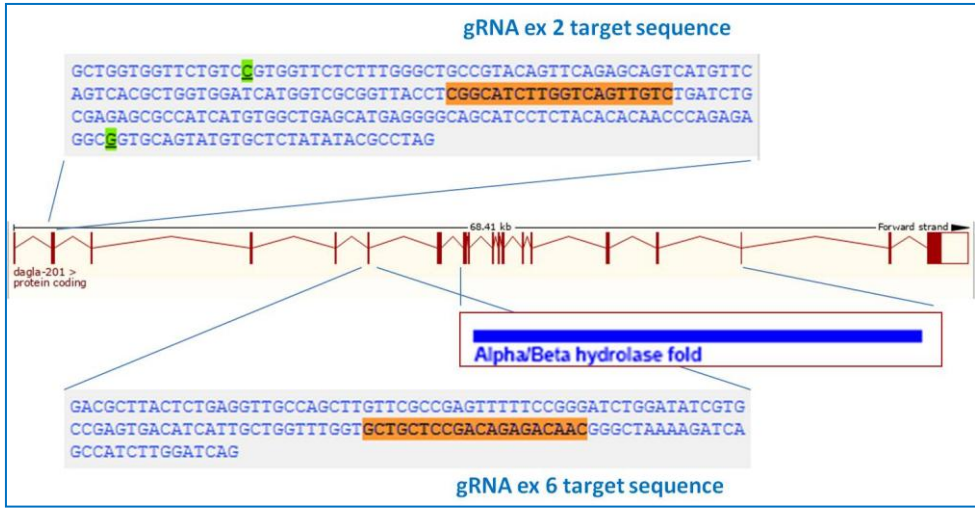
Figure 44: Representation of gRNAs binding sites in *dagla* gene. *dagla* gene consists of 20 exons. Sequences for gRNA synthesis, highlighted in orange, have been designed on the coding exons 2 and 6, located upstream of the protein catalytic domain (alpha/beta hydrolase fold), which starts at exon 8.
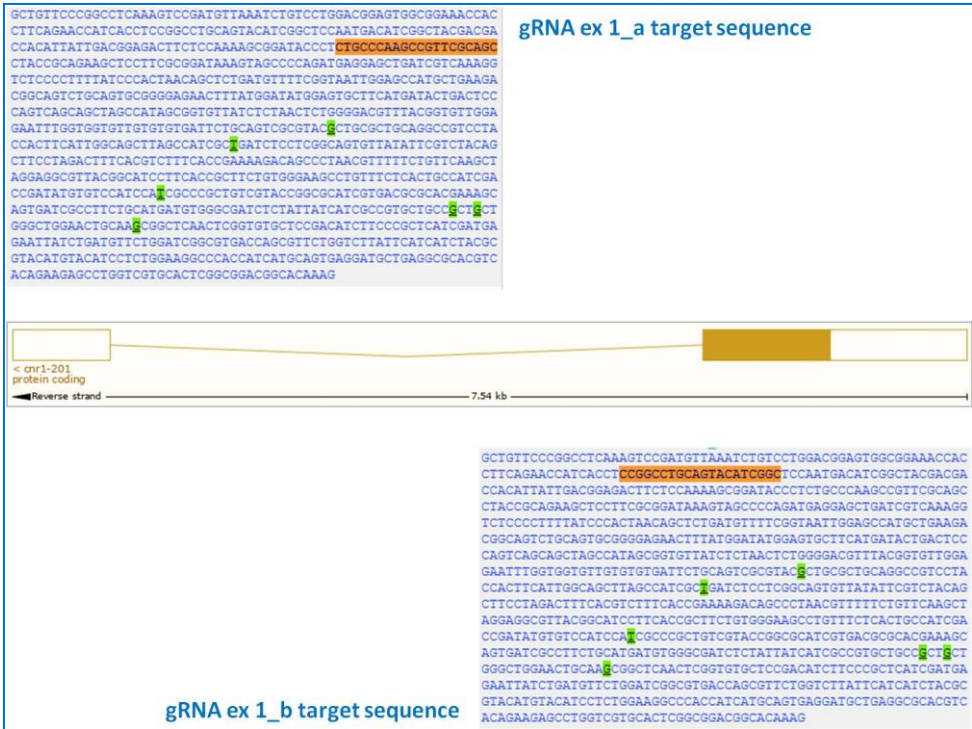
Figure 45: Representation of gRNAs binding sites in *cnr1* gene. *cnr1* gene consists of just 2 exons interspersed with a short intronic sequence. Both sequences for the synthesis of gRNAs, highlighted in orange, have been designed on the coding exons 1.

To synthesize template DNA required for the *in vitro* transcription, we employed a two-oligo PCR method (*Bassett et al*., 2013).

Zebrafish 1-cell stage embryos were injected with single gRNA and Cas9 mRNA.

F0 generation has been allowed to grow for three months and then crossed with the wild-type counterpart to select the founder. To this end, genomic DNA was isolated from a pool of F1 generation embryos, and gRNA binding region was analyzed by Sanger sequencing.

Up to now, only SoFa transgenic lines injected with the gRNAs directed against *daglα* gene exons 2 and 6 has been screened. Analyzing F1 generation by sequencing, we found samples exhibiting mutations both in exon 2 and in exon 6, with alteration of the reading frame (Fig. 46-47).
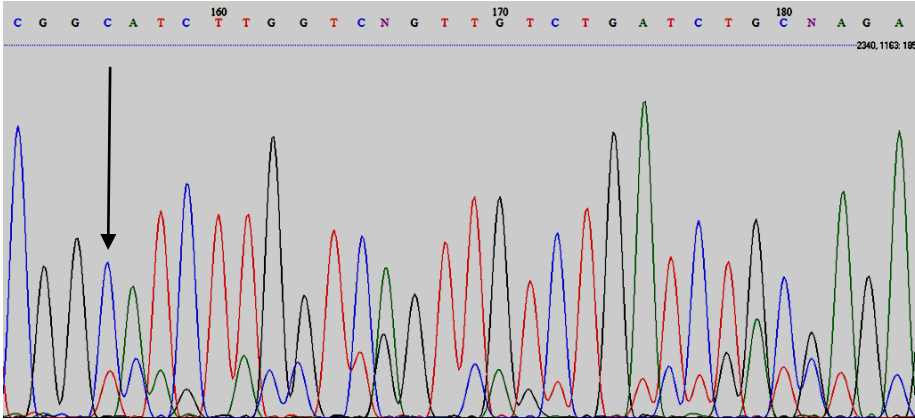
Figure 46: Electropherogram of the *daglα* mutated exon 2. The presence of double peaks indicates an alteration of the reading frame of the analyzed sample.
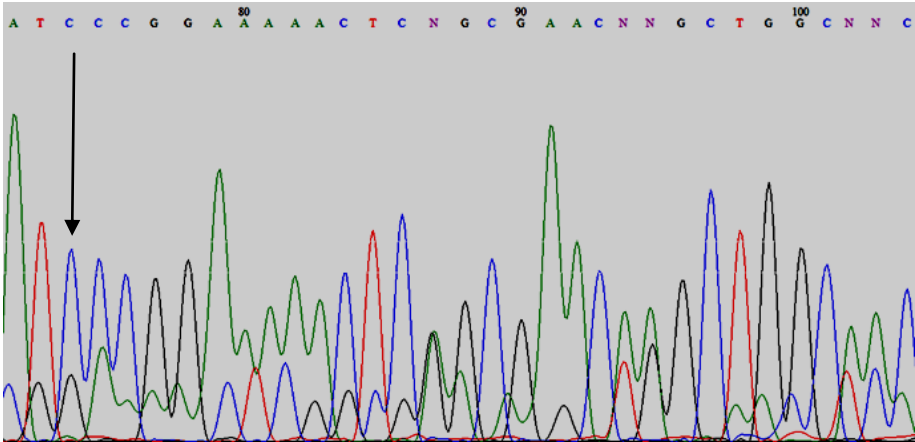
Figure 47: Electropherogram of the *daglα* mutated exon 6. The presence of double peaks indicates an alteration of the reading frame of the analyzed sample.

Spontaneous locomotion analysis was conducted on larvae that presented the above mutations (Fig. 48), finding that the alterations in both exons led to a significant reduction in motility, both in terms of distance moved and velocity, thus confirming the data on the locomotor behavioral assay, obtained by daglα-MOs.
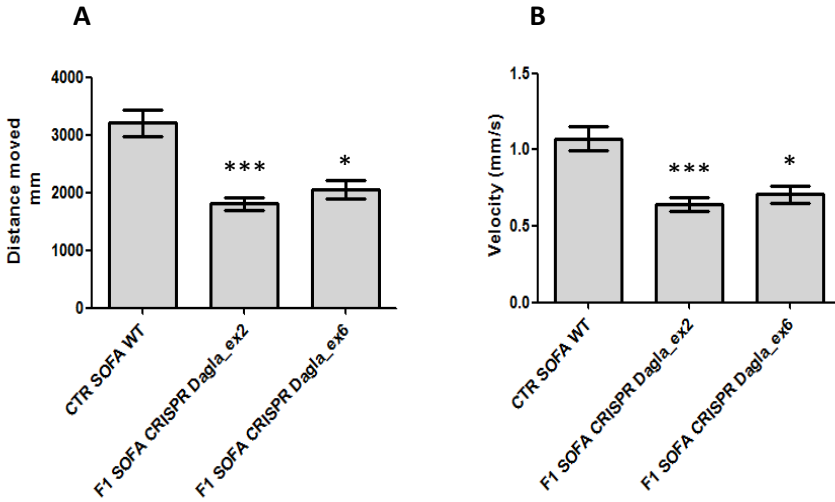
Figure 48: Locomotion is impaired in *daglα* CRISPR/Cas9 larvae at 5 dpf. F1 generation larvae of mutated animals displayed impaired spontaneous movements compared with control in term of distance moved (A) and velocity (B). This behavioral phenotype was quantitatively assessed by using Ethovision XT software analysis. Data are shown as means ± SEM of 3 independent experiments (repeated measures ANOVA *P < 0,05, ***P < 0.0005).

6. DISCUSSIONS AND CONCLUSIONS

On the basis of evolutionary and phylogenetic studies, the ECS seems to be conserved at least in vertebrates (*McPartland et al.*, 2006).

Although *cnr1* and *daglα* mRNA expression had been reported in distinct areas of zebrafish CNS (*Lam et al.*, 2006; *Watson et al.*, 2008), and bioinformatics studies suggested the existence of a complete ECS in this species (*McPartland et al.*, 2007), properties and actions of eCB signalling during zebrafish development have been subject of only few studies, despite clear advantages in using this model organism.

Here, we investigated the expression profiles of different genes known to be involved in endocannabinoid signalling during zebrafish development. Our observational gene expression studies contribute to the existing data about the endocannabinoid system and emphasize the benefit of this model in providing new insights.

Quantitative PCR analysis revealed that all examined canonical and non-canonical eCB receptors exhibited a time-dependent increase during zebrafish development, which likely reflects a specific modulation of eCB levels. Furthermore, substantially different developmental dynamics for AEA and 2-AG metabolism were observed. On one hand, genes that code for AEA biosynthetic (*nape-pld*, *abhd4*) and catabolic (*faah*) enzymes displayed a sequential increase in expression during development. A similar pattern was also found for *daglα*, the gene that encodes the main 2-AG anabolic enzyme, which exhibited the highest transcriptional increment among the examined genes. On the other hand, genes that code for 2-AG degradation enzymes (*ptgs2b*, *mgll*) showed expression levels that were

high in early embryos and decreased during the pre-hatching period that is characterized by important changes since hatched fish start new behavioral activities in response to free-swimming life and chemical cues (*Lindsay and Vogt*, 2004).

Zebrafish embryos displayed an active 2-AG turnover, as the Dagls/Magl activity ratio increased with developmental time, peaking between 48 and 72 hpf, which might explain the intense production of 2-AG during hatching. Of interest, it has been reported that pharmacologic antagonism of CB1 diminishes the hatching rate in zebrafish larvae (*Migliarini and Carnevali*, 2009). Taken together, these data suggest that the specific modulation of 2-AG synthesis during the first days of zebrafish development can play a role as endogenous stimulation of hatching.

Moreover, in this study, mass spectrometry analysis revealed that 2-AG levels were elevated among others eCBs, and was actively produced during zebrafish embryogenesis, suggesting its role as key factor in endocannabinoid signalling functions during zebrafish development.

Using whole-mount *in situ* hybridization to assess spatial and temporal gene expression, we identified CNS areas involved in 2-AG function during zebrafish development. We localized *daglα, daglβ* and *mgll* mRNAs, 2-AG anabolic and catabolic enzymes respectively, and we found that the expression of these three genes spatially overlap with that of *cnr1*, the main 2-AG receptor, in defined neuronal sub-populations within all main developing brain structures, such as telencephalon, optic area, retinal ganglion cells, cerebellum and rhomboencephalon (Fig. 20 F). These findings suggest that the 2-AG pathway is required in brain areas that are implicated in the control of locomotor and visual functions. Of interest,

these genes show also differential expression patterns, hinting that the outcome of 2-AG signaling may also be determined by other transmembrane proteins or that other monoacylglycerols produced by Daglα and other CB receptors might be involved in zebrafish brain development (*Ahn et al.*, 2008; *Di Marzo*, 2011; *Di Marzo and De Petrocellis*, 2012).

To study developmental functions of the eCB signalling pathway with respect to neurogenesis, we addressed the questions of how disruption of 2-AG biosynthesis impairs axon guidance and behavior, and how 2-AG controls development of functional neuronal circuits, as suggested by previous studies (*Watson et al.*, 2008, *Berghuis et al.*, 2007).

We report that 2-AG signaling and eCB receptor activation are required for axon growth in the eye and in defined areas of the developing brain, such as optic tectum, molecular layer of the cerebellum, and optic chiasm. Mechanisms by which ECS exerts its functions are complex and highly spatio-temporally and context dependent, but seem to have an impact on the motion and vision control.

We were able to manipulate expression of the zebrafish *daglα* gene by MO technology. Herein, the majority of specific brain regions that express 2-AG enzymes and receptors (*daglα*, *mgll*, and *cnr1*) show axonal defects in *daglα* morphant larvae.

It is interesting to note that in the *cnr1* zebrafish knockdown, the reticulospinal axons of the hindbrain cross abnormally the midline, with a failure in the formation of the forebrain anterior and posterior commissures (*Watson et al.*, 2008). In the present study, we gained experimental evidence that knockdown of the main 2-AG synthesis enzyme, *daglα*, is

associated with a reduced extension of cerebellum fiber length. Although apparently opposed by a topographic viewpoint, both 2-AG zebrafish models, *daglα* and *cnr1* knockdown, exhibit an aberrant axonal projection towards the midline, in support of the hypothesis that 2-AG can act as a chemoattractant of axon growth cones and regulates their midline crossing (controlaterality).

Impairment of retinotectal, cerebellar, and facial nerves in Daglα-depleted larvae indicates a localized effect on axon guidance and suggests a role for 2-AG in the development of functional locomotor and visual systems.

In addition to a central role of ECS in axogenesis and synaptogenesis, evidence is accumulating that the ECS mediates visual signalling by controlling axon transport and excitability in retinotectal circuitry (*Ryskamp et al*., 2014) and that it plays a role in the initiation and coordination of movement by modulating GABA, glutamate, and other neurotransmitters throughout the basal ganglia and cerebellum (*El Manira and Kyriakatos*, 2010; *Sañudo-Peña et al*., 2000).

In zebrafish, superficial tectal layers receive unprocessed visual information from retinal ganglion cells and contribute to larval visual system by coordination of eye and body movements *via* connections with cerebellar circuits (*Stuermer*, 1988; *Heap et al*., 2013; *Gahtan et al*., 2005). The zebrafish 2-AG knockdown model presented here displays compromised processing and/or transmission of visual inputs and motor outputs, thus providing a useful system to further investigate the role of the ECS in vision and locomotion. Indeed, zebrafish *daglα* morphants generated herein did suffer visual and swimming problems compared with uninjected sibling and standard control MO-injected larvae.

The consequences of Daglα depletion were that the swimming and visual performance was worse in 72 hpf and 5 dpf morphant larvae, respectively, compared with controls (Figs. 29 and 32). This closely reflected loss of motility (*El Manira and Kyriakatos*, 2010; *Song et al.*, 2012) and visual condition (*Ryskamp et al.*, 2014; *Cécyre et al.*, 2013; *Yoneda et al.*, 2013) that has been observed in other vertebrate model organisms.

The correlation between eCB signaling function and axonal and behavioral defects was further established by treatment of morphants with noladin ether, a CB1 agonist that differs from 2-AG because it is an ether and not an ester, and, as such, it is stable to enzymatic hydrolysis by Magl. Consistent with a crucial role exerted by Daglα in 2-AG biosynthesis in the brain, we demonstrated that incubation of *daglα* morphants with noladin ether confers partial rescue of axogenesis and spontaneous swimming.

Since we found that 2-AG reduction is responsible for motility alterations we hypothesized that this neuromodulator may play an important role in motor control *via* CB1 and CB2 activation. To validate this assumption, we treated zebrafish embryos with CB1 and CB2 receptor antagonists, showing that these animals displayed a defective swimming behavior, with a lower mean velocity and a lesser distance moved compared to the control larvae (Fig. 35-36). Therefore, these data lend support to the hypothesis that CB1 and CB2 receptors are needed for the proper function of the locomotor system.

Finally, the axonal outgrowth deficits that we detected here in zebrafish *daglα* morphants, together with the alterations in optokinetic performance, prompted us to gain new insight on the ECS role in the correct formation of axons in the developing retina and retino-tectal system.

For this purpose, we used different transgenic animals that express reporter genes in specific classes of neuronal cells and are powerful tools for the study of gene expression dynamics and neuronal network formation.

In the zebrafish transgnic line ath5:gap-gfp it is possible to follow the differentiation of retinal ganglion cells (RGCs).

We analyzed zebrafish 'ath5:gap-gfp' larvae at 5 dpf when the RGC are completely formed, finding that dagla-Tb1 MO-microinjected larvae showed abnormal optic nerve development, whose axons projected abnormally and strayed from the optic nerve before reaching the optic tectum (Fig. 37). Moreover, comparing the size of the tectal neuropil we observed that it was ~50% smaller on average in morphants than in their control counterparts (Fig. 38).

Furthermore, pharmacological treatments using antagonists suggested a putative role of CB1 receptor in the correct formation of the tectal neuropile in zebrafish transgenic line 'ath5:gap-gfp'.

These results lend support to the hypothesis that 2-AG, synthesized by Daglα, has an important role in the proper retinotectal axon guidance and in correct arborization of tectal neuropil, which also requires the activation of CB1 receptor for its complete formation.

To address the question if the ECS has a role also in retinal neurogenesis and eye circuit formation, we took advantage of the zebrafish SoFa transgenic line, in which all major retina neuronal subtypes are simultaneously labelled. Treatments on zebrafish embryos with a CB2 antagonist highlighted a potential role in the correct lamination of neuroretina, by regulating the positioning of interneurons (amacrine cells) in the inner plexiform layer of developing retina.

Of interest, we didn't reveal any significant changes in daglα-MO injected, as well as in CB1 antagonist treated SoFa embryos. This may suggest that the effects of CB2 receptor could be mediated by other endocannabinoids, different from 2-AG, that are present in the zebrafish retina. It remains to be understood whether this could be due to a defect of differentiation, proliferation, or migration.

In conclusion, our results point to the important role of eCBs as mediators in axonal outgrowth in defined area of developing brain, with implications in the control of vision and movement, highlighting that the well-established role of 2-AG in axon guidance is required in brain areas that control locomotor and optokinetic functions. On the other hand, the eCB receptors CB1 and CB2 can specifically regulate the formation of retinotectal system, and the differentiation and lamination of zebrafish neuroretina, respectively, as well as they are implicated in the control of swimming behaviour.

7. FUTURE PERSPECTIVES

In the light of the data obtained so far, our research project is intended to continue on the role of the endocannabinoid system in the formation of neuronal circuits involved in the development of visual and locomotor systems.

The 2-AG knocking-down phenotype, together with pharmacological treatments and the generation of mutant lines, will represent powerful tools for understanding the mechanisms of cell fate acquisition, for further insights of the specific molecular targets and components of ECS signalling mechanisms, and for defining new therapeutic approaches.

Although zebrafish can significantly advance the understanding of eCB biology with the use of pharmacological or genome editing approaches, the greatest contribution of this small model vertebrate to the field will likely result from studies enabled through combined approaches.

Any observed alterations in physiology or behavior could then be linked to specific molecular signaling cascades, which could be ideally analyzed with the use of comprehensive methodologies such as RNA sequencing and behavioral assays.

In conclusion, we propose to investigate the cellular/molecular mechanisms downstream of 2-AG signaling, in order to gain new insights on the poorly characterized role of the endocannabinoid system in vision and locomotion, studying the global dynamics of development and particularly the interactions between cell types. This study shows how such an integrative approach can be used to shed new light on the acquisition of neuronal fates and early steps of cell differentiation.

8. MATERIALS AND METHODS

8.1 Zebrafish maintenance and transgenic fish line

Zebrafish (*Danio rerio*) experiments were performed in accordance with the European Union animal welfare guidelines [European Communities Council Directive of September 22, 2010 (2010/63/ UE)]. Zebrafish were maintained according to standard procedures on a 14-h/10-h light/dark cycle at 28.5°C, as described previously (*Westerfield,* 2000).

Embryos were obtained from our animal colony by natural spawning and were maintained in E3 medium (5 mM NaCl, 0.17 mM KCl, 0.33 mM CaCl$_2$, 0.33 mM MgSO$_4$, 1x10^{-5}% methylene blue) and were staged according to hpf and morphologic criteria (*Kimmel et al.*, 1995). In particular, embryo euthanasia was performed via hypothermia shock by submerging the embryos in ice-cold water for at least 10 min to ensure death by hypoxia, or with an overdose of tricaine MS-222 (Sigma, E10521). All experiments were conducted on WT embryos at 24, 48, 72 hpf, and 5 dpf.

Homozygous Tg(Atoh5:GAP:EGFP) transgenic fishes were generated in Harris' laboratory: *Tg(pBatoh7:gap43-gfp)^{cb1}* ('*ath5:gap-gfp*'). They express a fluorescent protein [enhanced green fluorescent protein (EGFP)] fused to the GAP43 N-terminal palmitoylation signal, under the control of the zebrafish *ath5* promoter (*Zolessi et al*., 2006).

The polychrome transgenic line Atoh7:gapRFP/Ptf1a:cytGFP/Crx:gapCFP (SoFa) was characterize by William A. Harris' group and were generated by crossing following single with double transgenic lines: Atoh7:gapRFP (*Zolessi et al*., 2006), Ptf1a:cytGFP (*Godinho et al*., 2005), Crx:gapCFP (*Suzuki et al*., 2013), described previously.

All transgenic lines were bred each other to obtain transgenic embryos for imaging experiments conducted on homozygous embryos at 72 hpf and 5 dpf.

8.2 Quantitative PCR analysis

Embryos and larvae were staged following standard parameters (*Kimmel et al.*, 1995). Total RNA was isolated from a pool of 20 animals per group using Trizol (Thermo Fisher Scientific, Waltham, MA, USA) and treated with DNase I (Thermo Fisher Scientific), and were reverse transcribed with the SuperScript III RT reaction kit (Thermo Fisher Scientific) according to manufacturer instructions. Of starting RNA, 10-20 ng was used for quantitative PCR analysis using IQ SybrGreen Supermix (Bio-Rad, Hercules, CA, USA) with primers designed with AlleleID (Table 5) on a CFX 384 optical thermal cycler (Bio-Rad). Data analysis was performed by using CFXManager software (Bio-Rad) using *eef1a1l1* (*eukaryotic translation elongation factor 1 alpha 1, like 1*) as reference gene and was expressed as relative mRNA levels with SEM of triplicate reactions. Statistical significance was determined with the REST 2009 software (Qiagen, Valencia, CA, USA).

8.3 Measurement of ECs AEA, 2-AG, and EC-like PEA and OEA from whole zebrafish

Eggs, embryos, and larvae were collected at different developmental time points. Extraction, purification, and quantification of eCBs were performed as previously described (*Bisogno and DiMarzo*, 2007; *Matias et al.*, 2007). In brief, embryos were pestel homogenized and extracted with CHCl3/MeOH/Tris-HCl 50 mM, pH 7.5 (2:1:1 vol/vol) that contained internal standards ([H]8-AEA 10 pmol; [H]5-2-AG, [H]5-PEA, and [H]4-

OEA50 pmol each). The lipid-containing organic phase was dried down, weighed, and pre-purified by open-bed chromatography on silica gel. Fractions were obtained by eluting the column with 99:1, 90:10, and 50:50 (vol/vol) CHCl3/MeOH. The 90:10 fraction was used for AEA, 2-AG, PEA, and OEA quantification by liquid chromatography - atmospheric pressure chemical ionization - mass spectrometry by using a Shimadzu high-performance liquid chromatography apparatus (LC-10ADVP) coupled to a Shimadzu (LCMS-2020) quadrupole mass spectrometry via a Shimadzu atmospheric pressure chemical ionization interface (Shimadzu, Kyoto, Japan) as previously described (*Matias et al.*, 2007). Amounts of eCBs in embryos, quantified by isotope dilution with the above mentioned deuterated standards, were expressed as picomols per milligram of protein as the weight of the dried organic phase was too low to determine total lipid contents.

8.4 Magl and Dagls enzymatic activity studies on zebrafish embryo and larvae

A pool of 50 embryos/larvae for each time point was homogenized. Once we isolated the membrane fraction, 2-AG hydrolysis was measured by incubating 100 mg protein/sample in 50 mM Tris-HCl, pH 7, at 37°C for 20 min with synthetic 2-arachidonoyl-[3H]glycerol properly diluted with unlabeled 2-AG. After incubation, the amount of [3H]glycerol produced was measured by scintillation counting of the aqueous phase after extraction of the incubation mixture with 2 volume equivalents of CHCl3/MeOH1:1 (vol/vol). Dagls activity was assessed as previously reported (*Bisogno et al.*, 2003) by using the membrane fraction (70 mg protein) from the same homogenized sample used for MAGL enzymatic

assay, and 1-[14C] oleoyl-2-arachidonoylglycerol as substrate [1.0 mCi/mmol, 25mM, synthesized as reported previously (*Bisogno et al.*, 2003)] in Tris-HCl buffer, pH7, for 20 min. After incubation, lipids were extracted with 2 volumes of CHCl3/CH3OH (2:1 vol/vol). Organic extracts, lyophilized under vacuum, were purified by using TLC on silica on polypropylene plates eluted in CHCl3/CH3OH/NH4OH (85:15:0.1 vol/vol) as the eluting solvent. Bands corresponding to [14C]oleic acid were cut and their radioactivity was measured with a β-counter. Enzymatic activities are reported as means of n = 3 experiments.

8.5 RNA probes production

Plasmids for synthetizing *cnr1* and *fgf8a* riboprobe were kindly provided by Prof. A. Graham (King's College-London, UK), and Prof. K. Rohr (University of Cologne- Cologne, DE).

For the riboprobes construction of *daglα*, *daglβ*, *cnr2*, *trpv1* and *gpr55* transcripts, the following steps were performed:

- RNA extraction and cDNA synthesis:

Whole zebrafish embryos at different stages (24, 48 and 72 hpf) were killed with an overdose of tricaine MS-222 (Sigma, E10521) and stored at -80°C in 1 ml Trizol® reagent (Thermo Fisher Scientific, 15596018) at least for 24 h for RNA extraction. Embryos were defrosted in ice and were homogenized using TissueLyser II (Qiagen). For separation phase, homogenized sample were incubated for 5' at R.T. to permit complete dissociation of the nucleoprotein complex. Then, 200 μl chloroform were added to homogenates and, after shaking vigorously for 15", samples were incubates for 3' at R.T.. After centrifugation, the aqueous phase was removed and the RNA purification was performed. RNA samples was

purified using 500 μl phenol/chloroform acid solution and, then, were centrifuged to obtain the aqueous phase. RNA samples were precipitated with a solution containing 500 μl 100% isopropanol, 30 μl sodium acetate and 1 μl glycogen as RNA carrier and were stored for 30' at -20°C.

After centrifugation, RNA pellet was washed in EtOH 70%. Isolated RNAs were diluted in 30 μl H_2O DEPC and stored at -80°C for further use.

For cDNA synthesis, 1 μg of RNA was reverse transcribed using QuantiTect® Reverse Transcription Kit (Qiagen, 205313) according to manufacturer's instructions using both oligo (dT) and random primers. Synthesized cDNA was stored at -20°C.

- <u>Amplification of desired DNA fragments and cloning in a suitable plasmid</u>

From the obtained cDNA were generated the template for *daglα*, *daglβ*, *cnr2*, *trpv1* and *gpr55* transcripts by PCR using the following primers:

Gene	Forward 5'-3'	Reverse 5'-3'
daglα	CTTCAGTTTCAGGCTCTCGC	GCACTTTGTTCCTCCAGCAA
daglβ	GTTTTGACGGATCTCTCGGC	GGATGATGGGCAGAGGGTAA
cnr2	CAGTGACTTTCCTGGCGAAC	GCCTGTCTGCACTCCTAGAA
gpr55	CCAACTCATCGACAGACTGTGA	TCGCCATTCTCCTCTCTTTCTG
trpv1	ATGCTGCTTACACCGACAGTTA	TCGCGTAATCCTTCCCTTCTTC

A zebrafish full-length *mgll* clone was obtained from an I.M.A.G.E. cDNA plasmid clone (IRBOp991A0923D) into the pME18S-FL3 vector (Unigene DR.106158; Entrez Gene 378960 – Source BioScience LifeScience).

This clone was amplified by PCR using the following primers for the subsequent subcloning:

Forward 5'-3': GATTTCTGCCTCCAGCATTCAGCCTG

Reverse 5'-3': TAAAGTAGAGATGTGATTGGACAGGGG.

All the obtained fragments were subcloned into pCR™II-TOPO® vector (Invitrogen) according to manufacturer's instructions, and the sequences and insertion directionality were checked for automatic sequencing for capillary electrophoresis at the Molecular Biology and Bioinformatics Unit (Stazione Zoologica Anton Dohrn − Napoli), by using Applied Biosystems (Life Technologies) 3730 Analyzer 48 capillaries.

- Digoxigenin-labeled antisense riboprobes synthesis

To produce digoxigenin and fluorescein (*fgf8a*) − labeled antisense riboprobes, the templates were linearized and transcribed with the appropriate restriction enzyme and RNA polymerase (Table 7).

TABLE 7: ENZYMES for ANTISENSE RIBOPROBES PRODUCTION		
TEMPLATE	RESTRICTION ENZYME	RNA POLYMERASE
daglα	NotI	Sp6
daglβ	NotI	Sp6
mgll	KpnI	T7
cnr1	EcoRV	Sp6
trpv1	EcoRV	Sp6
cnr2	NotI	Sp6
gpr55	EcoRV	Sp6
fgf8a	XhoI	T7

8.6 Whole mount in situ hybridization (WISH)

WISH analyses were performed as previously described (*Westerfield*, 2000). Briefly, zebrafish embryos at different stages (24, 48 and 72 hpf) were anaesthetized with tricaine MS-222 and fixed in 4% paraformaldeide (PFA) overnight at 4°C. Larvae were washed in 1X PBS 3 times 10 minutes and dehydrated in a MeOH series for storage in 100% MeOH at -20°C until further use. Embryos were rehydrated stepwise in methanol ∕ PBS and finally put back in PBT (PBS 1X Tween 0,1%).

Samples were incubated in proteinase K (10μg/ml in PBT) for 5' (24 hpf), 15' (48 hpf), 30' (72 hpf). Reactions were stopped by rinsing in PBT followed by post fixation in 4% PFA in 1X PBS for 20 min at R.T. and by rinsing four times in PBT. Zebrafish embryos were pre-hybridized for 3 h at 63°C in hybridization buffer and, then, they were incubated O.N. in the hybridization solution containing 200 ng of the probe at 63°C (probe was denatured for 10 min at 95°C). The probes were removed by 30' step-wise washes in 100, 75, 50 and 25% hybridization buffer and 2X SSC, in 2X SSC for 10', in 0.2X SSC for 30', in 10 mM PIPES and 0.5 M NaCl for 10' and, finally, in maleic buffer tween-20 (MBT). Subsequently, zebrafish embryos were incubated in 2% Roche Blocking Reagent (Roche Applied Science, code 11096176001) for 2 h and, then, left in Fab fragments from polyclonal anti-digoxigenin antibodies, conjugated to alkaline phosphatase (Anti-Digoxigenin-AP, Fab fragments, Roche Applied Science, code 11093274910) at a 5.000-fold dilution in blocking reagent O.N. at 4°C. After several washes in MBT, embryos were incubated in a staining buffer and, then, in BM Purple chromogenic substrate (Roche Applied Science, code 11 442 074 001) until staining was sufficiently developed. After

stopping the reaction, embryos were post fixed in 4% PFA in 1X PBS for 20' and, finally, stored in 95% glycerol at 4°C.

Double-fluorescent WISH was performed as previously indicated (*Brend and Holley*, 2009).

Whole mount chromogenic zebrafish samples were imaged on a Zeiss AxioImager.M1 microscope with 10X or 20X objective. Whole mount fluorescent zebrafish preparations mounted on slides were imaged on a Zeiss LSM 710 laser scanning confocal microscope with 20X objective. Excitation and emission wavelengths were set according to the fluorophore used. All experiments were conducted in triplicates.

8.7 MO knockdown

- <u>Zebrafish embryo injection</u>

MO injection was used to block specific gene translation. For *daglα* and *mgll* knockdown experiments, antisense MO oligonucleotides designed to bind to the start codon (dagla-Tb1 and mgll-Tb1), to the *daglα* exon 3 splice donor site (dagla-Sb1), and to the *mgll* exon 2 splice donor site (mgll-Sb1) were purchased from Gene Tools (Philomath, OR, USA). MO sequences were as follows:

dagla-Tb1: 5' – TGCCCGGCATCACTGCCCTGAAACA – 3';

dagla-Sb1: 5' – GTGTTCACAGTGTACGTCTTACCTA – 3';

mgll-Tb1: 5' – CATGTCCCCGCTGAGGGTTGAGTCA – 3';

mgll-Sb1: 5' – TATGTCATCTCACACTTACTTCGGA – 3'.

Upon receiving lyophilized MOs, a 1 mM stock solution in sterile water was prepared and stored at -20°C. Titration of MOs to find effective concentrations is shown in Fig. 23. Wildtype zebrafish were injected into the yolk at 1–2 cell stages with desired MO concentration (300 μM) in

sterile water using phenol red at 0.05% as an injection indicator. Control embryos were injected with standard control MO (300 µM).

Embryos were lined up on a plastic dish against a glass slide in a medium-free environment. Injections were performed using 0.78 mm needles pulled with a needle puller (1.0 mm OD × 0.78 mm, Harvard Apparatus; puller: Pul-1, World Precision Instruments) and 1 nl of volume was pressure injected using an air-pressure injector (Picospritzer II; Intracel).

For RT-PCR analysis of dagla and mgll splicing products after MO injection, total RNA was isolated from a pool of 100 embryos at 24 hpf using Trizol (Thermo Fisher Scientific) and was reverse transcribed with QuantiTect Reverse Transcription Kit (Qiagen), as described above.

Primers were designed in exon 3 and exon 4 of *daglα*:

forward: 5'-CGAGAGCGCCATCATGTGGC-3'

reverse: 5'-CGAGGGCGAGGTTCTTAGCG-3'

and in exon 2 and exon 3 of *mgll*:

forward: 5'-ATGCCGGAACCGAGGGACT-3'

reverse: 5'-CGTGGTCGTGGCGAACACCA-3'.

1 µg of cDNA was amplified for RT-PCR analysis and reaction conditions were performed as follows: 95°C for 5 min, followed by 30 cycles of 95°C for 1 min, 55°C for 1 min, 72°C for 1 min, and a final extension step of 72°C for 10min. PCR products were visualized by using 1.5% agarose gel electrophoresis, subcloned into pCR™II-TOPO® vector (Invitrogen), and then subjected to automatic sequencing for capillary electrophoresis at the Molecular Biology and Bioinformatics Unit (Stazione Zoologica Anton Dohrn – Napoli), by using Applied Biosystems (Life Technologies) 3730 Analyzer 48 capillaries.

8.8 Pharmacological treatments and exposure windows

To perform dose-response curve in order to identify sub-lethal drug concentrations, six groups of 30 fertilized eggs were placed in individual wells of 6-well plate. The AM251 (Tocris, 1117/1), SR141716 (Tocris, 0923/10), AM630 (Tocris, 1120/10) treatment began at 7 hpf until 5 dpf. Each group was exposed to 0,5 μM, 1 μM, 2,5 μM, 5 μM, and 10 μM. An untreated control group of 20 fertilized eggs was examined in parallel. For each group (control and treated) DMSO at final concentration of 0.1% was added. Observations for any developmental effects due to treatment were made at 24, 48, 72 hpf and 5 dpf. Mortality and morphological deformities of embryos were recorded and photographed. Dead embryos were removed immediately once observed. Test drug solutions were renewed daily. Once we have selected the sub-lethal drug (10 μM for AM251 and AM630, 5μM for SR141716) concentrations for our study, groups of 30 fertilized eggs were exposed to drug treatments from 7 hpf until to 5 dpf. The above-mentioned experiments were performed in biological triplicates.

8.9 Whole mount immunohistochemistry

Immunostaining was done by using standard whole-mount immunostaining protocol with Vectastain elite ABC kit (Vector Laboratories, Burlingame, CA, USA) (*Westerfield*, 2000). Zebrafish larvae at 72 hpf were anaesthetized with tricaine, MS-222, and fixed in 4% paraformaldeide (PFA) overnight at 4°C. Larvae were washed 3 times in 1X PBS for 10 minutes and dehydrated in a MeOH series for storage in 100% MeOH at -20°C until further use. Animals were rehydrated stepwise in methanol/PBS, and then putted in PBS-Triton 0.8%. To remove pigmentation, zebrafish larvae were bleached with a bleaching solution containing potassium

hydroxide and hydrogen peroxide for 30'. Samples were, then, permeabilized with proteinase K (10µg/ml) for 30' at RT, washed in in PBS-Triton 0.8% and post- fixed in PFA for 20'. Larvae were incubated with blocking solution of 5% normal horse serum (NHS) for 1 h at R.T. on a shaker. Samples were incubated O.N. in blocking solution containing the monoclonal anti-acetylated tubulin primary antibody (Sigma-Aldrich, St. Louis,MO, USA) at 1:1000 concentration. After several washes in PBS-Triton 0.8%, samples were incubated with an hydrogen peroxide solution diluted in MeOH to block endogenous peroxidases and, then, with an anti-mouse IgG biotinylated secondary antibody (1:200), diluted in blocking solution O.N. at 4°C on shaker.

After several washes in PBS-Triton 0.8%, samples were incubated with avidine-biotine solution (Vectastain ABC kit, PK6102) and, finally, the incubation with the chromogenic substrate 3,3'-diaminobenzidine (DAB) was performed according to manufacturer instructions. For DAB detection, 1 µl of 0.6% H_2O_2/ml DAB solution was added, until staining was sufficiently developed. For detailed analysis, embryos were postfixed in 4% paraformaldehyde for 20 min at room temperature, washed in PBS that contained 0.1% Tween 20, and gradually transferred to 90% glycerol and stored at 4°C. Whole mount chromogenic zebrafish samples were imaged by using a Zeiss AxioImager.M1 microscope equipped with Axiocam digital camera (Zeiss) with 10X or 20X objective.

To detect and quantify superficial neuropil layer (SNL) axons, a manual counting was performed. Statistical significance of axon phenotype measurements was determined with Prism (version 6; GraphPad Software, La Jolla, CA, USA). Statistical analysis was performed by using Kruskal-

Wallis test followed by Dunn's multiple comparison test. All experiments were conducted in triplicates.

8.10 Optokinetic response

Large-field movements in the visual environment induce spontaneous, compensatory eye movements known as optokinetic responses (OKRs). In brief, larvae [5 days post fertilization (dpf)] were embedded in 3% pre-warmed (28°C) methylcellulose in a Petri dish to prevent body movements without affecting eye movements. The Petri dish was surrounded by a drum screen, upon which computer-generated stimulus patterns can be projected (PLV-Z3000; Sanyo, Moriguchi, Japan). Stimulus patterns consisted of vertical black-and-white sinusoidal gratings rotating around the larvae. Larvae were illuminated by infrared emitting diodes (peak 940 nm, BL0106-15-28; Kingbright, Taipei, Taiwan) from below and were recorded by an infrared-sensitive CCD camera (GuppyF-038B NIR; AlliedVision, Exton, PA, USA) from above. To determine contrast sensitivity, a spatial frequency of 20 cycles/360° and an angular velocity of 7.5°/s were applied with varying contrast (5, 10, 20, 40, 70, and 100%). To examine spatial sensitivity, an angular velocity of 7.5/s and 70% of maximum contrast was applied with varying spatial frequency (7, 14, 21, 28, 42, and 56 cycles/360°). To explore temporal sensitivity, maximum contrast and a spatial frequency of 20 cycles/360° were applied with varying angular velocity (5, 10, 15, 20, 25, 30°/s). Data were analyzed and figures were prepared by SPSS (version 22.0; Chicago, IL, USA).

8.11 Locomotor assays

Locomotor analysis was performed using Noldus EthoVision DanioVision (Noldus, Leesburg, VA, USA) technology, a fully automated, high-

throughput system designed for quantitative analysis of locomotory performance. It consists of an observation chamber, a high-quality digital camera, and Etho-Vision XT software. Fish larvae (72 hpf and 5 dpf) were placed one-per-well in a 96-well plate with clear bottoms in pre-warmed (28°C) E3 medium. Locomotion was observed using the lightON/lighOFF protocol. After an adaptation period of 10 min to a LED illumination source used to provide an even distribution of light across the multiwell plate, larvae were subjected to a light stimulus with 100% white light intensity for 10 min, after which they were returned to a condition of darkness for other 10 min. This repeated 2 times. Tracking duration was 50 min. All experiments were conducted in a room separate from the main zebrafish facility and the presence of the experimenter in the recording room was limited to the initial minute of recording in order to minimize extraneous stimuli. All videos were recorded between the 10:00 am and 2:00 pm. For the recording of movements and post-experimental data processing, movement was recorded and automatically analyzed by the EthoVision XT software package. All recording and analysis were achieved in real time. Data analysis enables immediate recognition of parameters, such as total distance moved and mean velocity. Locomotor parameters were calculated for 12 embryos per group and over three different video acquisitions, and averaged for each treatment.

8.12   Transgenic lines imaging

Atoh5:GAP:EGFP zebrafish transgenic line morphological analysis was done at 5 dpf, when the tectum is fully innervated. MO-injected and pharmacological treated zebrafish embryos were fixed with 4% PFA and then rinsed 3 times in 1X PBS at 5 dpf and kept at 4°C for a minimum of

24 h. For visualization of labeled axons, both eyes were removed using dissection pins and larvae were mounted laterally in a custom-made glass bottom dish in 1.2% low-melting-point agarose (24–28°C gelling point; Promega). Images were acquired using a PerkinElmer Spinning Disk UltraVIEW ERS; Olympus IX81 Inverted confocal microscope, and 30X UPLSAPO objectives (NA 1.3) water-immersion objective. Images were analyzed using Volocity 3D Image Analysis Software (RRID:SCR_002668; PerkinElmer).

SoFa zebrafish transgenic line morphological analysis was done at 3 and 5 dpf, when the retina is fully differentiated. Zebrafish larvae were fixed for 3 h in 4% PFA at RT, rinsed $3 \times$ in 1X PBS, and put in 30% sucrose in 1X PBS over night. Embryos were embedded in Tissue-TEK OCT compound (SAKURA) and quick frozen on dry ice or at -80°C. Transverse retina sections with a 20 μm thickness were cut using a cryostat (CM3050S; Leica)

Slides were washed 3×10 min in PBS, drained off, and mounted with FluorSave reagent. All slides were imaged using a PerkinElmer Spinning Disk UltraVIEW ERS; Olympus IX81 Inverted microscope, and 30X UPLSAPO objectives (NA 1.3) water-immersion objective. Images were analyzed using Volocity 3D Image Analysis Software (RRID:SCR_002668; PerkinElmer).

8.13 Genome Editing using CRISPR/Cas9 Technology

- sgRNA design and template synthesis

sgRNAs were designed using the design tool at https://chopchop.rc.fas.harvard.edu, which finds and ranks all 23-bp sgRNA sequences ending in the NGG motif. It also outputs predictable off-

target sites on the basis of sequence relatedness. Because of a restriction of the T7 RNA polymerase in our synthesis, only sgRNAs that began with a 5′ G nucleotide were chosen. To synthesize the template DNA required for the in vitro transcription, we employed a two-oligo PCR method (*Bassett et al*., 2013). First, an oligo scaffold containing the RNA loop structure required for recognition by Cas9 was synthesized; this was common to all of the sgRNAs generated. Next, a unique oligo containing a T7 binding site, the 20 nucleotides specific to the sgRNA and 20 bases of homology to the scaffold oligo was synthesized. PCR was performed using these two oligos such that they templated off each other and the full sgRNA sequence was created. The scaffold oligo sequence was: 5′ - GATCCGCACCGACTCGGTGCCACTTTTTCAAGTTGATAACGGAC TAGCCTTATTTTAACTTGCTATTTCTAGCTCTAAAAC − 3′ and the gene-specific oligo sequence was 5′- AATTAATACGACTCACTATA(N20)GTTTTAGAGCTA GAAATAGC- 3′, where (N20) refers to the 20 nucleotides of the sgRNA that bound the genome (excluding the NGG motif, Table 6). The full-length PCR product then was 5′-AATTAATACGACTCACTATA (N20) GTTTTAGAGCTAGAAATAGCAAGTTAAAATAAGGCTAGTCCGTT ATCAACTTGAAAAAGTGGCACCGAGTCGGTGCGGATC-3′. The PCR reaction included 2.5 µL H2O, 12.5 µL 2X Phusion Master Mix (New England BioLabs, M0531L), 5 µL scaffold oligo (10 µM, synthesized at Sigma-Aldrich), and 5 µL sgRNA oligo (10 µM, synthesized at Sigma-Aldrich) and was run in a thermocycler under the following program: 95°C for 30 s; 40 cycles of 95°C for 10 s, 60°C for 10 s, and 72°C for 10 s; and 72 °C for 5 min. This PCR product was purified and used as a template for

the in vitro transcription reaction. All DNA purifications were performed on columns (Zymo Research, D4014).

- RNA in vitro transcription for sgRNA and Cas9

For synthesis of Cas9-encoding mRNA, we used pT3Ts-nCas9n from the Chen lab, obtained via Addgene (46757). The plasmid was linearized using XbaI (New England BioLabs, R0145S), and DNA was purified. 1 µg of linear plasmid was used in an in vitro transcription reaction (T3 mMessage mMachine, Life Technologies, AM1348M). For sgRNA synthesis, 1 µg of guide-template PCR product was used in a T7 in vitro transcription half-reaction (MEGAscript T7, Life Technologies, AM1334M). Both RNA products were cleaned by column (Zymo Research, R1016). A Nanodrop spectrophotometer was used to ensure purity and check concentrations.

- Injection of Cas9-encoding mRNA and sgRNA

All injections contained 500 ng/µL Cas9-encoding mRNA. All sgRNAs were diluted to 50 ng/µL. 1 nL of Cas9-sgRNA mix was used for all injections.

- DNA isolation and screenening

A pool of 10 embryos of F1 generation was lysed in NTES solution (Tris pH 8.0 50 mM; EDTA pH 8,0 50 mM; NaCl 0,1M; SDS 10%) plus 0,3 U/mg of proteinase K solution (Roche PCR Grade recombinant Cat 3 115 828), rotated and heated at 55°C over night. The digested material was spinned at 13,000 rpm for 5' to separate skin from digested tissue. At the supernatant were added saturated NaCl and vortexed aggressively for 10-30 sec, and then spinned for 10' at 13,000 rpm. The supernatant was transferred in absolute ethanol and inverted a sufficient number of times to obtain maximum concentration of the precipitate DNA mass. The DNA

was spulled out and washed in 70% ethanol, and finally dissolved in Milli-Q water at 60°C for 10'. 100 ng of genomic DNA were then used for PCR amplification. We amplified by PCR the gRNA target region of *daglα* exon 2 and exon 6 with the following primers:

daglα exon 2 forward: 5' – ATTGTCCCTTTGTGTTCCAAAT – 3'

daglα exon 2 reverse: 5' – TCTGGGTTGTGTGTAGAGGATG – 3'

daglα exon 6 forward: 5' – CTTACTCTGAGGTTGCCAGCTT – 3'

daglα exon 6 reverse: 5' – CTAAACCCACGATTTTGCAGAC – 3'.

The PCR products were then purified by QIAquick PCR Purification Kit (QIAGEN) according to manufacturer's instructions, and the sequences were checked for automatic sequencing for capillary electrophoresis at the Molecular Biology and Bioinformatics Unit (Stazione Zoologica Anton Dohrn – Napoli), by using Applied Biosystems 3730 Analyzer 48 capillaries (Life Technologies), to check if there were mutations and thus recognize the founders.

8.14 Statistical analyses

For multiple group comparisons, either Kruskal-Wallis or 1-way ANOVA tests were used. The significance of differences between 2 unpaired groups was determined by Student's t test. $P < 0.01$ or $P < 0.05$ was taken as a minimum level of significance. Data are expressed as means ± SEM or SD.

9. REFERENCES

Abbott LF, Regehr WG (2004) "Synaptic computation". Nature 431:796–803.

Aguado T, Monory K, Palazuelos J, Stella N, Cravatt B, Lutz B, Marsicano G, Kokaia Z, Guzman M, Galve-Roperh I (2005) "The endocannabinoid system drives neural progenitor proliferation". FASEB J 19:1704–1706.

Aguado T, Palazuelos J, Monory K, Stella N, Cravatt B, Lutz B, Marsicano G, Kokaia Z, Guzman M, Galve-Roperh I (2006) "The endocannabinoid system promotes astroglial differentiation by acting on neural progenitor cells". J Neurosci 26:1551–1561.

Ahn K, McKinney MK, Cravatt BF. (2008) "Enzymatic pathways that regulate endocannabinoid signaling in the nervous system" Chemical reviews.; 108:1687–1707.

Alberini CM (2009). "Transcription factors in long-term memory and synaptic plasticity". Physiological Reviews. 89 (1): 121–45.

Alexander SP, Kendall DA. (2007) "The complications of promiscuity: endocannabinoid action and metabolism". British journal of pharmacology 152: 602–623.

Alger BE (2002). "Retrograde signaling in the regulation of synaptic transmission: focus on endocannabinoids". Prog Neurobiol 68: 247–286

Almeida AD, Boije H, Chow RW, He J, Tham J, Suzuki SC, Harris WA (2014) "Spectrum of Fates: a new approach to the study of the developing zebrafish retina", Development 141(9): 1971–1980

Argaw A, Duff G, Zabouri N et al. (2011) "Concerted action of CB1 cannabinoid receptor and deleted in colorectal cancer in axon guidance," The Journal of Neuroscience 31 (4): 1489–1499.

Avanesov A and Malicki J (2004) "Approaches to Study Neurogenesis in the Zebrafish Retina" Methods in cell biology Chapter 16 76: 333-384.

Avilion AA, Nicolis SK, Pevny LH, Perez L, Vivian N, Lovell-Badge R (2003) "Multipotent cell lineages in early mouse development depend on SOX2 function". Genes and Development 17 (1): 126-140.

Baier H, Klostermann S, Trowe T, Karlstrom RO, Nusslein-Volhard C, Bonhoeffer F. (1996) "Genetic dissection of the retinotectal projection". Development 123: 415–425.

Baker D, Pryce G, Davies WL, Hiley CR (2006). "In silico patent searching reveals a new cannabinoid receptor". Trends in Pharmacological Sciences. 27 (1): 1–4.

Bassett AR, Tibbit C, Ponting CP, Liu JL. (2013) "Highly efficient targeted mutagenesis of Drosophila with the CRISPR/Cas9 system". Cell Rep. 4, 220–228.

Bear MF (1996) "A synaptic basis for memory storage in the cerebral cortex". Proc Natl Acad Sci USA 93:13453–13459.

Berghuis P, Rajnicek AM, Morozov YM, Ross RA, Mulder J, Urban GM, Monory K, Marsicano G, Matteoli M, Canty A, Irving AJ, Katona I, Yanagawa Y, Rakic P, Lutz B, Mackie K, Harkany T (2007) "Hardwiring the brain: endocannabinoids shape neuronal connectivity". Science 316:1212–1216.

Bisogno T, Delton-Vandenbroucke I, Milone A, Lagarde M, and Di Marzo V (1999) "Biosynthesis and inactivation of N-arachidonoylethanolamine (anandamide) and Ndocosahexaenoylethanolamine in bovine retina," Archives of Biochemistry and Biophysics 370 (2): 300–307.

Bisogno T, Howell F, Williams G, Minassi A, Cascio MG, Ligresti A, Matias I, Schiano-Moriello A, Paul P, Williams EJ, Gangadharan U, Hobbs C, Di Marzo V, Doherty P (2003) "Cloning of the first sn1-DAG

lipases points to the spatial and temporal regulation of endocannabinoid signaling in the brain". J Cell Biol 163:463–468.

Bisogno T and Di Marzo V (2007) "Short- and long-term plasticity of the endocannabinoid system in neuropsychiatric and neurological disorders. Pharmacol. Res. 56, 428–442

Blackburn PR, Campbell JM, Clark KJ, Ekker SC. (2013) "The CRISPR system--keeping zebrafish gene targeting fresh". Zebrafish 10: 116–118.

Bouaboula M, Poinot-Chazel C, Marchand J, Canat X, Bourrié B, Rinaldi-Carmona M, Calandra B, Le Fur G, Casellas P (1996). "Signaling pathway associated with stimulation of CB2 peripheral cannabinoid receptor. Involvement of both mitogen-activated protein kinase and induction of Krox-24 expression". European Journal of Biochemistry / FEBS. 237 (3): 704–11.

Brend T, Holley SA (2009) "Zebrafish whole mount highresolution double fluorescent in situ hybridization". J. Vis. Exp. 25, 1229

Brustein E, Saint-Amant L, Buss RR, Chong M, McDearmid JR, Drapeau P (2003) "Steps during the development of the zebrafish locomotor network" Journal of Physiology 97 (1): 77-86.

Burrill, J, Easter S (1995) "The first retinal axons and their microenvironment in zebrafish cryptic pioneers and the pretract". J. Neurosci. 15: 2935–2947.

Butler AB, Hodos W (1996). "Comparative Vertebrate Neuroanatomy: Evolution and Adaptation". New York: Wiley-Liss

Buss R, Drapeau P (2001) "Synaptic drive to motoneurons during fictive swimming in the developing zebrafish". Journal of Neurophysiology 86 (1): 197-210.

Campbell JM, Hartjes KA, Nelson TJ, Xu X, Ekker SC. (2013) "New and TALENted genome engineering toolbox" Circulation research 113: 571–587

Caterina MJ, Schumacher MA, Tominaga M, Rosen TA, Levine JD, Julius D (1997). "The capsaicin receptor: a heat-activated ion channel in the pain pathway". Nature. 389 (6653): 816–24.

Cavodeassi F, Kapsimali M, Wilson S, Young R (2009) "Forebrain: early development". Squire, L. R. (ed.). Encyclopedia of Neuroscience. (pp. 321-325). Elsevier: Oxford: Academic Press

Cécyre B, Zabouri N, Huppé-Gourgues F,. Bouchard JF, Casanova C (2013) "Roles of cannabinoid receptors type 1 and 2 on the retinal function of adult mice" Investigative Ophthalmology and Visual Science 54 (13): 8079–8090.

Chen J, Matias I, Dinh T et al. (2005) "Finding of endocannabinoids in human eye tissues: implications for glaucoma," Biochemical and Biophysical Research Communications 330 (4): 1062–1067.

Chevaleyre V, Takahashi KA, Castillo PE. (2006) "Endocannabinoidmediated synaptic plasticity in the CNS". Annu Rev Neurosci 29: 37–76.

Cherif H, Argaw A, Cécyre B, et al. (2013) "GPR55 participates to the development of the nervous system," in Proceedings of the 43rd AnnualMeeting of the Society for Neuroscience, SanDiego,Calif, USA.

Clark T (ed.) (1981) ''Visual Responses in Developing Zebrafish (Brachydanio rerio)'' University of Oregon, Eugene, OR.

Cui M, Honore P, Zhong C, Gauvin D, Mikusa J, Hernandez G, Chandran P, Gomtsyan A, Brown B, Bayburt EK, Marsh K, Bianchi B, McDonald H, Niforatos W, Neelands TR, Moreland RB, Decker MW, Lee CH, Sullivan JP, Faltynek CR (2006). "TRPV1 receptors in the CNS play a key role in

broad-spectrum analgesia of TRPV1 antagonists". J. Neurosci. 26 (37): 9385–93.

Demuth DG, Molleman A (2006). "Cannabinoid signalling". Life Sciences. 78 (6): 549–63.

Destexhe A, Marder E. (2004). "Plasticity in single neuron and circuit computations". Nature 431: 789–795.

Devane WA, Hanuš L, Breuer A, Pertwee RG, Stevenson LA, Griffin G, Gibson D, Mandelbaum A, Etinger A, Mechoulam R (1992) "Isolation and structure of a brain constituent that binds to the cannabinoid receptor". Science 258(5090): 1946-9

Diana MA, Levenes C, Mackie K, Marty A. (2002) "Short-term retrograde inhibition of GABAergic synaptic currents in rat Purkinje cells is mediated by endogenous cannabinoids". J Neurosci 22: 200–208.

Dijkhuizen PA, Ghosh A (2005) "BDNF regulates primary dendrite formation in cortical neurons via the PI3-kinase and MAP kinase signaling pathways". J Neurobiol 62:278–288.

Di Marzo V, De Petrocellis L (2012) "Why do cannabinoid receptors have more than one endogenous ligand? Philos. Trans. R. Soc. Lond. B Biol. Sci. 367, 3216–3228

Di Marzo V (2011) "Endocannabinoid signaling in the brain: biosynthetic mechanisms in the limelight". Nature neuroscience 14: 9–15.

Di Marzo V (2008) "Endocannabinoids: synthesis and degradation". Rev Physiol Biochem Pharmacol 160: 1–24.

Di Marzo V (2008) "Targeting the endocannabinoid system: to enhance or reduce?" Nature Reviews Drug Discovery 7, 438-455.

Doniach T and Musci T (1995). "Induction of anteroposterior neural pattern in Xenopus: evidence for a quantitative mechanism". Mechanisms and Development, 53 (3): 405-413.

Duff G, Argaw A, Cecyre B, et al., 2013 "Cannabinoid receptor CB2 modulates axon guidance" PLoS ONE 8 (8) Article ID e70849.

Easter S, Nicola G (1996) "The development of vision in the zebrafish (Danio rerio)". Dev. Biol. 180: 646–663.

Eaton RC, Lee RK, Foreman MB (2001) "The Mauthner cell and other identified neurons of the brainstem escape network of fish" Progress in Neurobiology 63 (4): 467-485.

Egertova M, Giang DK, Cravatt BF, Elphick MR (1998) "A new perspective on cannabinoid signalling: complementary localization of fatty acid amide hydrolase and the CB1 receptor in rat brain". Proc R Soc Lond B Biol Sci 265:2081–2085.

El Manira A, Kyriakatos A, Nanou E, Mahmood R. (2008). "Endocannabinoid signaling in the spinal locomotor circuitry". Brain Res Rev 57: 29–36.

El Manira A, Kyriakatos A. (2010) "The role of endocannabinoid signaling in motor control". Physiology (Bethesda) 25, 230–238

Elphick MR, Egertová M (2001). "The neurobiology and evolution of cannabinoid signalling". Philosophical Transactions of the Royal Society of London. Series B, Biological Sciences. 356 (1407): 381–408.

Fernández-Ruiz J, Berrendero F, Hernández ML, Ramos JA (2000). "The endogenous cannabinoid system and brain development". Trends Neurosci. (1):14-20.

Freund TF, Katona I, Piomelli D. (2003) "Role of endogenous cannabinoids in synaptic signaling". Physiol. Rev. 83, 1017–1066.

Fride E. (2004). "The endocannabinoid-CB(1) receptor system in pre- and postnatal life". Eur J Pharmacol. 500(1-3):289-97.

Fukumitsu H, Ohtsuka M, Murai R, Nakamura H, Itoh K, Furukawa S (2006) "Brain-derived neurotrophic factor participates in determination of neuronal laminar fate in the developing mouse cerebral cortex". J Neurosci 26:13218–13230.

Galve-Roperh I, Sanchez C, Cortes ML, del Pulgar TG, Izquierdo M, Guzman M (2000) "Antitumoral action of cannabinoids: involvement of sustained ceramide accumulation and extracellular signal-regulated kinase activation". Nat Med 6:313–319.

Galve-Roperh I, Aguado T, Rueda D, Velasco G, Guzman M (2006) "Endocannabinoids: a new family of lipid mediators involved in the regulation of neural cell development". Curr Pharm Des 12:2319–2325.

Galve-Roperh I, Aguado T, Palazuelos J, Guzman M (2007) "The endocannabinoid system and neurogenesis in health and disease". Neuroscientist 13:109–114.

Gao Y, Vasilyev DV, Goncalves MB, Howell FV, Hobbs C, Reisenberg M, Shen R, Zhang MY, Strassle BW, and Lu P et al. (2010) "Loss of retrograde endocannabinoid signaling and reduced adult neurogenesis in diacylglycerol lipase knock-out mice". J Neurosci 30:2017–2024.

Gahtan E, Tanger P, Baier H. (2005) "Visual prey capture in larval zebrafish is controlled by identified reticulospinal neurons downstream of the tectum". J. Neurosci. 25, 9294–9303

Gerdeman GL. (2008). "Endocannabinoids at the Synapse: Retrograde Signaling and Presynaptic Plasticity in the Brain" Chapter 11 Cannabinoids and the Brain Springer Science + Business Media, LLC: 203-236.

Godinho L, Mumm JS, Williams PR, Schroeter EH, Koerber A, Park SW, Leach SD, Wong ROL (2005). "Targeting of amacrine cell neurites to

appropriate synaptic laminae in the developing zebrafish retina". Development 132, 5069-5079

Gramage E, Li J, Hitchcock P (2014) "The expression and function of midkine in the vertebrate retina" Br J Pharmacol. 171(4): 913-23.

Grotenhermen, F. (2012) "The Therapeutic Potential of Cannabis and Cannabinoids". Dtsch Arztebl Int. 109, 495–501.

Guzman M, Sanchez C, Galve-Roperh I (2002) "Cannabinoids and cell fate". Pharmacol Ther 95:175–184.

Guzman M (2003) "Cannabinoids: potential anticancer agents". Nat Rev Cancer 3:745–755.

Hanuš L, Abu-Lafi S, Fride E, Breuer A, Vogel Z, Shalev DE, Kustanovich I, Mechoulam R (2001) "2-Arachidonyl glyceryl ether, an endogenous agonist of the cannabinoid CB1 receptor". Proc. Natl. Acad. Sci. USA 98, 3662–3665

Harkany T, Guzman M, Galve-Roperh I, Berghuis P, Devi LA, Mackie K (2007) "The emerging functions of endocannabinoid signaling during CNS development". Trends Pharmacol Sci 28:83–92.

Harkany T, Keimpema E, Barabás K, Mulder J. (2008). "Endocannabinoid functions controlling neuronal specification during brain development". Mol Cell Endocrinol. Apr 16;286(1-2 Suppl 1):S84-90.

Haug MF, Biehlmaier O, Mueller KP, Neuhauss SCF (2010) "Visual acuity in larval zebrafish: behavior and histology". Front. Zool. 7, 8

He JC, Gomes I, Nguyen T, Jayaram G, Ram PT, Devi LA, Iyengar R (2005) "The G alpha(o/i)- coupled cannabinoid receptor-mediated neurite outgrowth involves Rap regulation of Src and Stat3". J Biol Chem 280:33426–33434.

Heap LA, Goh CC, Kassahn KS, Scott EK (2013) "Cerebellar output in zebrafish: an analysis of spatial patterns and topography in eurydendroid cell projections". Front. Neural Circuits 7, 53

Hebb DO (1949) "Organization of Behavior". New York: Wiley.

Heifets BD, Castillo PE (2009). "Endocannabinoid signaling and long-term synaptic plasticity". Annu Rev Physiol 71: 283–306.

Herkenham M, Lynn AB, Little MD, Johnson MR, Melvin LS, de Costa BR, Rice KC. (1990) "Cannabinoid receptor localization in brain". Proc Natl Acad Sci USA. 87(5):1932-6.

Herkenham M, Lynn AB, de Costa BR, Richfield EK (1991) Neuronal localization of cannabinoid receptors in the basal ganglia of the rat. Brain Res 547:267–274.

Horch HW, Katz LC (2002) "BDNF release from single cells elicits local dendritic growth in nearby neurons". Nat Neurosci 5:1177–1184.

Howlett AC, Barth F, Bonner TI, Cabral G, Casellas P, Devane WA, Felder CC, Herkenham M, Mackie K, Martin BR, Mechoulam R, Pertwee RG (2002) International Union of Pharmacology. XXVII. "Classification of cannabinoid receptors". Pharmacol Rev 54:161–202.

Hsu KL, Tsuboi K, Adibekian A, Pugh H, Masuda K, and Cravatt BF (2012) "DAGLb inhibition perturbs a lipid network involved in macrophage inflammatory responses". Nat Chem Biol 8:999–1007

Huang SM, Bisogno T, Trevisani M, Al-Hayani A, De Petrocellis L, Fezza F, Tognetto M, Petros TJ, Krey JF, Chu CJ, Miller JD, Davies SN, Geppetti P, Walker JM, Di Marzo V (2002). "An endogenous capsaicin-like substance with high potency at recombinant and native vanilloid VR1 receptors". Proc. Natl. Acad. Sci. U.S.A. 99 (12): 8400–5.

Huang YY, Neuhauss SCF (2008) "The optokinetic response in zebrafish and its applications" Frontiers in Bioscience 13: 1899-1916,

Ito M. (1972) "Neural design of the cerebellar motor control system". Brain Res 40: 81–84.

Járai Z, Wagner JA, Varga K, Lake KD, Compton DR, Martin BR, Zimmer AM, Bonner TI, Buckley NE, Mezey E, Razdan RK, Zimmer A, Kunos G (1999). "Cannabinoid-induced mesenteric vasodilation through an endothelial site distinct from CB1 or CB2 receptors". Proc. Natl. Acad. Sci. U.S.A. 96 (24): 14136–41.

Jessel T. (2000) "Neuronal specification in the spinal cord: inductive signals and transcriptional codes". Nature Reviews Genetics 1 (1): 20-29.

Johns DG, Behm DJ, Walker DJ, Ao Z, Shapland EM, Daniels DA, Riddick M, Dowell S, Staton PC, Green P, Shabon U, Bao W, Aiyar N, Yue TL, Brown AJ, Morrison AD, Douglas SA (2007). "The novel endocannabinoid receptor GPR55 is activated by atypical cannabinoids but does not mediate their vasodilator effects". Br. J. Pharmacol. 152 (5): 825–31.

Jordan JD, He JC, Eungdamrong NJ, Gomes I, Ali W, Nguyen T, Bivona TG, Philips MR, Devi LA, Iyengar R (2005) "Cannabinoid receptor-induced neurite outgrowth is mediated by Rap1 activation through Gαo/i-triggered proteasomal degradation of Rap1GAPII". J Biol Chem 280:11413–11421.

Jusuf PR and Harris WA (2009) "Ptf1a is expressed transiently in all types of amacrine cells in the embryonic zebrafish retina" Neural Development 4:34.

Kaczocha M, Glaser ST, Deutsch DG (2009). "Identification of intracellular carriers for the endocannabinoid anandamide". Proceedings of the National Academy of Sciences of the United States of America. 106 (15): 6375–6380.

Kano M, Ohno-Shosaku T, Hashimotodani Y, Uchigashima M, Watanabe M (2009). "Endocannabinoid-mediated control of synaptic transmission". Physiol Rev 89: 309–380.

Kapur A, Zhao P, Sharir H, Bai Y, Caron MG, Barak LS, Abood ME (2009). "Atypical responsiveness of the orphan receptor GPR55 to cannabinoid ligands". The Journal of Biological Chemistry. 284 (43): 29817–27.

Karlstrom RO, Trowe T, Klostermann S, Baier H, Brand M, Crawford AD, Grunewald B, Haffter, P, Hoffmann H, Meyer SU, et al. (1996) "Zebrafish mutations affecting retinotectal axon pathfinding". Development 123: 427–438.

Katona I, Sperlagh B, Sik A, Köfalvi A, Vizi ES, Mackie K, Freund TF (1999) "Presynaptically located CB1 cannabinoid receptors regulate GABA release from axon terminals of specific hippocampal interneurons". J Neurosci 19:4544–4558.

Katona I, Urban GM, Wallace M, Ledent C, Jung KM, Piomelli D, Mackie K, Freund TF (2006) Molecular composition of the endocannabinoid system at glutamatergic synapses. J Neurosci 26:5628–5637.

Katona I, Freund TF. "Endocannabinoid signaling as a synaptic circuit breaker in neurological disease". (2008) Nat Med 14: 923–930.

Katz PS, Frost WN. (1996) Intrinsic neuromodulation: altering neuronal circuits from within. Trends Neurosci 19: 54–61.

Keimpema E, Barabas K, Morozov YM, Tortoriello G, Torii M., Cameron G, Yanagawa Y, Watanabe M, Mackie K, Harkany T. (2010) "Differential subcellular recruitment of monoacylglycerol lipase generates spatial specificity of 2-arachidonoyl glycerol signaling during axonal pathfinding". J. Neurosci. 30, 13992–14007

Kettunen P, Krieger P, Hess D, El Manira A. (2002) "Signaling mechanisms of metabotropic glutamate receptor 5 subtype and its endogenous role in a locomotor network". J Neurosci 22: 1868–1873.

Kettunen P, Kyriakatos A, Hallen K, El Manira A (2005). "Neuromodulation via conditional release of endocannabinoids in the spinal locomotor network". Neuron 45: 95–104.

Kimmel CB, Ballard WW, Kimmel SR, Ullmann B, Schilling TF (1995) "Stages of embryonic development of the zebrafish". Dev. Dyn. 203, 253–310.

Klemke RL, Cai S, Giannini AL, Gallagher PJ, de Lanerolle P, Cheresh DA (1997). "Regulation of cell motility by mitogen-activated protein kinase". The Journal of Cell Biology. 137 (2): 481–92.

Kondo S, Kondo H, Nakane S, Kodaka T, Tokumura A, Waku K, Sugiura T. (1998) "2-Arachidonoylglycerol, an endogenous cannabinoid receptor agonist: identification as one of the major species of monoacylglycerols in various rat tissues, and evidence for its generation through CA2+-dependent and -independent mechanisms". FEBS Lett 429(2):152-6

Kreitzer AC, Regehr WG. (2001) "Cerebellar depolarization-induced suppression of inhibition is mediated by endogenous cannabinoids". J Neurosci 21: RC174.

Kreitzer AC, Regehr WG. (2001) "Retrograde inhibition of presynaptic calcium influx by endogenous cannabinoids at excitatory synapses onto Purkinje cells". Neuron 29: 717–727.

Kreitzer AC, Malenka RC. (2008) "Striatal plasticity and basal ganglia circuit function". Neuron 60: 543–554.

Krug II RG and. Clark KJ. (2015) "Elucidating Cannabinoid Biology in Zebrafish (Danio rerio)" Gene 570 (2): 168–179.

Kyriakatos A, El Manira A. (2007). "Long-term plasticity of the spinal locomotor circuitry mediated by endocannabinoid and nitric oxide signaling". J Neurosci 27: 12664–12674.

Lagler K, Bardach J, Miller R (1967) "Ichthyology: the study of fishes", 2nd ed. New York: John Wiley.

Lam CS, Rastegar S, Strahle U. (2006) "Distribution of cannabinoid receptor 1 in the CNS of zebrafish" Neuroscience 138: 83–95.

Lan H, Vassileva G, Corona A, Liu L, Baker H, Golovko A, Abbondanzo SJ, Hu W, Yang S, Ning Y, Del Vecchio RA, Poulet F, Laverty M, Gustafson EL, Hedrick JA, Kowalski TJ (2009). "GPR119 is required for physiological regulation of glucagon-like peptide-1 secretion but not for metabolic homeostasis". The Journal of Endocrinology. 201 (2): 219–30.

Latek, D; Kolinski, M; Ghoshdastider, U; Debinski, A; Bombolewski, R; Plazinska, A; Jozwiak, K; Filipek, S (2011). "Modeling of ligand binding to G protein coupled receptors: Cannabinoid CB1, CB2 and adrenergic β 2 AR". Journal of Molecular Modeling. 17 (9): 2353–66.

Li Z, Joseph NM, Easter SS. (2000) "The morphogenesis of the zebrafish eye, including a fate map of the optic vesicle" Dev. Dyn. 218: 175–188.

Lindsay SM, Vogt RG (2004) "Behavioral responses of newly hatched zebrafish (Danio rerio) to amino acid chemostimulants". Chem. Senses 29, 93–100

López EM, Tagliaferro P, Onaivi ES, López-Costa JJ (2011). "Distribution of CB2 cannabinoid receptor in adult rat retina". Synapse. 65 (5): 388–92.

Lumsden A and Krumlauf R (1996). "Patterning the vertebrate neuraxis". Science, 274 (5290): 1109-1115.

Macdonald R, Wilson S (1997). "Distribution of Pax6 protein during eye development suggests discrete roles in proliferative and differentiated visual cells". Dev. Genes Evol. 206: 363–369.

Macdonald R, Scholes J, Strahle, U, Brennan C, Holder N, Brand M, Wilson SW (1997) "The Pax protein Noi is required for commissural axon pathway formation in the rostral forebrain" Development 124, 2397–2408.

Mackie K, Stella N. (2006). "Cannabinoid receptors and endocannabinoids: evidence for new players". AAPS J 8: E298–E306.

Mailleux P, Parmentier M, Vanderhaeghen JJ. (1992) "Distribution of cannabinoid receptor messenger RNA in the human brain: an in situ hybridization histochemistry with oligonucleotides. Neurosci Lett. 143(1-2):200-4.

Marsicano G, Goodenough S, Monory K, Hermann H, Eder M, Cannich A, Azad SC, Cascio MG, Gutierrez SO, van der Stelt M, Lopez- Rodriguez ML, Casanova E, Schutz G, Zieglgansberger W, Di Marzo V, Behl C, Lutz B. (2003) "CB1 cannabinoid receptors and on-demand defense against excitotoxicity". Science 302: 84–88.

Matias I, Wang JW, Moriello AS, Nieves A, Woodward DF, Di Marzo V (2006) "Changes in endocannabinoid and palmitoylethanolamide levels in eye tissues of patients with diabetic retinopathy and age-related macular degeneration" Prostaglandins Leukotrienes and Essential Fatty Acids, 75 (6): 413–418.

Matias I, Gonthier MP, Petrosino S, Docimo L, Capasso R, Hoareau L, Monteleone P, Roche R, Izzo AA, and Di Marzo V (2007) "Role and regulation of acylethanolamides in energy balance: focus on adipocytes and b-cells". Br. J. Pharmacol. 152, 676–690

Matyas F, Yanovsky Y, Mackie K, Kelsch W, Misgeld U, Freund TF (2006) "Subcellular localization of type 1 cannabinoid receptors in the rat basal ganglia". Neuroscience 137:337–361.

Mayden RL, Tang, K, Conway KW, Freyhof J, Chamberlain S, Haskins M, Schneider L, Sudkamp M, et al. (2007) "Phylogenetic relationships of Danio within the order Cypriniformes: A framework for comparative and

evolutionary studies of a model species". Journal of Experimental Zoology Part B: Molecular and Developmental Evolution. 308B (5): 642–54.

McHugh D; Hu SS-J; Rimmerman N; Juknat A; Vogel Z; Walker JM; Bradshaw HB (2010). "N-arachidonoyl glycine, an abundant endogenous lipid, potently drives directed cellular migration through GPR18, the putative abnormal cannabidiol receptor". BMC Neuroscience. 11: 44.

McHugh D, Tanner C, Mechoulam R, Pertwee RG, Ross RA (2008). "Inhibition of human neutrophil chemotaxis by endogenous cannabinoids and phytocannabinoids: evidence for a site distinct from CB1 and CB2". Mol. Pharmacol. 73 (2): 441–50.

McKinney MK, Cravatt BF, 2005. "Structure and function of fatty acid amide hydrolase". Annu Rev Biochem 74: 411–432.

McPartland JM, Matias I, Di Marzo V, Glass M (2006) "Evolutionary origins of the endocannabinoid system". Gene 370, 64–74

McPartland, J. M., Glass, M., Matias, I., Norris, R. W., and Kilpatrick, C. W. (2007) A shifted repertoire of endocannabinoid genes in the zebrafish (Danio rerio). Mol. Genet. Genomics 277, 555–570.

Migliarini B, Carnevali O (2009) "A novel role for the endocannabinoid system during zebrafish development. Mol. Cell. Endocrinol. 299, 172–177

Molina-Holgado E, Vela JM, Arevalo-Martin A, Almazan G, Molina-Holgado F, Borrell J, Guaza C (2002) "Cannabinoids promote oligodendrocyte progenitor survival: involvement of cannabinoid receptors and phosphatidylinositol-3 kinase/Akt signaling". J Neurosci 22:9742–9753.

Moriconi A, Cerbara I, Maccarrone M, Topai A (February 2010). "GPR55: Current knowledge and future perspectives of a purported "Type-3" cannabinoid receptor". Current Medicinal Chemistry. 17 (14): 1411–29.

Mueller KP, Schnaedelbach OD, Russig HD, Neuhauss SCF (2011) "VisioTracker, an Innovative Automated Approach to Oculomotor Analysis". J. Vis. Exp. (56), e3556.

Nawrocki W (ed.) (1985) ''Development of the Neural Retina in the Zebrafish, Brachydanio rerio'' University of Oregon, Eugene, OR

Ning Y, O'Neill K, Lan H, Pang L, Shan LX, Hawes BE, Hedrick JA (2008). "Endogenous and synthetic agonists of GPR119 differ in signalling pathways and their effects on insulin secretion in MIN6c4 insulinoma cells". British Journal of Pharmacology. 155 (7): 1056–65.

Nusbaum MP, Blitz DM, Swensen AM, Wood D, Marder E (2001). "The roles of co-transmission in neural network modulation". Trends Neurosci 24: 146– 154.

Ohno-Shosaku T, Maejima T, Kano M. (2001) "Endogenous cannabinoids mediate retrograde signals from depolarized postsynaptic neurons to presynaptic terminals". Neuron 29: 729–738.

Onaivi ES (2006). "Neuropsychobiological evidence for the functional presence and expression of cannabinoid CB2 receptors in the brain". Neuropsychobiology. 54 (4): 231–46.

Oster SF, Deiner M, Birgbauer E, Sretavan DW (2004) "Ganglion cell axon pathfinding in the retina and optic nerve". Semin Cell Dev Biol 15, 125–136.

Overton HA, Babbs AJ, Doel SM, Fyfe MC, Gardner LS, Griffin G, Jackson HC, Procter MJ, Rasamison CM, Tang-Christensen M, Widdowson PS, Williams GM, Reynet C (2006). "Deorphanization of a G protein-coupled receptor for oleoylethanolamide and its use in the discovery of small-molecule hypophagic agents". Cell Metab. 3 (3): 167–75.

Pacher P, Mechoulam R (2011). "Is lipid signaling through cannabinoid 2 receptors part of a protective system?". Prog Lipid Res. 50 (2): 193–211.

Pagotto U, Marsicano G, Cota D, Lutz B, Pasquali R (2006). "The emerging role of the endocannabinoid system in endocrine regulation and energy balance". Endocrine Reviews. 27 (1): 73–100.

Papan C, Campos-Ortega J (1999) "Region-specific cell clones in the developing spinal cord of zebrafish". Development genes and evolution. 209 (3): 135-144.

Pertwee, R.G. (2006) "The pharmacology of cannabinoid receptors and their ligands: an overview". Int J Obes (Lond). 30 (Suppl 1): S13–8.

Petros TJ, Rebsam A, Mason CA (2008) "Retinal axon growth at the optic chiasm: to cross or not to cross". Annu Rev Neurosci 31, 295–315.

Petrosino S, Schiano Moriello A, Cerrato S, Fusco M, Puigdemont A, De Petrocellis L, Di Marzo V (2016) "The anti-inflammatory mediator palmitoylethanolamide enhances the levels of 2-arachidonoyl-glycerol and potentiates its actions at TRPV1 cation channels". British Journal of Pharmacology 173: 1154–1162

Pettit DA, Harrison MP, Olson JM, Spencer RF, Cabral GA. (1998) "Immunohistochemical localization of the neural cannabinoid receptor in rat brain". J Neurosci Res. Feb 1;51(3):391-402.

Piomelli D. (2003) "The molecular logic of endocannabinoid signaling". Nat Rev Neurosci 4: 873–884.

Pizzorno L, (2011) New Developments in Cannabinoid-Based Medicine: An Interview with Dr. Raphael Mechoulam". Longevity Medicine Review.

Poggi L, Vitorino M, Masai I, Harris WA (2005) "Influences on neural lineage and mode of division in the zebrafish retina in vivo". J Cell Biol., 171: 991-999.

Reese BE (2011) "Development of the retina and optic pathway". Vision Res 51, 613–632

Reisenberg M, Singh PK, Williams G, Doherty P, (2012) The diacylglycerol lipases: structure, regulation and roles in and beyond endocannabinoid signalling. Philos Trans R Soc Lond B Biol Sci. 367(1607): 3264–3275.

Rinner O, Rick JM, Neuhauss SCF (2005) "Contrast Sensitivity, Spatial and Temporal Tuning of the Larval Zebrafish Optokinetic Response" Investigative Ophthalmology & Visual Science 46 (1): 137-142.

Robles E, Smith SJ, and Baier H. (2011) Characterization of genetically targeted neuron types in the zebrafish optic tectum. Front. Neural Circuits 5, 1

Ross RA (2003). "Anandamide and vanilloid TRPV1 receptors" Br J Pharmacol. 140(5): 790–801.

Ross RA (2009). "The enigmatic pharmacology of GPR55". Trends in Pharmacological Sciences. 30 (3): 156–63.

Rouzer CA, Marnett LJ (2008). "Non-redundant functions of cyclooxygenases: oxygenation of endocannabinoids". J. Biol. Chem. 283, 8065–8069

Rueda D, Navarro B, Martinez-Serrano A, Guzman M, Galve-Roperh I (2002) "The endocannabinoid anandamide inhibits neuronal progenitor cell differentiation through attenuation of the Rap1/B-Raf/ERK pathway". J Biol Chem 277:46645–46650.

Ryberg E, Larsson N, Sjögren S, Hjorth S, Hermansson NO, Leonova J, Elebring T, Nilsson K, Drmota T, Greasley PJ (2007). "The orphan receptor GPR55 is a novel cannabinoid receptor". Br. J. Pharmacol. 152 (7): 1092–1101.

Ryskamp DA, Redmon S, Jo AO, Krizaj D (2014) "TRPV1 and endocannabinoids: emerging molecular signals that modulate mammalian vision". Cells 3, 914–938

Saint-Amant L, Drapeau P (1998) "Time course of the development of motor behaviors in the zebrafish embryo". Journal of Neurobiology 37 (4): 622-632.

Saint-Amant, L, Drapeau P (2000) "Motoneuron activity patterns related to the earliest behavior of the zebrafish embryo" The Journal of Neuroscience 20 (11): 3964-3972.

Sañudo-Peña MC, Romero J, Seale GE, Fernandez-Ruiz JJ, Walker JM (2000) "Activational role of cannabinoids on movement". Eur. J. Pharmacol. 391, 269–274

Savinainen JR and Laitinen JT (2004) "Detection of cannabinoid CB1, adenosine A1, muscarinic acetylcholine, and GABA(B) receptor-dependent G protein activity in transducindeactivated membranes and autoradiography sections of rat retina" Cellular and Molecular Neurobiology. 24 (2): 243–256.

Savinainen, JR; Saario, SM; Laitinen, JT (2012). "The serine hydrolases MAGL, ABHD6 and ABHD12 as guardians of 2-arachidonoylglycerol signalling through cannabinoid receptors". Acta physiologica (Oxford, England). 204 (2): 267–76.

Schlicker E, Timm J, Gothert M (1996) "Cannabinoid receptormediated inhibition of dopamine release in the retina," Naunyn-Schmiedeberg'sArchives of Pharmacology.354 (6): 791–795.

Schmitt E, and Dowling J (1994) "Early eye morphogenesis in the Zebrafish, Brachydanio rerio" J. Comp. Neurol. 344: 532–542.

Shen M, Thayer SA (1998) "The cannabinoid agonist Win55,212-2 inhibits calcium channels by receptor-mediated and direct pathways in cultured rat hippocampal neurons". Brain Res 783:77–84.

Shvartsman SY, Coppey M, Berezhkovskii AM (2009). "MAPK signaling in equations and embryos". Fly. 3 (1): 62–7.

Shoemaker JL, Ruckle MB, Mayeux PR, Prather PL (2005). "Agonist-directed trafficking of response by endocannabinoids acting at CB2 receptors". The Journal of Pharmacology and Experimental Therapeutics. 315 (2): 828–38.

Sickle MDV, Duncan M, Kingsley PJ, Mouihate A; Urbani P, Mackie K; Stella N, Makriyannis A; Piomelli D (2005). "Identification and Functional Characterization of Brainstem Cannabinoid CB2 Receptors". Science. 310 (5746): 329–332.

Song ZH, Zhong M (2000) "CB1 cannabinoid receptor-mediated cell migration". J Pharmacol Exp Ther 294:204–209.

Song J, Kyriakatos A, El Manira A. (2012) "Gating the polarity of endocannabinoid-mediated synaptic plasticity by nitric oxide in the spinal locomotor network". J. Neurosci. 32, 5097–5105

Spemann H and Mangold H (2001) "Induction of embryonic primordia by implantation of organizers from a different species". International Journal of Developmental Biology, 45 (1): 13-38.

Stein PSG, Grillner S, Selverston AI, Stuart DG (1997) "Neurons, Networks, and Motor Behavior". Cambridge.

Streit A, Sockanathan S, Pérez L, Rex M, Scotting P, Sharpe P, et al. (1997). "Preventing the loss of competence for neural induction: HGF/SF, L5 and Sox-2". Development, 124 (6): 1191-1202.

Streit A, Berliner A, Papanayotou C, Sirulnik A, Stern C (2000) "Initiation of neural induction by FGF signalling before gastrulation". Nature, 406 (6791): 74-78.

Stuermer CA (1988) "Retinotopic organization of the developing retinotectal projection in the zebrafish embryo". J. Neurosci. 8: 4513–4530.

Sugiura T, Itoh K, Waku K, Hanahan DJ (1994) Proceedings of Japanese conference on the Biochemistry of Lipids, 36, 71-74

Sugiura T, Kondo S, Sukagawa A, et al. (1995). "2-Arachidonoylglycerol: a possible endogenous cannabinoid receptor ligand in brain". Biochem. Biophys. Res. Commun. 215 (1): 89–97.

Sugiura T, Kobayashi Y, Oka S, Waku K.(2002). "Biosynthesis and degradation of anandamide and 2-arachidonoylglycerol and their possible physiological significance". Prostaglandins Leukot Essent Fatty Acids 66: 173–192.

Surmeier DJ, Plotkin J, Shen W. (2009) "Dopamine and synaptic plasticity in dorsal striatal circuits controlling action selection". Curr Opin Neurobiol 19: 621–628.

Suzuki SC, Bleckert A, Williams PR, Takechi M, Kawamura S, Wong ROL (2013). "Cone photoreceptor types in zebrafish are generated by symmetric terminal divisions of dedicated precursors". Proc. Natl. Acad. Sci. U.S.A. 110, 15109-15114

Swaminath G (Dec 2008). "Fatty acid binding receptors and their physiological role in type 2 diabetes". Archiv der Pharmazie. 341 (12): 753–61.

Tanimura A, Yamazaki M, Hashimotodani Y, Uchigashima M, Kawata S, Abe M, Kita Y, Hashimoto K, Shimizu T, and Watanabe M et al. (2010). "The endocannabinoid 2 arachidonoylglycerol produced by diacylglycerol lipase alpha mediates retrograde suppression of synaptic transmission". Neuron 65:320–327.

Tessier-Lavigne M, Goodman C (1996) "The molecular biology of axon guidance". Science 274 (5290): 1123-1133.

Thorn Perez C, Hill RH, El Manira A, Grillner S. (2009) "Endocannabinoids mediate tachykinin-induced effects in the lamprey locomotor network". J Neurophysiol 102: 1358–1365.

Trowe T, Klostermann S, Baier H, Granato M, Crawford AD, Grunewald B, Hoffmann H, Karlstrom RO, Meyer SU, Muller B, et al. (1996)

"Mutations disrupting the ordering and topographic mapping of axons in the retinotectal projection of the zebrafish, Danio rerio" Development 123: 439–450

Twitchell W, Brown S, Mackie K (1997) "Cannabinoids inhibit N- and P/Q-type calcium channels in cultured rat hippocampal neurons". J Neurophysiol 78:43–50.

Ventimiglia R, Mather PE, Jones BE, Lindsay RM (1995) "The neurotrophins BDNF, NT-3 and NT-4/5 promote survival and morphological and biochemical differentiation of striatal neurons in vitro". Eur J Neurosci 7:213–222.

Viader A, Ogasawara D, Joslyn CM, Sanchez-Alavez M, Mori S, Nguyen W, Conti B, Cravatt BF (2015). "A chemical proteomic atlas of brain serine hydrolases identifies cell type-specific pathways regulating neuroinflammation". eLife 5:e12345

Yazulla S (2008) "Endocannabinoids in the retina: from marijuana to neuroprotection," Progress in Retinal and Eye Research. 27 (5): 501–526.

Yoneda T, Kameyama K, Esumi K, Daimyo Y, Watanabe M, Hata Y (2013) "Developmental and visual input-dependent regulation of theCB1 cannabinoidreceptor inthemouse visual cortex". PLoS One 8, e53082

Yoshida T, Fukaya M, Uchigashima M, Miura E, Kamiya H, Kano M, Watanabe M (2006) "Localization of diacylglycerol lipase-alpha around post-synaptic spine suggests close proximity between production site of an endocannabinoid, 2-arachidonoyl-glycerol, and presynaptic cannabinoid CB1 receptor". J Neurosci 26:4740–4751.

Yoshino H, Miyamae T, Hansen G, Zambrowicz B, Flynn M, Pedicord D, Blat Y, Westphal RS, Zaczek R, and Lewis DA et al. (2011). "Postsynaptic diacylglycerol lipase mediates retrograde endocannabinoid suppression of inhibition in mouse prefrontal cortex". J Physiol 589:4857–4884.

Wang J, Ueda N (2009). "Biology of endocannabinoid synthesis system". Prostaglandins Other Lipid Mediat 89: 112–119.

Warrier A and Wilson M (2007) "Endocannabinoid signaling regulates spontaneous transmitter release from embryonic retinal amacrine cells" Visual Neuroscience 24(1): 25–35.

Watson S, Chambers D, Hobbs C, Doherty P, Graham A. (2008) "The endocannabinoid receptor, CB1, is required for normal axonal growth and fasciculation". Molecular and cellular neurosciences. 38: 89–97.

Weber B and Schlicker E (2001) "Modulation of dopamine release in the guinea-pig retina by Gi- but not by Gs- or Gq-protein coupled receptors" Fundamental and Clinical Pharmacology. 15 (6): 393–400.

Westerfield M (2000) "The Zebrafish Book. A Guide for the Laboratory Use of Zebrafish (Danio rerio)", 4th ed., University of Oregon Press, Portland, OR, USA

Williams EJ, Walsh FS, Doherty P (2003) "The FGF receptor uses the endocannabinoid signaling system to couple to an axonal growth response". J Cell Biol 160:481–486.

Wilson RI, Nicoll RA. (2002) "Endocannabinoid signaling in the brain". Science 296, 678–682

Zolessi FR, Poggi L, Wilkinson CJ, Chien CB, Harris WA (2006). "Polarization and orientation of retinal ganglion cells in vivo". Neural Dev. 1, 2 10.1186/1749-8104-1-2

Zygmunt PM, Ermund A, Movahed P, Andersson DA, Simonsen C, Jönsson BAG, Blomgren A, Birnir B, Bevan S, Eschalier A, Mallet C, Gomis A, Högestätt ED (2013) "Monoacylglycerols Activate TRPV1 – A Link between Phospholipase C and TRPV1". PLoS One 8 (12): e81618.